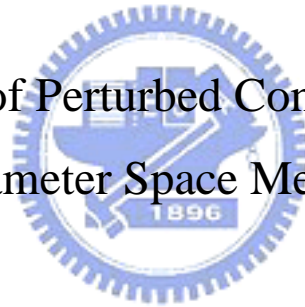# 國立交通大學

電機與控制工程學系

博 士 論 文

參數空間法用於擾動控制系統之分析與設計

Analysis and Design of Perturbed Control Systems Based on
Parameter Space Method

研 究 生：秦弘毅

指導教授：吳炳飛 博士

中 華 民 國 九 十 四 年 六 月

參數空間法用於擾動控制系統之分析與設計

Analysis and Design of Perturbed Control Systems Based on Parameter Space Method

研 究 生：秦弘毅　　　　　　　　　Student：Hung-I Chin

指導教授：吳炳飛 博士　　　　　　Advisor：Dr. Bing-Fei Wu

國 立 交 通 大 學

電 機 與 控 制 工 程 學 系

博 士 論 文

A Dissertation

Submitted to Department of Electrical and Control Engineering

College of Electrical Engineering and Computer Science

National Chiao Tung University

In Partial Fulfillment of the Requirements

for the Degree of

Doctor of Philosophy

in

Electrical and Control Engineering

June 2005

Hsinchu, Taiwan, Republic of China

中 華 民 國 九 十 四 年 六 月

參數空間法用於擾動控制系統之分析與設計

研究生：秦弘毅　　　　　　　　　　指導教授：吳炳飛 博士

國立交通大學電機與控制工程學系

摘　　　要

　　在實體系統中使用的模型通常是不準確的。在運作期間，系統中的參數常隨著時間和環境的變化而改變，或者由於使用之模型為簡化的模型，凡此種種原因皆可導致誤差的產生，所以針對特定準確的系統而進行之分析及設計是不完全實用的。在實際控制系統設計及分析時，穩健的系統穩定性，是重要的考慮因素。由於系統中非線性元件的存在，另一個必須考慮的重要現象為極限環的產生，而通常這是設計者不希望見到的，此類問題已經被許多的研究者討論過。對帶有非線性性質的擾動系統而言，如果能夠事先預測其極限環的行為，對設計者是極有助益的。利用描述函數法將非線性元件線性化，以預測其極限環的發生，已成功的使用在許多的應用上。

　　本論文旨在針對具有擾動參數的控制系統，提出一完整且有效之方法，利用參數空間法及穩定性的基本觀念，以分析其增益邊際和相位邊際，並且設計控制器，調整控制器的係數，以達到系統頻域的規格要求，例如增益邊際、相位邊際和敏感度。同時對有非線性元件的系統，預測其極限環的發生。車輛模型被使用為模擬的例子。藉著求解系統之特性方程式，在選定之系統參數平面或空間上，產生增益及相位邊界曲線，以圖解方式決定控制器係數的合格區域，以使整個系統之性能達到頻域規格的要求，以此法進行分析及設計。同樣的方法也應用於模糊控制系統穩定度的分析。以上提出之方法更進一步延伸至具有擾動參數的鎖相迴路系統的設計分析。部分系統參數在給定區域擾動，於參數平面上，以圖形顯示待決之目標參數區域，選定該區域範圍內之參數，使該鎖相迴路系統能達到規格之要求。本論文模擬的結果已驗証了預期達成之目標。

Analysis and Design of Perturbed Control Systems Based on Parameter Space Method

Student：Hung-I Chin   Advisor：Dr. Bing-Fei Wu

Department of Electrical and Control Engineering
National Chiao Tung University

ABSTRACT

The models used are usually imprecise and the parameters of physical systems vary with the operating conditions and time. Designing and implementing a system for a fixed and exact control plant is not usually practical in the natural environments. A inaccurate plant may result from a simplified model and uncertainties in system parameters can always occur in the physical world. Robustness stability is important in analysis and design of practical control systems. Another important phenomena to be considered is undesirable oscillations due to nonlinearities in a feedback closed system and it has been studied by many researchers. It is very instructive for the designer to predict the limit cycle behavior of a perturbed control system with nonlinearities. The describing function technique is mainly employed to predict the existence of constant amplitude oscillations of closed nonlinear systems and has been successfully used in many applications.

The main subject of this dissertation is to propose a novel method based on parameter space method and robust stability criteria to predict limit cycles occurred, analyze the system performances of gain margin and phase margin (GM and PM), and design a desired controller by adjusting the controller coefficients for perturbed control systems to meet specified conditions including GM, PM and sensitivity in frequency domain. A vehicle model is used as an example for simulation. With the help of gain and phase boundary curves resulting from the roots of the characteristic polynomial equation of closed control systems, a methodology is proposed for portraying regions in a selected designed parameter plane so that the performance of the whole system can meet the specified requirements with perturbed parameters varying in given intervals. The same approach is

extended to analyze the robust stability for a fuzzy control system. This dissertation also applies the above method on phase-locked loops (PLL) design by frequency domain approach for a perturbed PLL system. The desired system parameters of PLLs in the selected coordinate plane are determined in graphical portrayals. Simulation results have demonstrated and achieved the objectives as desired.

誌謝

這一路走來，有太多我需要感謝的人!

尤其是我的論文指導教授 吳炳飛老師。

在此我要由衷的向您和師母的關心表示十二萬分的謝意和敬意。由於您的鼎力協助、指導研究，並給予不斷的鼓勵，尤其遭遇挫折的時候，才使我越挫越能堅持。

特別感謝口試委員 鄧清政教授、張志永教授、林志民教授、鍾俊業教授、黃英哲教授，在百忙之中，願意撥冗參與口試，不吝給予鞭策和指導。

在研究過程中，彭昭暐博士經常給予協助和提供諸多建議，給予研究上極大的助益，多年來彭博士及淑美賢伉儷所展現的友誼關懷，尤其令我銘感五內，永誌難忘。

感謝 CSSP 實驗室的學弟妹們多年來提供的協助，您們的友情，給了我一切。您們的勤奮和努力，使也我印象深刻，值得向年輕的各位再學習，尤其是立山、世孟。

多年來，內人 素瑩體諒我就讀研究所博士班，課業繁重，協助我照料家庭及子女，免除後顧之憂，使我能潛心向學，最值得我感謝。希望在未來人生旅途上，能以實際行動，回報一二。也謝謝小兒 國鈞及小女 瑋苓的加油、鼓勵，給予我無比的勇氣。

有所遺憾的是博士班就讀期間，父親、母親相繼辭世，使我未能

多盡人子孝道，回饋養育恩情，謹於此，表達對我的父親 秦瓊樹先生、母親 秦黃含笑女士感恩及紀念之意。

「天行健，君子以自強不息」，人生就是不斷的學習過程。雖已年過半百，仍滿懷信心，願盡一己棉薄之力，將所學所知，進行對照，服務社會，希望有所助益。

再一次，恭謹的向所有關心、支持及協助我的人，表達最誠摯的謝意。

弘毅　　於交大 CSSP 實驗室

6/24/2005

Contents

List of Tables

List of Figures

List of Symbols

N describing function

ϕ phase shift

A amplitude of limit cycle

ω frequency of limit cycle

k gain

θ phase

Φ input signal range of fuzzy logic

$\mathbb{S}$ 2D perturbed parameter plane

$\mathbb{R}$ 3D perturbed parameter space

Chapter 1

Introduction

1.1 Motivations

Gain margin and phase margin are important specifications in the frequency domain for

the analysis and design of practical control systems and have served as important measures of

robustness analysis which is always of primary concern. This is because the models used are

usually imprecise and the parameters of all physical systems vary with the operating

conditions and time. They are usually obtained numerically or graphically by the use of

system frequency response like Bode plots. Studying for controller design to satisfy GM, PM

or sensitivity conditions was proposed by several articles such as in [1]-[6], There are also

many design methods to determine the parameters to meet different objectives [7]-[9].

Designing a controller for a fixed and exact control plant is not usually practical in the natural

environments. Due to the simplified models or the factors resulting from the changing

environments, the uncertainties in system parameters can always occur. Uncertain parameters

in a linear control system can be robustly analyzed by the parameter plane method or the

parameter space method [10]-[16]. By robust stability criteria a simple way of checking the

stability of perturbed interval polynomials, is to guarantee if all the polynomials have the

roots in the left-half plane [17]. The perturbed parameters will result in root-clusters, within

which the roots of the perturbed polynomials will be located. Usually, a change in a physical

quantity typically appears in more than one coefficient of the characteristic equation. Robust

Gamma-stability analysis for a perturbed vehicle plant was also studied [18]. The methods of

analyzing the gain-phase margin of a linear control system with adjustable parameters have

been developed [19]-[21]. Strictly speaking, the majority of the researches mentioned above

are not concentrated on the controller design for perturbed systems. Sensitivity functions are

usually used as a design specification to indicate the robustness of a system. In [6] and [8],

Yaniv and Nagurka proposed a robust controller design method satisfying GM, PM and

sensitivity constraints on the perturbed systems, not with the system parameters in uncertain

continuous intervals, but with the system uncertainties in the finite discrete set of gains and

pole locations.

Undesirable oscillation phenomena due to nonlinearities in a feedback closed system

have been studied by many publications [22]-[26] and it is important for the designer to

predict the limit cycle behavior of a perturbed vehicle system with nonlinearities. It is of

interest to know the frequency, amplitude, stability and instability of the limit cycle occurred.

The describing function technique is mainly employed to predict the existence of constant

amplitude oscillations of closed nonlinear systems and has been successfully used in many

applications although some limitations exist in the systems which don't satisfy the assumption

of filtering out the higher order harmonics [27]-[30].

In addition, some researchers have developed the experimental and analytic describing

functions of fuzzy controller in order to analyze the stability of fuzzy control systems [31-32].

Furthermore, the describing function technique to design a fuzzy controller for switching

DC-DC regulators was proposed by Gomariz et al [33]. The describing function was also

applied to find the bounds for the neural network parameters to have a stable system response

and generate limit cycles [34]. The results in [32] and [33] are extended to analyze the

stability of a fuzzy vehicle steering control system under the effects of system parameters and

gain-phase margin by the use of methods of describing function, parameter plane and a

gain-phase margin tester. A simple vehicle steering control model with perturbed parameters

is cited to verify the design procedure.

On the other hand, there are a large number of studies concentrated on the subject of

phase-locked loops (PLL) in the latest decades. The theoretical description of PLL was well

proposed [35]-[39]. A PLL is essentially a circuit that has a particular system lock its

frequency as well as the phase to those of the input applied to it. When the phase error is built

up in the locked state, a feedback mechanism acts on an oscillator called VCO so that the

error is reduced to a minimum and a phase output of VCO is really locked to the reference

input. There are a considerable number of applications in many areas. A technique using PLL

was established on motor speed control [40]. In the design of Global Positioning System

receivers, PLL is very useful especially in a noisy environment [41]. PLL was also applied in

the design of frequency synthesizer [42].

In this thesis, GM and PM performances are defined for a perturbed system with

uncertain continuous interval parameters and shown here graphically in the system parameter

space. By the use of parameter space method and robustness stability criteria, stability

boundary curves corresponding to specific GM and PM constraints are generated. Owing to

the complexity of the controller design for perturbed control systems, it is not an easy job to

find out a qualified controller together with the system plant with uncertain interval

parameters so that the whole closed system at every point in the perturbed system parameter

region satisfies all the three specifications of GM, PM and sensitivity. The main concern in

the controller design is to find a desired region in the controller coefficient plane so that the

performance of the whole system with uncertain parameters inside a perturbed space satisfies

given specifications. The desired controller will be determined graphically from a figure in

which a qualified controller coefficient area is to be found out. With the help of stability

boundary curves in the controller coefficient space, the objective of designing a suitable

controller meeting the specified requirements is achieved.

1.2 Organizations of the Dissertation

The dissertation is organized as follows. Chapter 1 is an introduction. Basic concepts are

described in Chapter 2. In Chapter 3, a perturbed vehicle control system whose gain margin

(GM) and phase margin (PM) are analyzed and for which a novel controller design method

satisfying the given specifications on GM, PM and sensitivity is developed. In Chapter 4, the

subject of predicting the limit cycle of a nonlinear perturbed vehicle control system under

specific gain-phase margin (GM/PM) constraints is addressed. The analysis of robust stability

for a fuzzy vehicle steering control system is considered in Chapter 5. In Chapter 6, a control

algorithm is presented for phase-locked loop (PLL) design with perturbed parameters

satisfying frequency-domain specifications. In Chapter 7, conclusions are given and

suggestions for future research are also proposed.

Chapter 2

Basic Concepts

2.1 Overview

This chapter presents a description about the way how to analyze and design a feedback control system with perturbed parameters varying in intervals by frequency approach. Parameter space method and robust stability criteria provide a technique to check the stability of perturbed control systems in a space with the coordinates of uncertain system parameters. By the use of a gain-phase margin tester, stability boundary curves are generated to determine gain and phase margins (GM and PM) in performance analysis. In the similar way, desired controller coefficients are going to be found out to meet given specifications for controller design. Sensitivity function is also considered in the controller design. With the nonlinearities inherent in the system, describing function method is used for predicting limit cycle occurred.

2.2 Robust Stability Criteria

Consider the characteristic polynomial of a feedback control system

$$P(s,q) = \sum_{i=0}^{n} d_i(q)s^i = d_0(q) + d_1(q)s + \cdots + d_n(q)s^n,$$
(2.1)

where $q = [q_1, q_2, \cdots q_n] \in \Re$ and $\Re$ is a set of allowable parameter domain space. Each q_i varies independently within the interval with $q_i \in [q_i^-; q_i^+], i = 1, 2 \cdots n$.

It has been shown that for real continuous coefficient functions $d_i(q)$ of the characteristic equation, a sufficient condition for robust stability is that (a) there exists a $q = q_o \in \Re$ such that $P(s, q)$ is stable; (b) $P(s, q)$ doesn't have any roots on the imaginary axis for any $q \in \Re$. It is easily tested by checking the stability of the characteristic polynomial $P(s, q_o)$ for an arbitrary $q_o \in \Re$. If no such q_o exists, the system is unstable. The condition (b) is satisfied if and only if the equation $P(s, q) = 0$ neither has a real root at $s = 0$, i.e.
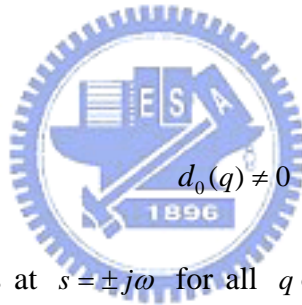
$$d_0(q) \neq 0 \tag{2.2}$$

nor an imaginary pair of roots at $s = \pm j\omega$ for all $q \in \Re$. Let $\Re_{j\omega}$ be the set of all real q such that the polynomial $P(s, q)$ has roots on the imaginary axis .

$$\Re_{j\omega} = \{q : P(j\omega, q) = 0 \quad \text{for} \quad \omega \geq 0\}. \tag{2.3}$$

The condition (b) also means that $\Re_{j\omega}$ does not intersect the parameter domain space $\Re$. The curve formed by the points q in $\Re_{j\omega}$ in the $q-\text{space}$ is the stability boundary curve. The perturbed feedback control system is stable at the points in the $q-\text{space}$ on one side of the stable boundary curve and it is unstable at the points on the other side. The above method can be used to determine where the system parameters in $\Re$ can be chosen.

2.3 Describing Function

It is generally useful for the describing function technique to be applied in engineering problems of control systems. Nonlinear systems are generally linearized by using the describing function method to predict the limit cycle for stability analysis. Assume a sinusoidal input $x(t) = A\sin(\omega t)$ with the amplitude A and the frequency ω to a nonlinear system $\mathbb{N}$ in Fig. 2.1 and $y(t)$ is the output signal and periodic. By the Fourier series,

$$y(t) = a_0 + \sum_{n=1}^{\infty}(a_n \sin(n\omega t) + b_n \cos(n\omega t)), \tag{2.4}$$

where

$$a_0 = \frac{1}{2\pi}\int_0^{2\pi} y(t)d(\omega t),$$
$$a_n = \frac{1}{\pi}\int_0^{2\pi} y(t)\sin n\omega t d(\omega t), \qquad n \neq 0, \tag{2.5}$$
$$b_n = \frac{1}{\pi}\int_0^{2\pi} y(t)\cos n\omega t d(\omega t), \qquad n \neq 0.$$

If the nonlinear system is symmetric about the origin, $a_0 = 0$. Let Y be a fundamental component of the Fourier series of $y(t)$ and $Y = a_1 + jb_1 = Y_1 \angle \theta_1$, where $Y_1 = \sqrt{a_1^2 + b_1^2}$ and $\theta_1 = \tan^{-1}\frac{b_1}{a_1}$. Y_1 is the amplitude of the fundamental component of the system output $y(t)$ and θ is the phase shift by Fourier series.

The describing function N of a symmetric nonlinear system is defined as [28]

$$N = \frac{Y_1}{A}\angle\theta_1 = \frac{a_1 + jb_1}{A}\angle\theta_1 \tag{2.6}$$

2.4 Parameter Space Method

Consider a perturbed closed control system with a gain-phase margin tester $ke^{-j\theta}$ and there are r nonlinear components in the system. Every nonlinear component has the complex describing function N_i $(i=1,2,....,r)$ that is a complex function of A and ω, which are the amplitude and frequency respectively of the input signal to the $i-th$ nonlinear element N_i and

$$N_i = N_{iR} + jN_{iI}. \tag{2.7}$$

Assume the closed characteristic equation is

$$
\begin{aligned}
&P(s,q,c,k,\theta,N_{1R},N_{1I}...,N_{rR},N_{rI}) \\
&= \text{the numerator of } [1+ke^{-j\theta}G(s,q,c,N_{1R},N_{1I}...,N_{mR},N_{mI},...,N_{rR},N_{rI})] \\
&= 0,
\end{aligned}
\tag{2.8}
$$

and

$$
\begin{aligned}
&P(s,q,c,k,\theta,N_{1R},N_{1I},...,N_{rR},N_{rI}) \\
&= \sum_{t=0}^{n} d_t(q,c,k,\theta,N_{1R},N_{1I},...,N_{rR},N_{rI})s^t \\
&= d_0(q,c,k,\theta,N_{1R},N_{1I},...,N_{rR},N_{rI})+d_1(q,c,k,\theta,N_1,...,N_r)s+\cdots \\
&\quad +d_n(q,c,k,\theta,N_{1R},N_{1I},...,N_{rR},N_{rI})s^n,
\end{aligned}
\tag{2.9}
$$

where $G(s,q,c,N_{1R},N_{1I}...,N_{rR},N_{rI})$ is an open loop transfer function of the system and c is a controller coefficient vector. $c=[c_0,c_1,.....c_m]$ and c_i is a controller coefficient to be designed for $i=0,1,2,.....m$.

$P(j\omega,q,c,k,\theta,N_{1R},N_{1I},...,N_{rR},N_{rI})$ may be written into the real part $U(\omega,q,c,k,\theta,N_{1R},N_{1I},$ $..,N_{rR},N_{rI})$ and imaginary part $V(\omega,q,c,k,\theta,N_{1R},N_{1I}...,N_{rR},N_{rI})$.

$$
\begin{aligned}
P(j\omega,q,c,k,\theta,N_{1R},N_{1I},...,N_{rR},N_{rI}) &= U(\omega,q,c,k,\theta,N_{1R},N_{1I}...,N_{rR},N_{rI})+ \\
&\quad jV(\omega,q,c,k,\theta,N_{1R},N_{1I},...,N_{rR},N_{rI}) \quad (2.10) \\
&= 0,
\end{aligned}
$$

where

$$U(\omega,q,c,k,\theta,N_{1R},N_{1I},...,N_{rR},N_{rI}) = r_0(q,k,\theta,N_{1R},N_{1I},...,N_{rR},N_{rI})$$
$$+ r_1(q,c,k,\theta,N_{1R},N_{1I},...,N_{rR},N_{rI})\omega$$
$$+ r_2(q,c,k,\theta,N_{1R},N_{1I},...,N_{rR},N_{rI})\omega^2 \qquad (2.11)$$
$$+ \cdots + r_n(q,c,k,\theta,N_{1R},N_{1I},...,N_{rR},N_{rI})\omega^n$$

and

$$V(\omega,q,c,k,\theta,N_{1R},N_{1I},...,N_{rR},N_{rI}) = i_0(q,k,\theta,N_{1R},N_{1I},...,N_{rR},N_{rI})$$
$$+ i_1(q,c,k,\theta,N_{1R},N_{1I},...,N_{rR},N_{rI})\omega$$
$$+ i_2(q,c,k,\theta,N_{1R},N_{1I},...,N_{rR},N_{rI})\omega^2 \qquad (2.12)$$
$$+ \cdots + i_n(q,c,k,\theta,N_{1R},N_{1I},...,N_{rR},N_{rI})\omega^n.$$

The equations

$$\begin{cases} U(\omega,q,c,k,\theta,N_{1R},N_{1I},...,N_{rR},N_{rI}) = 0 \\ V(\omega,q,c,k,\theta,N_{1R},N_{1I},...,N_{rR},N_{rI}) = 0 \end{cases} \qquad (2.13)$$

can be solved for q or for c.

2.4.1   Limit Cycle Prediction

For predicting the limit cycle resulting from nonlinearities N_i, (2.13) is solved   for q

given specific ω,c,k,θ and A in system performance analysis analytically or numerically.

Gain boundary curves will be generated from these q values in the q-parameter space by

varying ω given specific k and A with $\theta = 0^\circ$. Phase boundary curves will be

generated by varying ω given specific θ and A with $k = 1$. Every boundary curve

separates the parameter domain region into two areas as in Fig. 2.2. One is the asymptotically

stable region and the other is unstable. The limit cycle with amplitude A will happen if a

system parameter point q is in the unstable area, but it won't if q is in the stable area. The gain and phase margins of the perturbed control system will be analyzed from boundary curves geometrically. A specific gain or phase value corresponding to the boundary curve which is tangent to the perturbed parameter region as in Fig. 2.3 is defined as the GM and PM of the perturbed system for predicting the limit cycles occurring, respectively.

2.4.2 GM Analysis without Nonlinearities

If there is no nonlinear part in a perturbed system, $N_{1R}, N_{1I}, ..., N_{rR}$, and N_{rI} in (2.10)-(2.13) are omitted.

Equation (2.13) is rewritten into the following form

$$\begin{cases} U(\omega, q, c, k, \theta) = 0 \\ V(\omega, q, c, k, \theta) = 0 \end{cases} \tag{2.14}$$

Equation (2.14) can be solved for q with specific ω, c, k, θ. For gain margin analysis, a gain boundary curve is generated in $q-$space from the solutions q of (2.14) by varying ω for every k with $\theta = 0^O$. A specific gain k (dB) corresponding to the boundary curve which is tangent to the perturbed region $\Re$ is defined as the GM of the perturbed control system. It is also the minimal GM of the system within the entire region $\Re$. The GM of the control system at a point on one side of a specific gain boundary curve is greater than that at a point on the boundary curve. But it is less at the points on the other side.

2.4.3 PM Analysis without Nonlinearities

Equation (2.14) can be solved for q with respect to θ, given specific ω, c, k. Phase boundary curves are developed under the PM specification in a similar way with $k = 1$. They are generated in q-space from the solutions q of (2.14) by varying ω for every θ. The PM of the control system is defined as the phase value θ associated with the phase boundary curve which is tangent to the perturbed region $\Re$. It is the minimal PM for the whole system with the parameters inside $\Re$, too. The PM of the control system at a point on one side of a specific phase boundary curve is greater than that at a point on the boundary curve. But it is less at a point on the other side.

2.4.4   Controller Design
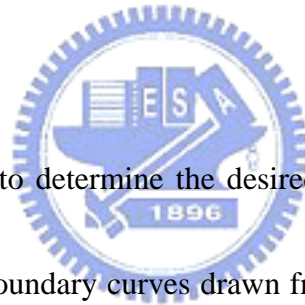
The controller design is to determine the desired controller coefficients in selected c -space. Based on gain-phase boundary curves drawn from the locations of the roots of (2.14) for c and the constant-sensitivity loci, the desired area in c-space is found so that the whole system with the controller in that area will meet specified conditions.

First, determine a gain region in c-space with the help of the gain boundary curves so that the controller with the coefficients in that region satisfies the specified GM constraints. Secondly, a phase-region is determined in c-space with the help of the phase boundary curves so that the controller with the coefficients in that region satisfies the specified PM conditions. Then, find out the common region of the previous mentioned gain and phase areas.

The controller coefficients in that region will satisfy both the user-defined GM and PM specifications.

2.5 Sensitivity Function

Sensitivity effects are often important to be considered in the design of control systems on frequency domain and can be used as a design specification to indicate the robustness of control system. The sensitivity function of the closed-loop transfer function *H(s)* with respect to the variations of the transfer function *G(s)* which is a subsystem of *H(s)* is defined as

$$S_{G(s)}^{H(s)} = \frac{\partial H(s)/H(s)}{\partial G(s)/G(s)} \tag{2.15}$$

or with respect to the variations of an element β in *H(s)* is given by

$$S_{\beta}^{H(s)} = \frac{\partial H(s)/H(s)}{\partial \beta/\beta} . \tag{2.16}$$
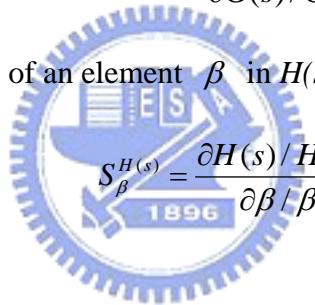
2.6 Concluding Remarks

In this chapter, basic concepts of performance analysis and controller design for perturbed control systems are addressed based on parameter space method and robust stability criteria. GM and PM are analyzed and the desired controller is determined by the proposed methods with the help of a gain-phase margin tester. Limit cycles are also predicted for perturbed systems with nonlinearities.
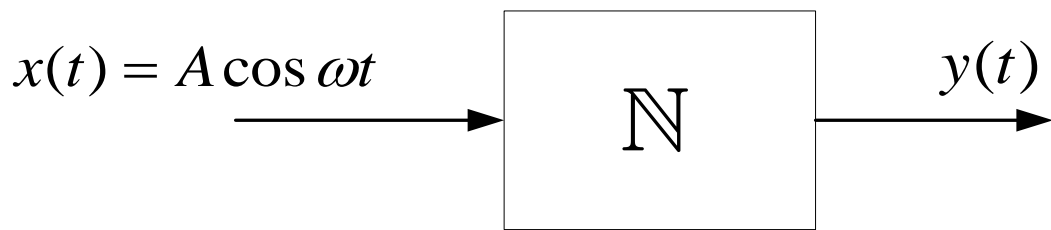
Fig. 2.1 A nonlinear system with input signal $x(t) = A\cos\omega t$
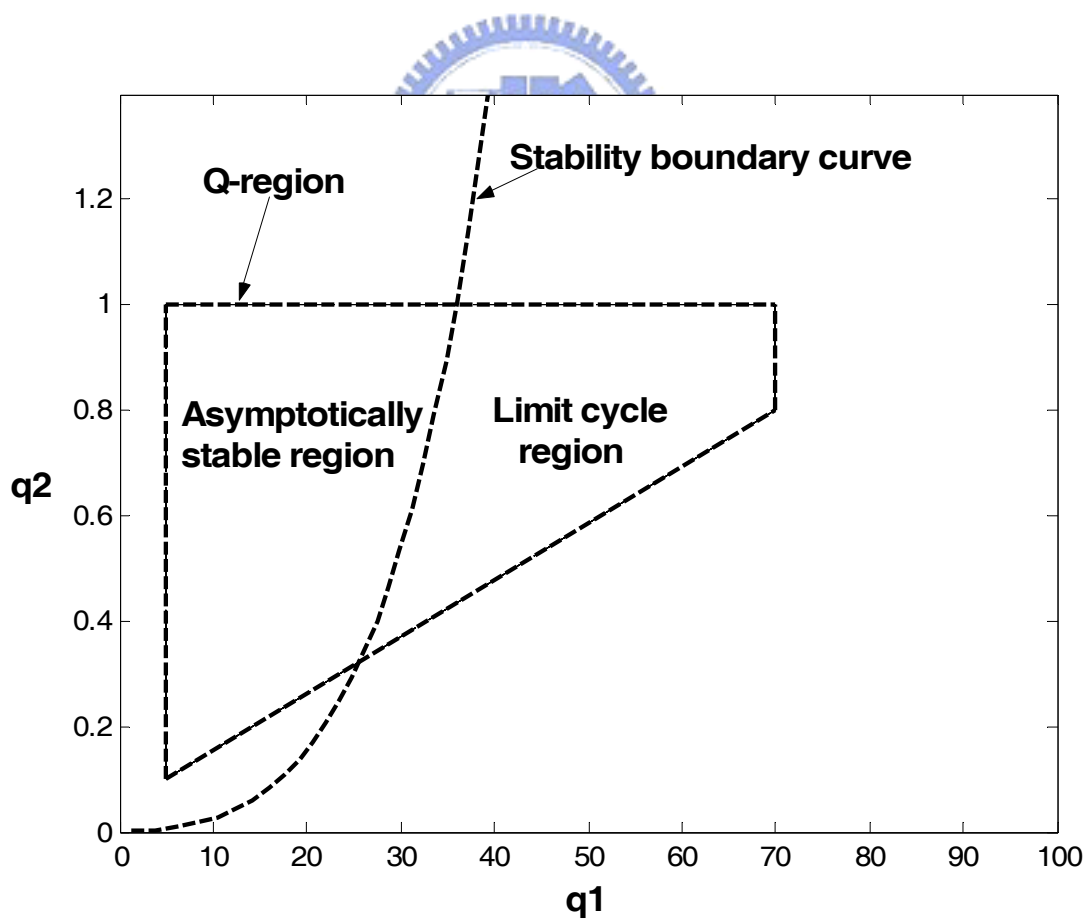
Fig. 2.2 Limit cycle boundary in a nonlinear system.
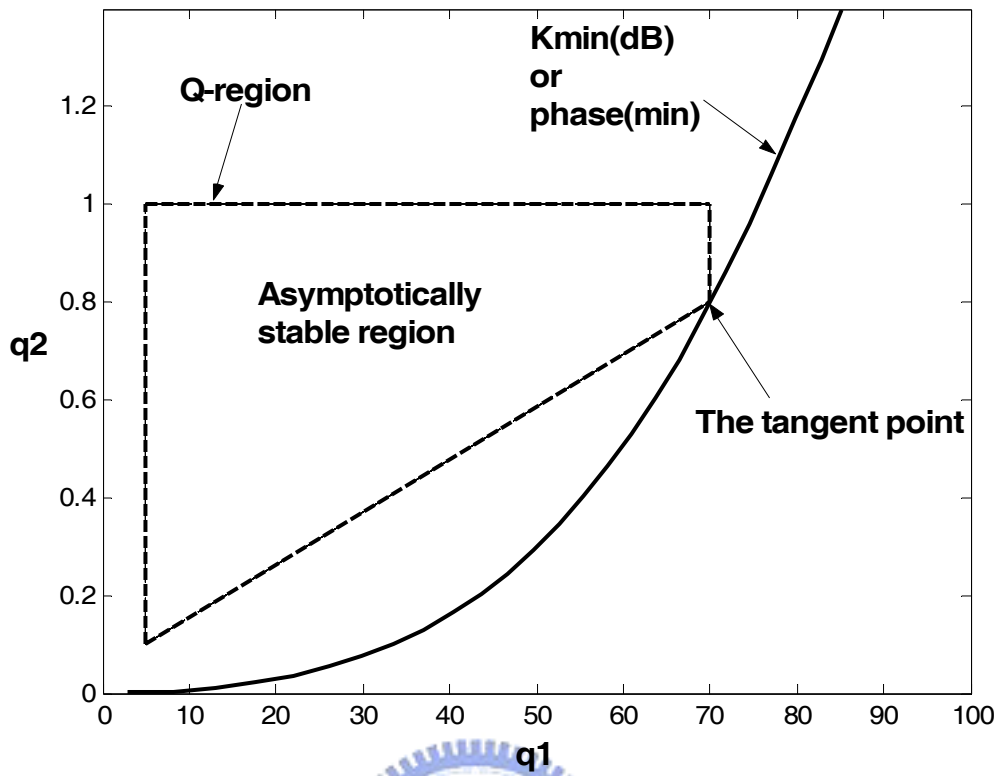
Fig. 2.3 Gain margin (or phase margin) for predicting
Limit cycle occurred in a nonlinear system.
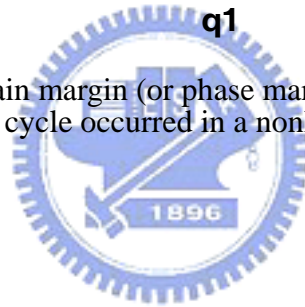
Chapter 3

Robust Control Design for Perturbed Systems by Frequency Domain Approach

3.1 Overview

The chapter presented here is concentrated on a perturbed vehicle control system whose gain margin (GM) and phase margin (PM) are analyzed and for which a novel controller design method satisfying the given specifications on GM, PM and sensitivity is developed. The approach is applied to the plants with uncertain parameters that vary in intervals. Based on the parameter space method and robust stability criteria, gain and phase boundary curves are generated from the characteristic polynomial of the system with which a gain-phase tester is included in series to perform system stability analysis and controller design. The main concern in the controller design is to find a region in the controller coefficient plane so that the performance of the uncertain system satisfies given specifications. The proposed method is applied to an example of a bus system. Simulation results are given for illustration to show the system performances on GM and PM and the desired controller meeting the specified conditions in frequency domain for the perturbed system is derived.

16

3.2 Sensitivity

Since in physical systems all the elements may change their properties with time and

environments, the considerations about the changes of the characteristics of the closed control

systems with respect to system parameter variations are always of big concern for a system

designer.

Consider a linear control feedback system illustrated in Fig. 3.1. The closed loop

feedback system has the transfer function given by

$$H(s,q,c) = \frac{C(s,c)G(s,q)}{1 + C(s,c)G(s,q)}, \tag{3.1}$$

where $C(s,c)$ is a controller with $c = [c_0, c_1, ... c_m]$ and c_i is a controller coefficient to be

designed for $i = 0,1,2,.....m$. $G(s,q)$ is a plant with a perturbed parameter vector

$q = [q_1, q_2, \cdots q_n] \in \Re$. $\Re$ is a set of allowable parameter domain space. Each q_i varies

independently within the interval with $q_i \in [q_i^-; q_i^+]$, $i = 1,2 \cdots n$.

Assume

$$C(s,c) = \frac{N_c(s,c)}{D_c(s)} \tag{3.2}$$

and

$$G(s,q) = \frac{N_G(s,q)}{D_G(s,q)}. \tag{3.3}$$

With a specific q, $H(s,q,c)$ is replaced by $H(s,c)$. The sensitivity function $S_{c_i}^{H(s,c)}$ with

respect to the controller coefficient c_i is defined as

$$S_{c_i}^{H(s,c)} = \frac{dH(s,c)/H(s,c)}{dc_i/c_i},$$ (3.4)

where $i = 0,1,2....m$. Substitute (3.1), (3.2) and (3.3) into (3.4), and the sensitivity function

$S_{c_i}^{H(s,c)}$ can be computed. Given a different constant s_0, the solutions of the equality

$\left| S_{c_i}^{H(j\omega)} \right|_{s=j\omega} = s_0$ for a controller coefficient c give constant-sensitivity loci in the $c-\text{space}$.

The controller coefficient c will be determined based on sensitivity specifications

corresponding to one of those loci. A system being very insensitive to parameter variations is

considered to be a good control system.

3.3 Stability Boundary Analysis

Consider a gain-phase tester $ke^{-j\theta}$ included in series with the original control system as

in Fig. 3.2, and its transfer function is given by

$$H(s,q,c,K,\theta) = \frac{Ke^{-j\theta}C(s,c)G(s,q)}{1+Ke^{-j\theta}C(s,c)G(s,q)}.$$ (3.5)

The characteristic polynomial is $P(s,q,c,k,\theta)$ and

$$P(s,q,c,k,\theta) = \text{the numerator of } [1+ke^{-j\theta}C(s,c)G(s,q)]$$
$$= \sum_{i=0}^{n} d_i(q,c,k,\theta)s^i$$
$$= d_0(q,c,k,\theta) + d_1(q,c,k,\theta)s + \cdots + d_n(q,c,k,\theta)s^n$$ (3.6)

By the use of the parameter space method and robust stability criteria, system stability

performance on GM and PM is analyzed by generating gain and phase boundary curves. For

perturbed control systems in which the parameters of the characteristic polynomial lie within

given intervals, the minimum of all the GM values of the system at the points inside the entire

perturbed region in the parameter space is defined to be the GM of the system. The PM of the

system is defined in the same way.

3.3.1   Parameter Space Method

The parameter space method is a good analytical technique to perform system analysis in

the selected system parameter plane for a control system which is described by its

characteristic polynomial, the roots of which generate stability boundary curves in the

parameter plane. The characteristic polynomial on the $j\omega$-axis $P(j\omega, q, c, k, \theta)$ may be

written into the real part $U(\omega, q, c, k, \theta)$ and the imaginary part $V(\omega, q, c, k, \theta)$.

$$P(j\omega, q, c, k, \theta) = U(\omega, q, c, k, \theta) + jV(\omega, q, c, k, \theta)$$
$$= 0 \qquad , \qquad (3.7)$$

where

$$U(\omega, q, c, k, \theta) = r_0(q, c, k, \theta) + r_1(q, c, k, \theta)\omega + r_2(q, c, k, \theta)\omega^2 + \cdots + r_n(q, c, k, \theta)\omega^n \quad (3.8)$$

and

$$V(\omega, q, c, k, \theta) = i_0(q, c, k, \theta) + i_1(q, c, k, \theta)\omega + i_2(q, c, k, \theta)\omega^2 + \cdots + i_n(q, c, k, \theta)\omega^n \quad (3.9)$$

The equations

$$\begin{cases} U(\omega, q, c, k, \theta) = 0 \\ V(\omega, q, c, k, \theta) = 0 \end{cases} \qquad (3.10)$$

can be solved analytically or numerically for q or c. Gain and phase boundary curves are

generated both in $q-$space from the solutions q for GM and PM analysis and in $c-$space from the solutions c for the controller design under specified conditions.

In the analysis of GM and PM, a fixed controller is used to analyze the system performance, and (3.7)-(3.10) don't depend on c. The gain and phase margins of the perturbed vehicle system will be analyzed geometrically in 2 and 3 dimensions from stability boundary curves.

In controller design, (3.10) can be solved for c with specific ω, k, θ and q in a similar way. Gain and phase boundary curves are developed in the $c-$space according to different gain k and θ, respectively.

3.3.2   Gain Margin Analysis
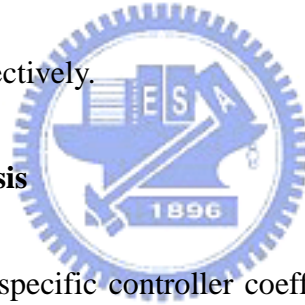
Let $\theta = 0^{\mathrm{O}}$ and c be a specific controller coefficient in Fig. 3.2. Equations (3.7) and (3.10) are rewritten into the forms

$$P(j\omega, q, k) = U(\omega, q, k) + jV(\omega, q, k)$$
$$= 0 \tag{3.11}$$

and

$$\begin{cases} U(\omega, q, k) = 0 \\ V(\omega, q, k) = 0 \end{cases}, \tag{3.12}$$

where

$$U(\omega, q, k) = r_0(q, k) + r_1(q, k)\omega + r_2(q, k)\omega^2 + \cdots + r_n(q, k)\omega^n \tag{3.13}$$

and

$$V(\omega, q, k) = i_0(q, k) + i_1(q, k)\omega + i_2(q, k)\omega^2 + \cdots + i_n(q, k)\omega^n. \qquad (3.14)$$

A gain boundary curve is generated in $q-\text{space}$ from the solutions q of (3.12) by varying

ω for every k. By varying k the curve is approaching to the parameter region $\mathfrak{R}$

gradually and finally intersect with $\mathfrak{R}$. A specific gain k (dB) corresponding to the

boundary curve which is tangent to the parameter perturbed region $\mathfrak{R}$ is defined as the GM

of the perturbed control system. It is also the minimal GM of the system within the entire

region $\mathfrak{R}$. The GM of the control system at a point on one side of a specific gain boundary

curve is greater than that at a point on the boundary curve. But it is less at the points on the

other side.

3.3.3 Phase Margin Analysis
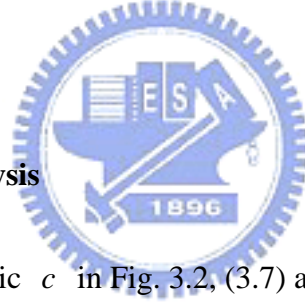
Given $k = 1$ and a specific c in Fig. 3.2, (3.7) and (3.10) are rewritten into the forms

$$\begin{aligned} P(j\omega, q, \theta) &= U(\omega, q, \theta) + jV(\omega, q, \theta) \\ &= 0 \end{aligned} \qquad (3.15)$$

and

$$\begin{cases} U(\omega, q, \theta) = 0 \\ V(\omega, q, \theta) = 0 \end{cases}, \qquad (3.16)$$

where

$$U(\omega, q, \theta) = r_0(q, \theta) + r_1(q, \theta)\omega + r_2(q, \theta)\omega^2 + \cdots + r_n(q, \theta)\omega^n \qquad (3.17)$$

and

$$V(\omega, q, \theta) = i_0(q, \theta) + i_1(q, \theta)\omega + i_2(q, \theta)\omega^2 + \cdots + i_n(q, \theta)\omega^n. \qquad (3.18)$$

Phase boundary curves are developed under the PM specification in a similar way. They are generated in q-space from the solutions q of (3.16) by varying ω for every θ. The PM of the control system is defined as the phase value θ associated with the phase boundary curve which is tangent to the perturbed region $\Re$. It is the minimal PM for the whole system with the parameters inside $\Re$, too. The PM of the control system at a point on one side of a specific phase boundary curve is greater than that at a point on the boundary curve. But it is less at a point on the other side.

3.3.4   Controller Design

The controller design is based on gain-phase boundary curves which are drawn in c-space from the locations of the roots of the polynomial equation (3.10) with respect to different k and θ, and the constant-sensitivity loci which are drawn based on the solutions of the $\left| S_{C_i}^{H(j\omega)} \right|_{s=j\omega} = s_0$ for the controller coefficient c in c-space with respect to the given sensitivity constant s_0. The desired coefficients are determined under the constraints of specified GM, PM and sensitivity. Systems with high stability and low sensitivity are desired.

Based on the discussions mentioned above, the design algorithm is as the followings:

Step 1: Set up user-defined specifications on GM, PM and sensitivity.

Step 2: For every system parameter q at the vertices of the perturbed system parameter region in q-plane, draw the gain boundary curves corresponding to the specified GM and

0dB in c-plane by solving (3.12).

Step 3: For every q at the vertices of the perturbed system parameter region in q-plane, draw the phase boundary curves corresponding to the specified PM and 0° in c-plane by solving (3.16).

Step 4: Sketch the sensitivity constant loci from the solutions of the sensitivity equation $\left|S_{c_i}^{H(j\omega)}\right|_{s=j\omega} = s_0$ for c, given s_0.

Step 5: Determine a gain region in $c-\text{space}$ with the help of the gain boundary curves as in step 2 so that the controller with the coefficients in that region satisfies the specified GM constraints.

Step 6: Determine a phase-region in $c-\text{space}$ with the help of the phase boundary curves as in step 3 so that the controller with the coefficients in that region satisfies the specified PM constraints.

Step 7: Find out the common region of the determined gain and phase ones as in steps 5 and 6. The controller with the coefficients in that region is the desired one satisfying the specified GM and PM conditions.

Step 8: Choose a point in $c-\text{space}$ on a specified sensitivity constant locus which passes through the common region as in step 7. Then the controller coefficient at that point satisfies all the three specified constraints of GM, PM and sensitivity. If no such sensitivity locus exists,

tradeoff has to be made among the three specified conditions.

3.4 An Example and Simulation Results

In this simulation, a Daimler Benz 0305 bus [18] is adopted. Its linearized system with

actuator input δ =steering angle rate, and output y=displacement of front antenna, has the

following transfer function

$$G(s, q_1, q_2) = \frac{609.8q_1^2 q_2 s^2 + 388600 q_1 s + 48280 q_1^2}{s^3 (q_1^2 q_2^2 s^2 + 1077 q_1 q_2 s + 16.8 q_1 q_2 + 270000)}, \qquad (3.19)$$

where the parameter $q_1 = v$ is the bus velocity, and the other parameter $q_2 = \dfrac{m}{u}$.

m: the mass of the bus (tons). u : road friction coefficient (0.5 for wet road, 1 for dry road).
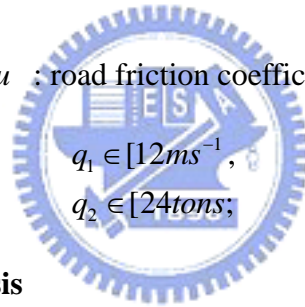
$$\begin{aligned} q_1 &\in [12ms^{-1}, \quad 20ms^{-1}] \\ q_2 &\in [24tons; \quad 32tons] \end{aligned}. \qquad (3.20)$$

3.4.1   GM and PM Analysis

The controller used is taken as given by

$$C(s) = \frac{2344s^2 + 10938s + 9375}{s^3 + 50s^2 + 1250s + 15625} \qquad (3.21)$$

and was determined by Muench [18].

Case 1 : 2D GM/PM Analysis in $q_1 - q_2$ Plane . Consider the system parameter $q = [q_1, q_2]$

with an uncertain parameter region $\mathbb{S}$ as in Fig. 3.3 for studying GM/PM performances.

The $\mathbb{S}$ – parameter region is

$$\begin{cases} 12 \le q_1 \le 20 \\ 24 \le q_2 \le 32 \end{cases} \qquad (3.22)$$

and the closed-loop characteristic polynomials is as in (3.6). By substituting $s = j\omega$ into the

numerator of the above polynomials and by lengthy computation, the coefficients of the real

part polynomial $U(\omega, q, k, \theta)$ with a specific c in (3.8) are

$$
\begin{aligned}
r_0 &= 4.5262 \times 10^8 q_1^2 k \cos(\theta), \\
r_1 &= (3.6431 \times 10^9 q_1 + 5.2808 \times 10^8 q_1^2) \times k \sin(\theta), \\
r_2 &= (-4.2505 \times 10^9 q_1 - 5716875 q_1^2 q_2 - 1.1316 \times 10^8 q_1^2) \times k \cos(\theta), \\
r_3 &= -(6669992.4 q_1^2 q_2 + 9.1087 \times 10^8 q_1) k \sin(\theta), \\
r_4 &= 16828125 q_1 q_2 + 21000 q_1^2 q_2 + 3375 \times 10^5 + 1429371.2 k q_1^2 q_2 \cos(\theta), \qquad (3.23) \\
r_5 &= 0, \\
r_6 &= -1250 q_1^2 q_2^2 - 16.8 q_1^2 q_2 - 53850 q_1 q_2 - 270000, \\
r_7 &= 0, \\
r_8 &= q_1^2 q_2^2.
\end{aligned}
$$

In (3.9), the coefficients of the imaginary part polynomial $V(\omega, q, k, \theta)$ are

$$
\begin{aligned}
i_0 &= -4.5262 \times 10^8 k q_1^2 \sin(\theta), \\
i_1 &= (3.6431 \times 10^9 q_1 + 5.2808 \times 10^8 k q_1^2 \cos(\theta), \\
i_2 &= (4.2505 \times 10^9 q_1 + 5716875 q_1^2 q_2 + 1.1316 \times 10^8 q_1^2) \times k \sin(\theta), \\
i_3 &= -262500 q_1^2 q_2 - 4218750000 - 6669992.4 \times k q_1^2 q_2 k \cos(\theta) \\
&\quad -9.1087 \times 10^8 k q_1 \cos(\theta), \\
i_4 &= -1429371.2 k q_1^2 q_2 \sin(\theta), \qquad\qquad\qquad\qquad (3.24) \\
i_5 &= 15625 q_1^2 q_2^2 + 840 q_1^2 q_2 + 1346250 q_1 q_2 + 135 \times 10^5, \\
i_6 &= 0, \\
i_7 &= -50 q_1^2 q_2^2 - 1077 q_1 q_2, \\
i_8 &= 0.
\end{aligned}
$$

Solve the equations

$$
\begin{cases}
U(\omega, q, k, \theta) = 0 \\
V(\omega, q, k, \theta) = 0
\end{cases}, \qquad (3.25)
$$

for q by varying k and θ, and the stable boundary representation curves for gain and

phase margins are shown as in Figs. 3.4 and 3.5 in the $q_1 - q_2$ plane, respectively. We are

only interested in positive solutions $q_1 > 0$ and $q_2 > 0$ for practical reasons. The GM of the

perturbed control system with the domain region $\mathbb{S}$ is -4.3dB and its PM is 19.336° as seen

in Figs. 3.4 and 3.5, respectively. In general, the specifications on the stability robustness

point of view are $GM \geq 3dB$ and $PM \geq 30^\circ$, which the system with the original controller

(3.21) doesn't satisfy. A new controller is designed in the following section and its

performance is improved significantly.

The gain boundary curves associated with different gains shown in Fig. 3.4 reveal that

the GM of the control system at a point on one side of a specific gain boundary curve is

greater than that at a point on the curve. But it is less at a point on the other side.
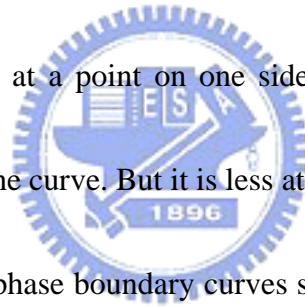
Similarly in Fig. 3.5, the phase boundary curves show that the PM of the control system

at a point on one side of a specific phase boundary curve is greater than that at a point on the

curve. But it is less at a point on the other side. At the point A $((q_1, q_2) = (20, 32))$ in both

Figs.3.4 and 3.5 the system has the minimal GM and PM of all the points within the entire $\mathbb{S}$

region.

Case 2 : 3D GM/PM Analysis in $m - v - u$ Space.

Select $q = [q_1, q_2, q_3] = [m, v, u]$ in the block diagram of the closed system in Fig. 3.2. The

perturbed parameter space $\mathbb{R}$ as in Fig. 3.6 as follows

$$\begin{cases} 24 \le m/u \le 32 \\ 12 \le v \le 20 \\ 0.5 \le u \le 1 \end{cases}.$$

(3.26)

Gain and phase boundary curves in the $m-v-u$ parameter space are generated from

the solutions for q to (3.12) and (3.16), respectively. Those curves corresponding to

different k and θ by varying the frequency ω are shown in Figs. 3.7 and 3.8. A specific

gain k (dB) corresponding to a boundary curve which is tangent to the perturbed region $\mathbb{R}$

at a point on the edge $\overline{EF}$ of $\mathbb{R}$ is defined as the GM of the system. It is also the minimal

GM of the perturbed control system within $\mathbb{R}$. Its PM is defined in the same way. The

system with uncertain parameters within the $\mathbb{R}-space$ has GM=-4.3dB and PM $=19.336^{\circ}$.

3.4.2   Controller Design
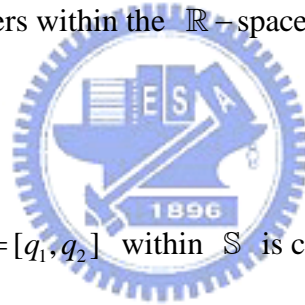
The system parameter $q = [q_1, q_2]$ within $\mathbb{S}$ is considered for the controller design.

Assume the controller to be designed is given as

$$C(s) = \frac{c_2 s^2 + c_1 s + c_0}{s^3 + 50s^2 + 1250s + 15625},$$

(3.27)

where c_0, c_1 and c_2 are the controller coefficients to be designed under the user-specified

constraints and the system parameter domain is within the region $\mathbb{S}$ as in Fig. 3.3. Equation

(3.21) is a special case of (3.27) with $c_0 = 9375$, $c_1 = 10938$ and $c_2 = 2344$.

1) Controller Design for $GM \ge 3dB$ and $PM \ge 30^0$

The design problem of interest is to find all the controller coefficients c_0, c_1 and c_2

that satisfy user-specified conditions of GM, and PM. According to the design steps as above,

27

a coefficient region in $c-\text{space}$ is to be found out by the use of gain and phase boundary curves associated with different k and θ.

By solving (3.10), the coefficients of the real part of the characteristic polynomial $U(\omega,q,c,k,\theta)$ in (3.8) are

$$
\begin{aligned}
r_0 &= 48280c_0q_1^2k\cos(\theta),\\
r_1 &= (388600c_0q_1+48280c_1q_1^2)\times k\sin(\theta),\\
r_2 &= -(388600c_1q_1+609.8c_0q_1^2q_2+48280c_2q_1^2)k\cos(\theta),\\
r_3 &= -(609.8c_1q_1^2q_2+388600c_2q_1)k\sin(\theta),\\
r_4 &= 16828125q_1q_2+21000q_1^2q_2+3375\times10^5,\\
&\quad+609.8q_1^2q_2c_2k\cos(\theta),\\
r_5 &= 0,\\
r_6 &= -1250q_1^2q_2^2-16.8q_1^2q_2-53850q_1q_2-270000,\\
r_7 &= 0,\\
r_8 &= q_1^2q_2^2.
\end{aligned}
\tag{3.28}
$$

The coefficients of the imaginary part of the polynomial $V(\omega,q,c,k,\theta)$ in (3.9) are

$$
\begin{aligned}
i_0 &= -48280c_0q_1^2k\sin(\theta),\\
i_1 &= (388600c_0q_1+48280c_1q_1^2)\times k\cos(\theta),\\
i_2 &= (388600c_1q_1+609.8c_0q_1^2q_2+48280c_2q_1^2)\\
&\quad\times k\sin(\theta),\\
i_3 &= -262500q_1^2q_2-4218750000-609.8c_1q_1^2\\
&\quad\times q_2k\cos(\theta)-388600c_2q_1k\cos(\theta),\\
i_4 &= -609.8c_2q_1^2q_2k\sin(\theta),\\
i_5 &= 15625q_1^2q_2^2+840q_1^2q_2+1346250q_1q_2\\
&\quad+135\times10^5,\\
i_6 &= 0,\\
i_7 &= -50q_1^2q_2^2-1077q_1q_2,\\
i_8 &= 0,
\end{aligned}
\tag{3.29}
$$

where $q=(q_1,q_2)$ is a specific point within $\mathbb{S}$ and (3.10) is rewritten into the following one.

$$\begin{cases} U(\omega,c,k,\theta)=0 \\ V(\omega,c,k,\theta)=0 \end{cases}. \tag{3.30}$$

Two controller coefficients of c_0, c_1 and c_2 are chosen as adjustable parameters and the other one is fixed for this design. By solving (3.30), a shaded area is determined by gain and phase boundary curves from the solutions for (c_0, c_1) pairs with $c_2 = 2344$ under GM and PM specifications given as above in $c_0 - c_1$ plane, as shown in Fig. 3.9.

For the vertices A,B,C and D of $\mathbb{S}$ as in Fig. 3.3, stability boundary curves are plotted to determine the qualified shaded area. Two gain boundary curves are obtained associated with $k = 0\text{dB}$ and 3dB given $\theta = 0^\circ$ for each vertex. In a similar way, two phase boundary ones are also generated corresponding to $\theta = 0^\circ$ and $\theta = 30^\circ$ with $k = 1$.

Let $c_0 = 9375$. Select c_1 and c_2 as adjustable coefficients. Gain and phase stability curves are generated in the same way in $c_1 - c_2$ plane and the shaded region within which c_1 and c_2 satisfy specified constraints is founded, as shown in Fig. 3.10.

In Figs. 3.9 and 3.10 the desired controller coefficients can be chosen according to the specified gain and phase constraints. The controller coefficient is selected from the above shaded region so that the whole system with the chosen controller has the desired specifications. With the designed controller, Tables 3.1 and 3.2 show the GM and PM of the system operating at several points within the region $\mathbb{S}$. The Bode plots of magnitude and phase are provided in Figs. 3.11 and 3.12.

2) The constant-sensitivity loci

Compute $S_{c_i}^{H(s,c)}$ for $i = 0,1,2$ by substituting Eqs. (3.1)-(3.3) and (3.27) into (3.4) as the followings:

$$S_{c_0}^{H(s,c)} = \frac{c_0 D_c(s) D_G(s)}{N_c(s,c)(D_c(s)D_G(s) + N_c(s,c)N_G(s))}, \tag{3.31}$$

$$S_{c_1}^{H(s,c)} = \frac{s c_1 D_c(s) D_G(s)}{N_c(s,c)(D_c(s)D_G(s) + N_c(s,c)N_G(s))}, \tag{3.32}$$

and

$$S_{c_2}^{H(s,c)} = \frac{s^2 c_2 D_c(s) D_G(s)}{N_c(s,c)(D_c(s)D_G(s) + N_c(s,c)N_G(s))}. \tag{3.33}$$

Let $c_2 = 2344$. The constant-sensitivity loci in Fig. 3.13, are plotted in $c_0 - c_1$ plane from the solutions to the equality $\left| S_{c_i}^{H(j\omega)} \right|_{s=j\omega} = s_{01}$, where s_{01} is a specified sensitivity constant and $i = 0,1$. Gain and phase boundary curves in Fig. 3.11 are plotted with the system operating at the point A in the region $\mathbb{S}$. If the specified sensitivity locus passes through the shaded area as in Fig. 3.9, a point on the locus is chosen and the controller at this location in $c_0 - c_1$ plane is desired. The point Q_1 on the sensitivity locus with the constraint $\left| S_{c_0}^{H(j\omega)} \right|_{s=j\omega} = \left| S_{c_1}^{H(j\omega)} \right|_{s=j\omega} = 0.001$ is chosen for the controller with $c_0 = 180.7, c_1 = 18.83$ and $c_2 = 2344$. The system at the point A in $\mathbb{S}$ has GM=4.13dB and $PM = 37.1^\circ$. Its performance on stability has been improved.

Let $c_0 = 9375$. The solutions to the equality $\left| S_{c_i}^{H(j\omega)} \right|_{s=j\omega} = s_{12}$, where $i = 1,2$, give a plot of the constant-sensitivity loci in $c_1 - c_2$ plane, as shown in Fig. 3.14. Choose the point

Q_2 in Fig. 3.14 with $c_1 = 410$ and $c_1 = 6000$ on the sensitivity locus $\left|S_{C_1}^{H(j\omega)}\right|_{s=j\omega}\Big| = $

$\left|S_{C_2}^{H(j\omega)}\right|_{s=j\omega}\Big| = 10^{-7}$ and the system operating at the point B in $\mathbb{S}$ has GM=6.08dB and

$PM = 31^{\circ}$.

3.5 Concluding Remarks

This chapter introduces a new method on performance analysis and controller design by

frequency domain approach for a perturbed control system. Based on the parameter space

method and robust stability criteria, the performances of a perturbed vehicle control system

are analyzed in graphical portrayals. With the help of gain and phase boundary curves

resulting from the roots of the system characteristic polynomial equation, the GM and PM

have been obtained. In controller design, a methodology is proposed for portraying regions in

a selected controller coefficient plane so that the designed controller is to meet the specified

requirements on GM, PM and sensitivity. Simulation results demonstrate the objectives have

been achieved as desired.
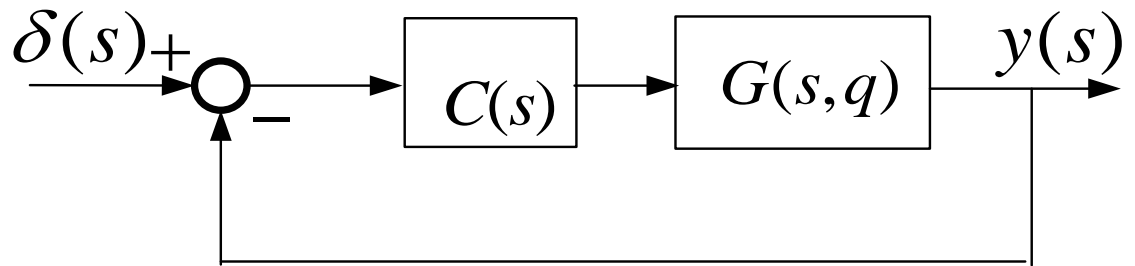
Fig. 3.1 The perturbed vehicle control system with uncertain parameter q.
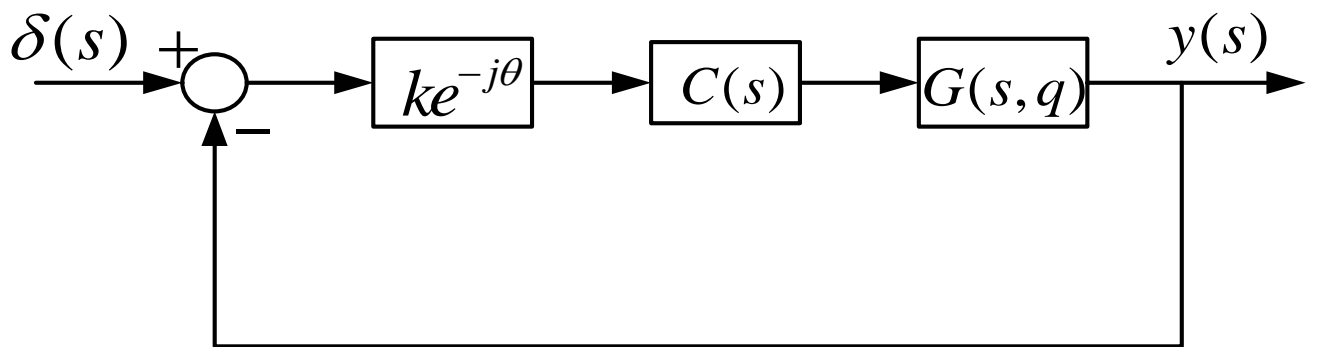
Fig. 3.2 The perturbed vehicle control system in series with a gain-phase tester.
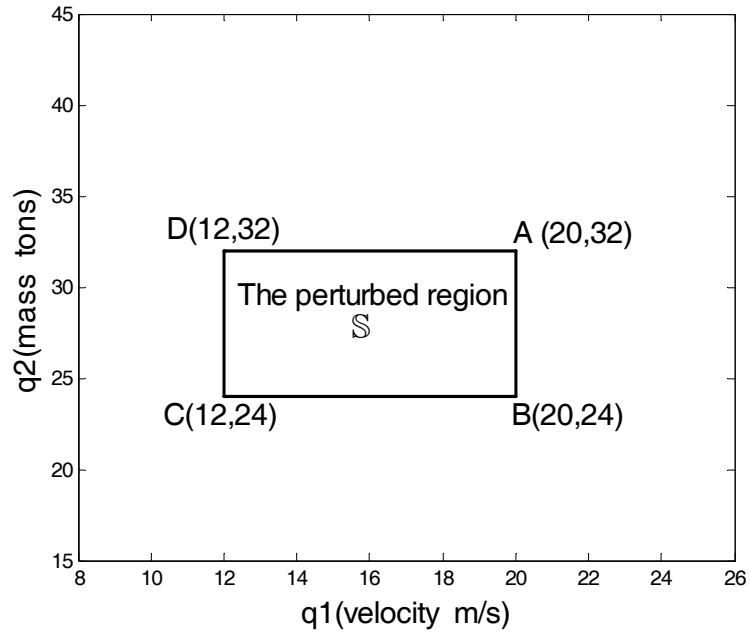
Fig. 3.3 The parameter domain region $\mathbb{S}$ in q1-q2 plane.
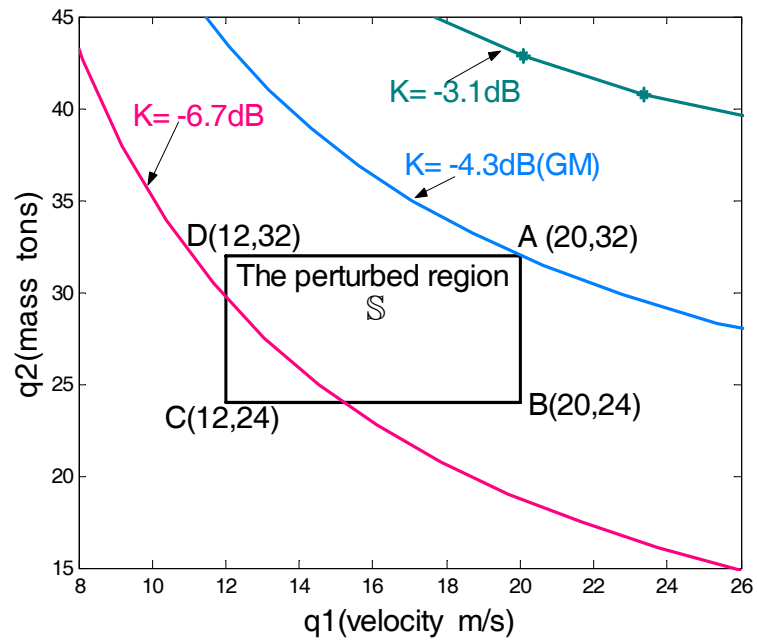
Fig. 3.4 Gain boundary curves by varying k with GM=-4.3dB.
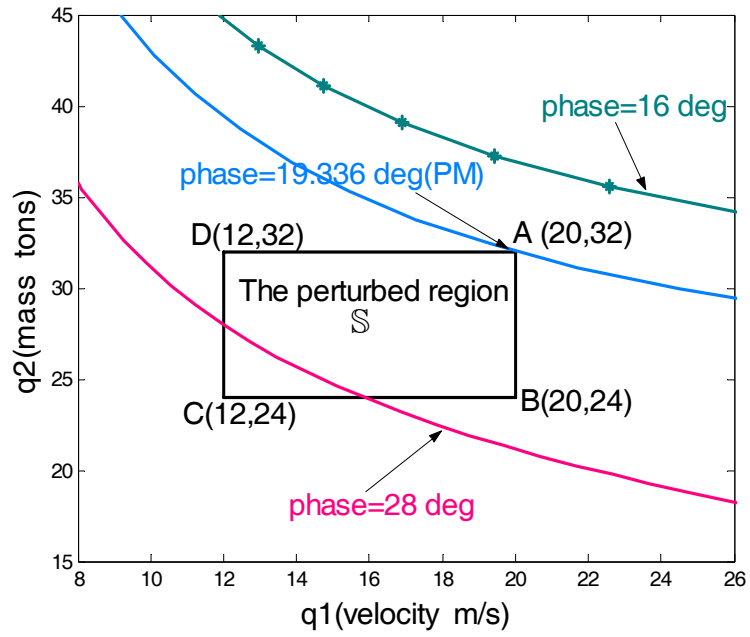
Fig. 3.5 Phase boundary curves by varying θ with PM=19.336°.
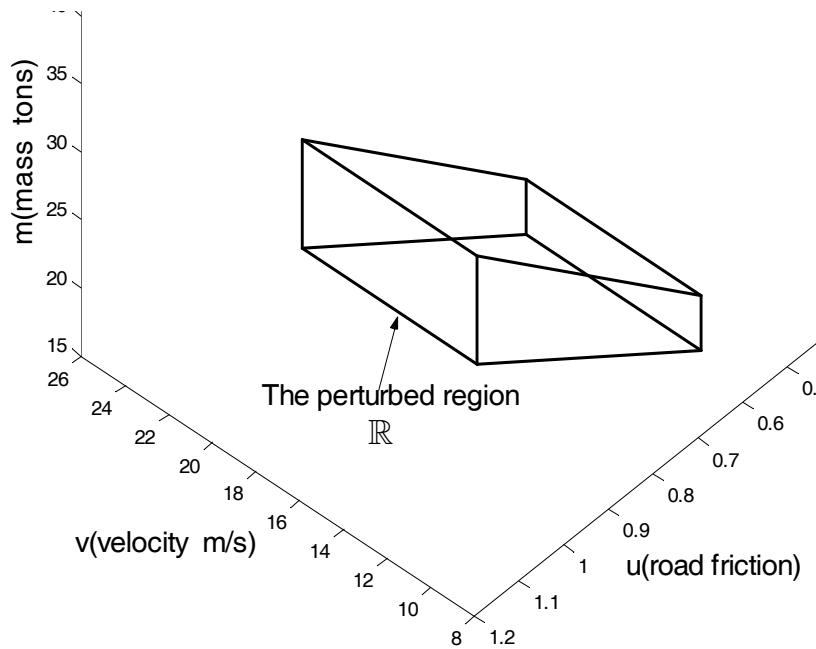
Fig. 3.6 The 3D perturbed parameter space $\mathbb{R}$ with 3 uncertain parameters m, v and u.
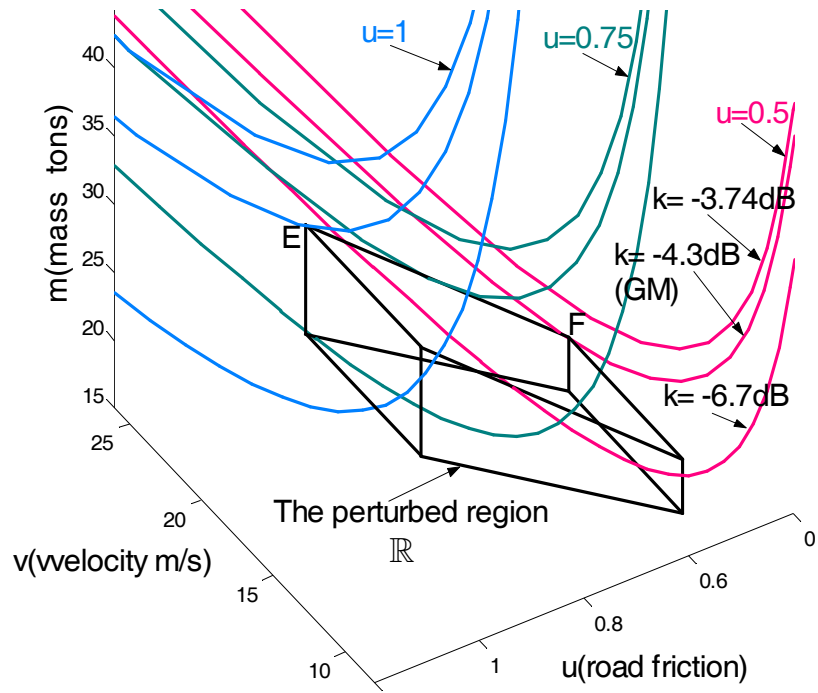
Fig. 3.7 Gain boundary curves in 3D with by varying k with GM=-4.3dB.
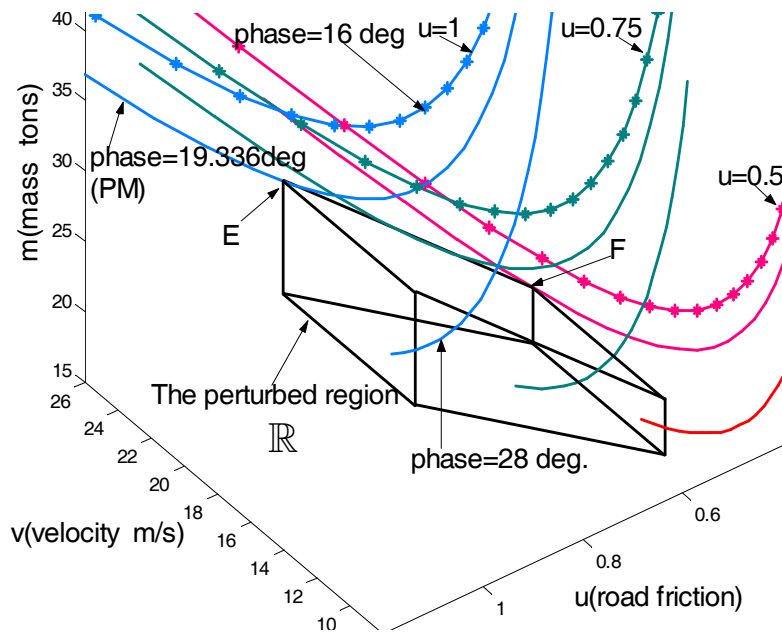
Fig. 3.8 Phase boundary curves in 3D with PM=19.336° .
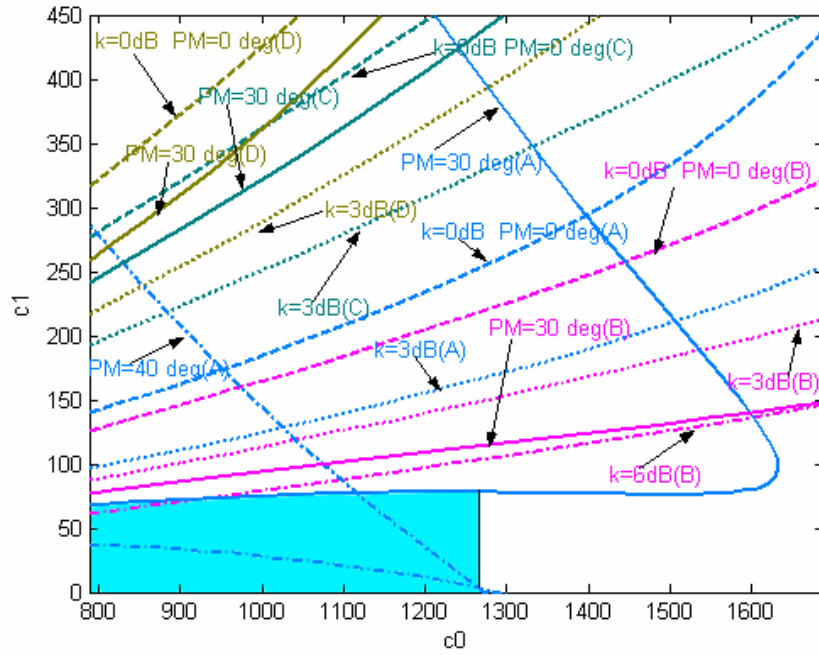
Fig. 3.9 The controller coefficient region for $GM \geq 3dB$ and $PM \geq 30^0$ as indicated in the shaded area in $c_0 - c_1$ plane with $c_2 = 2344$.
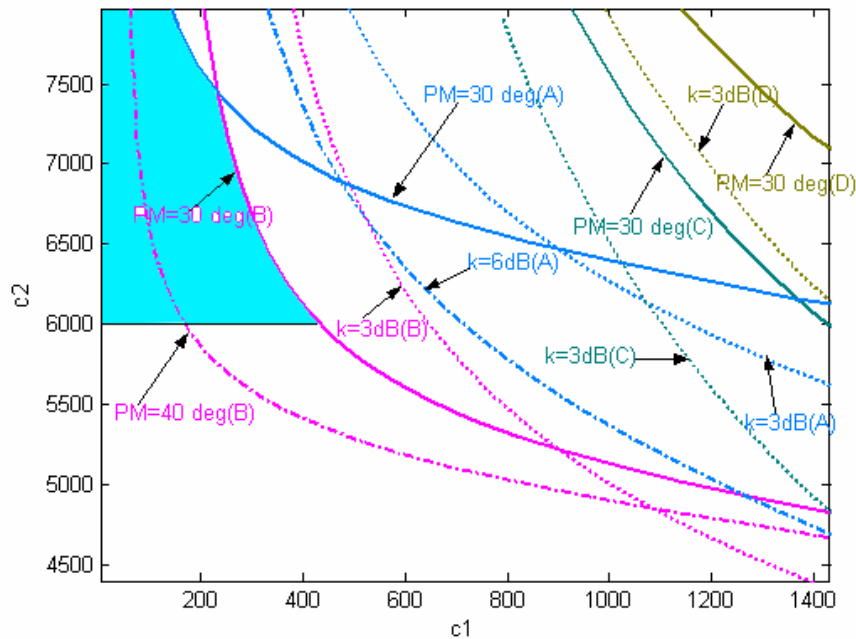
Fig. 3.10 The controller coefficient region for $GM \geq 3dB$ and $PM \geq 30^0$ as indicated in the shaded area in $c_1 - c_2$ plane with $c_0 = 9375$

Table 3.1 The GM and PM of the system with $c_2 = 2344$

$c_0 = 180.7, \quad c_1 = 18.83$		
Location inside $\mathbb{S}$	GM	PM
Point A(20,32)	4.13dB	37.1^0
Point B(20,24)	3.18dB	35^0
Point C(12,24)	9.76dB	67.1^0
Point D(12,32)	10.3dB	64.5^0
Point(17,30)	5.73dB	46.5^0

Table 3.2 The GM and PM of the system with $c_o = 9375$

$c_1 = 410, \quad c_2 = 6000$		
Location inside $\mathbb{S}$	GM	PM
Point A(20,32)	8.48dB	57^0
Point B(20,24)	6.08dB	31^0
Point C(12,24)	6.29dB	55.7^0
Point D(12,32)	8.64dB	67.7^0
Point(14,26)	6.87dB	57.9^0
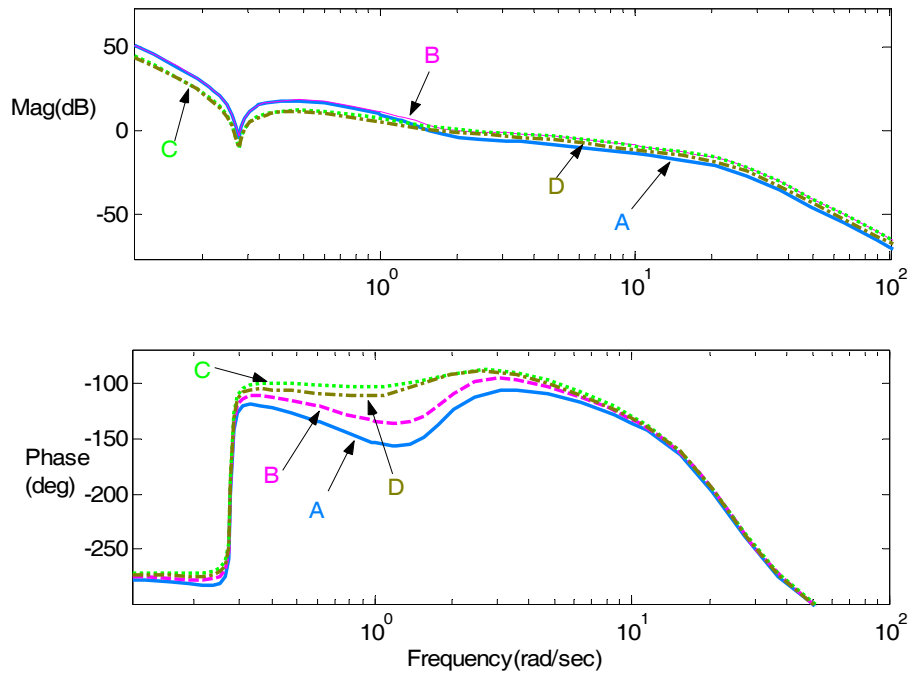
Fig. 3.11 Bode plots of magnitude and phase with $c_0 = 180.7, c_1 = 18.83$ and $c_2 = 2344$ at four vertices of the perturbed region $\mathbb{S}$.
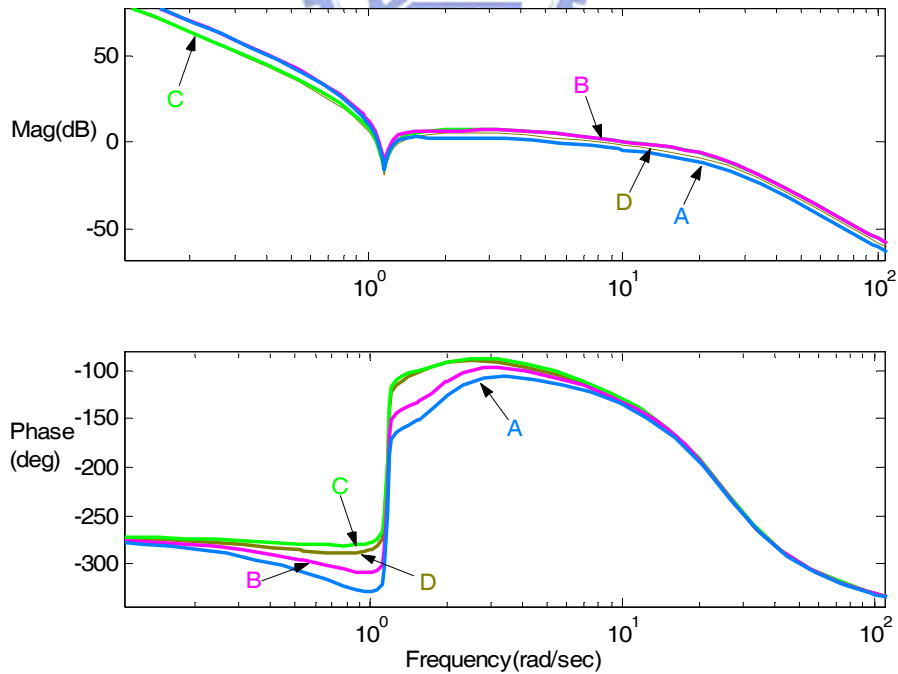
Fig. 3.12 Bode plots of magnitude and phase with $c_0 = 9375, c_1 = 410$ and $c_2 = 6000$ at four vertices of the perturbed region $\mathbb{S}$.
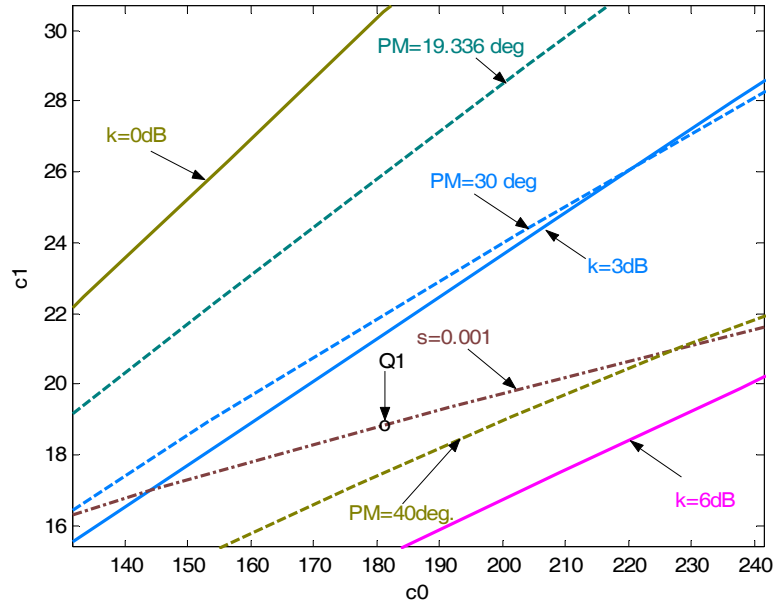
Fig. 3.13 A chosen controller at the point Q_1 with $c_0 = 180.7, c_1 = 18.83$ and $c_2 = 2344$ based on the control system at the vertex A $(20,32)$ of the perturbed parameter region $\mathbb{S}$.
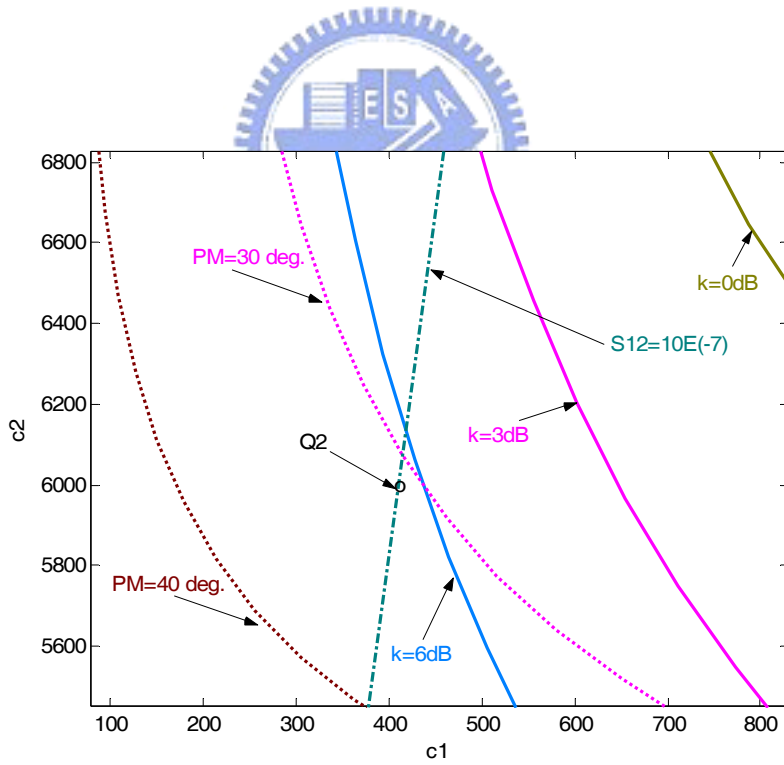
Fig. 3.14 A chosen controller at the point Q_2 with $c_0 = 9375, c_1 = 410$ and $c_2 = 6000$ based on the control system at the vertex B $(20,24)$ of the perturbed parameter region $\mathbb{S}$.

Chapter 4

Gain-Phase Margin Analysis of Nonlinear Perturbed Vehicle Control Systems for Limit Cycle Prediction

4.1 Overview

The chapter is concentrated on the subject of predicting the limit cycle of a nonlinear perturbed vehicle control system under specific gain-phase margin (GM/PM) constraints. A gain-phase margin tester is included in series with the perturbed vehicle system to perform the GM/PM analysis. GM and PM are determined from the gain and phase values of the gain-phase margin tester at which the undesirable limit cycle caused by nonlinearities of the system with uncertain parameters occurs. The nonlinear elements in this system are linearized by the method of the conventional describing functions. By the use of the parameter space method, describing function method and stability criteria, a concise and clear way will be given in the geometric representation in the parameter coordinate to show the gain-phase margin performances for a nonlinear vehicle control system with uncertain parameters which are the velocity, road friction and car weight of the plant. The proposed method is applied to a

car model and simulation results are presented to illustrate the GM and PM performances for

the limit cycle.

4.2 Preliminary

Consider a perturbed closed control system with a gain-phase margin tester ($ke^{-j\theta}$) and it

is assumed that there exist r nonlinear elements inside the perturbed nonlinear vehicle

system as illustrated in Fig. 4.1. The closed loop feedback system has the transfer function

given by

$$H(s,q,K,\theta,N_1,...,N_m,...,N_r)$$
$$= \frac{Ke^{-j\theta}G(s,q,N_1,...,N_m,...,N_r)}{1+Ke^{-j\theta}G(s,q,N_1,...,N_m,...,N_r)}, \tag{4.1}$$

where $G(s,q,N_1,...,N_m,...,N_r)$ is the open loop transfer function with the describing

function $N_i(i=1,2,....r)$ of nonlinear parts. q is a perturbed vector with $q=[q_1,q_2,\cdots q_n]$

$\in \Re$, and $\Re$ is a set of allowable domain space of the system plant parameters. N_i is a

complex function of the input amplitude and frequency to the $i-\text{th}$ nonlinear element and

$$N_i = N_{iR} + jN_{iI}. \tag{4.2}$$

The closed characteristic polynomial equation is written into

$$P(s,q,k,\theta,N_{1R},N_{1I}...,N_{rR},N_{rI})$$
$$= \text{the numerator of } [1+ke^{-j\theta}G(s,q,N_{1R},N_{1I}...,N_{mR},N_{mI},...,N_{rR},N_{rI})] \tag{4.3}$$
$$= 0,$$

and

$$P(s, q, k, \theta, N_{1R}, N_{1I}, ..., N_{rR}, N_{rI})$$

$$= \sum_{i=0}^{n} d_i(q, k, \theta, N_{1R}, N_{1I}, ..., N_{rR}, N_{rI}) s^i$$

$$= d_0(q, k, \theta, N_{1R}, N_{1I}, ..., N_{rR}, N_{rI}) + d_1(q, k, \theta, N_1, ..., N_r) s + \cdots \qquad (4.4)$$

$$+ d_n(q, k, \theta, N_{1R}, N_{1I}, ..., N_{rR}, N_{rI}) s^n$$

$$= U(j\omega, q, k, \theta, N_{1R}, N_{1I}, ..., N_{rR}, N_{rI}) + jV(\omega, q, k, \theta, N_{1R}, N_{1I}, ..., N_{rR}, N_{rI}).$$

Assume $d_i(q, k, \theta, N_{1R}, N_{1I}, ..., N_{rR}, N_{rI})$ is a real continuous function.

The equation

$$\begin{cases} U(\omega, q, k, \theta, N_{1R}, N_{1I}, ..., N_{rR}, N_{rI}) = 0 \\ V(\omega, q, k, \theta, N_{1R}, N_{1I}, ..., N_{rR}, N_{rI}) = 0 \end{cases} \qquad (4.5)$$

can be solved for q given specific ω, k, θ and A analytically or numerically. Gain

boundary curves will be generated from these q values in the q-parameter space by

varying ω given specific k and A with $\theta = 0^\circ$. Phase boundary curves will be

generated by varying ω given specific θ and A with $k = 1$. The gain and phase margins

of the perturbed vehicle system for the limit cycle will be analyzed from boundary curves

geometrically in 2 and 3 dimensions. A specific gain or phase value corresponding to the

boundary curve which is tangent to the perturbed parameter region is defined as the gain or

phase margin for predicting the limit cycles, respectively.

4.3 Problem Solution

The block diagram of the perturbed vehicle system with nonlinear elements N_1 and

N_2 is illustrated as in Fig. 4.2. The transfer function of a vehicle control model used for the

investigations with the input δ_F =the front wheel deflection angle and the output r =the yaw

rate around the vertical axis is [22].

$$G_{r/\delta_F}(s) = \frac{1.415\times10^{10}\mu^2 v + 1.382\times10^8 \mu v^2 s}{(4\times10^{10}\mu^2 + 56500 m\mu v^2) + 587225 m\mu v s + 1.9932 m^2 v^2 s^2} \qquad (4.6)$$

The steering actuator is modeled as a linear dynamic system with the actuator bandwidth

$\omega_a = 4\pi$,

$$G_a(s) = \frac{\omega_a^2}{s^2 + \sqrt{2}\omega_a s + \omega_a^2}. \qquad (4.7)$$

The closed loop characteristic polynomial is

$$\begin{aligned}
&P(s,q,k,\theta,N_1,N_2)\\
&= \text{the numerator of } [1 + ke^{-j\theta}G(s,q,N_1,N_2)]\\
&= 0.
\end{aligned} \qquad (4.8)$$

Assume that the input signals to the nonlinear elements N_1 and N_2 are $x_1(t) = A_1 \sin \omega t$

and $x_2(t) = A_2 \sin \omega t$, where N_1 is the describing function of a saturation element and

$$N_1(A_1) = \begin{cases} 1 & \text{for } A_1 < R_1 \\ X(A_1) & \text{for } A_1 > R_1 \end{cases},$$
$$X(A_1) = \frac{2}{\pi}\left[\sin^{-1}(\frac{R_1}{A_1}) + \frac{R_1}{A_1}\sqrt{1-(\frac{R_1}{A_1})^2} \right], \qquad (4.9)$$

and N_2 is that of a rate limiter element,

$$N_2(A_2) = \frac{4R_2}{\pi A_2}. \qquad (4.10)$$

Assume $x_1(t)$ is chosen as the reference input signal. A_2 can be expressed as a

function of A_1 and ω, when A_1 and ω are known. By (4.4) the coefficients of the real

part of the characteristic polynomial are

$$r_o = 1.415 \times 10^{10} k N_1 N_2 \omega_a^2 m \mu^2 v \cos(\theta),$$

$$r_1 = 75500 k N_1 N_2 \omega_a^2 m^2 \mu v^2 \sin(\theta),$$

$$r_2 = -(4.00145 \times 10^{10} m \mu^2 + 56500 m^2 \mu v^2)(\omega_a^2 + \sqrt{2} N_2 \omega_a)$$
$$\quad -587225 m^2 \mu v N_2 \omega_a^2,$$

$$r_3 = 0,$$

$$r_4 = 4.00145 \times 10^{10} m \mu^2 + 56500 m^2 \mu v^2$$
$$\quad + 587225 m^2 \mu v (\sqrt{2} \omega_a + N_2) + 1.9932 m^3 v^2 \times$$
$$\quad (\omega_a^2 + \sqrt{2} N_2 \omega_a),$$

$$r_5 = 0,$$

$$r_6 = -1.9932 m^3 v^2.$$

$$(4.11)$$

The coefficients of the imaginary part of the polynomial are

$$i_o = -1.415 \times 10^{10} k N_1 N_2 m \mu^2 v \omega_a^2 \sin(\theta),$$

$$i_1 = (4.00445 \times 10^{10} m \mu^2 + 56500 m^2 \mu v^2) N^2 \omega_a^2 +$$
$$\quad 75500 k N_1 N_2 m^2 \mu v^2 \omega_a^2 \cos(\theta),$$

$$i_2 = 0,$$

$$i_3 = -(4.00445 \times 10^{10} m \mu^2 - 56500 m^2 \mu v^2)(\sqrt{2} \omega_a + N_2)$$
$$\quad + 587225 m^2 \mu v (\omega_a^2 + \sqrt{2} N_2 \omega_a) - 1.9932 m^3 v^2 N_2 \omega_a^2,$$

$$i_4 = 0,$$

$$i_5 = 587225 m^2 \mu v + 1.9932 m^3 v^2 (\sqrt{2} \omega_a + N_2),$$

$$i_6 = 0.$$

$$(4.12)$$

4.3.1 Case 1: Gain-phase Margin Analysis in $v - \mu$ Plane

Consider the perturbed parameter $q = [q_1, q_2] = [v, \mu]$ for analyzing gain and phase margins. The system parameter $q_1 = v$ is the vehicle velocity, $q_2 = \mu$ is the road friction, and the car weight is $m = 1830 Kg$. The perturbed parameter region Q in the $v - \mu$ plane is illustrated in Fig. 4.3.

$$Q \text{ region} \begin{cases} \dfrac{7v + 30}{650} \leq \mu \leq 1 \\ 5 \leq v \leq 70 \end{cases} \qquad (4.13)$$

Gain margin is the minimal gain $k_{\min}$ (dB) of the gain-phase tester ($ke^{-j\theta}$) with $\theta = 0^\circ$ such

that a limit cycle with a specific amplitude is generated and the gain boundary curve

corresponding to $k_{\min}$ which is tangent to the perturbed parameter region Q is observed.

Phase margin is the minimal phase $\theta_{\min}$ of the gain-phase tester ($ke^{-j\theta}$) with $k=1$ such that

a limit cycle is generated and the phase boundary curve corresponding to $\theta_{\min}$ which is

tangent to the perturbed parameter region Q is observed.

Based on the previous analysis, some limit cycle loci with the gain $k=1$ and the phase

$\theta = 0^\circ$ of the gain-phase tester are depicted as in Fig. 4.3. In Figs. 4.4 and 4.5, the gain and

phase boundary curves are generated. It is obviously observed that the gain and phase margins

of the perturbed vehicle system are 0.772dB and 9.4126 deg, respectively. The time

response shown in Fig. 4.6 has demonstrated the consistence with the results in Fig. 4.4 and

Fig. 4.5.

4.3.2   Case2: Gain-phase Margin Analysis in $v - \mu - m$ Space

The perturbed parameter $q = [q_1, q_2, q_3] = [m, \mu, v]$ are considered for analyzing gain and

phase margins. The system parameter $q_1 = m$ is the car mass, $q_1 = \mu$ is the road friction and

$q_3 = v$ is the vehicle velocity.

The perturbed parameter space $\mathbb{R}$ in the $\mu - v - m$ coordinate is illustrated in Fig. 4.7.

$$\mathbb{R} \quad \text{region} \begin{cases} \dfrac{7v+30}{650} \leq \mu \leq 1 \\ 5 \leq v \leq 70 \\ 1730\text{K}g \leq m \leq 2330\text{K}g \end{cases} \tag{4.14}$$

In the similar way, the 3D gain and phase boundary curves corresponding to different vehicle

weights are also shown in Figs.4.7 and 4.8. For example, the gain and phase margins for the vehicle weight equal to 1730Kg are 0.922 dB and 12.12 deg, respectively.

4.4 Concluding Remarks

In this chapter, some effective techniques are presented involving describing function methods, parameter space methods, and a gain-phase margin tester. The methods in previous studies are extended to analyze GM and PM performances of a vehicle plant with three parameters in a perturbed space for predicting the limit cycle occurred by using a gain-phase tester and 3D graphical representations are also provided to give a concise and clear way to study the robustness stability of the system with nonlinearities. The method proposed here would further be extended to be used in a system with more than three perturbed parameters.
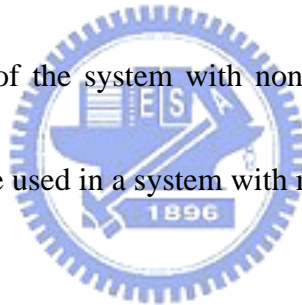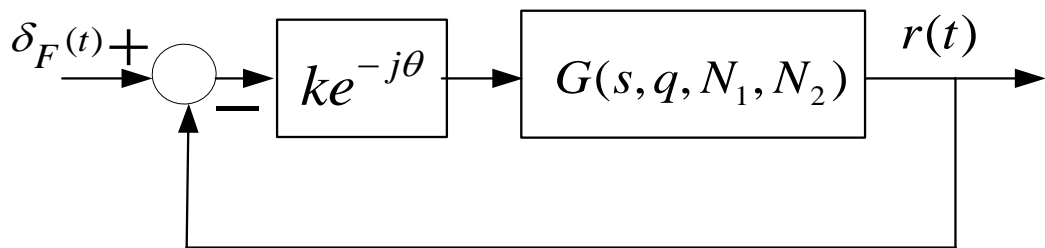
Fig. 4.1 The block diagram of a nonlinear control system with a gain-phase margin tester.
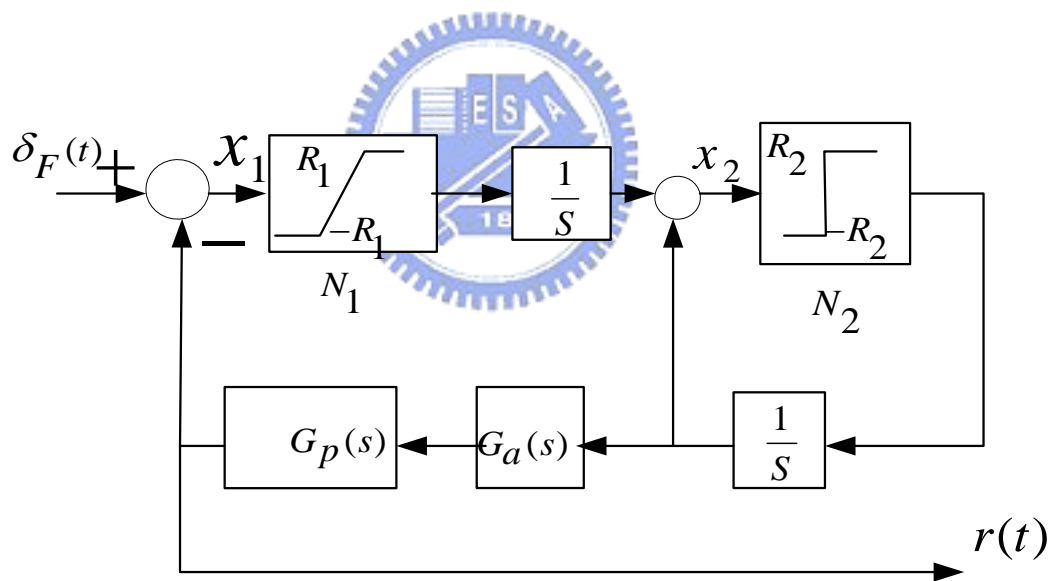
Fig. 4.2 The block diagram of the perturbed nonlinear system.
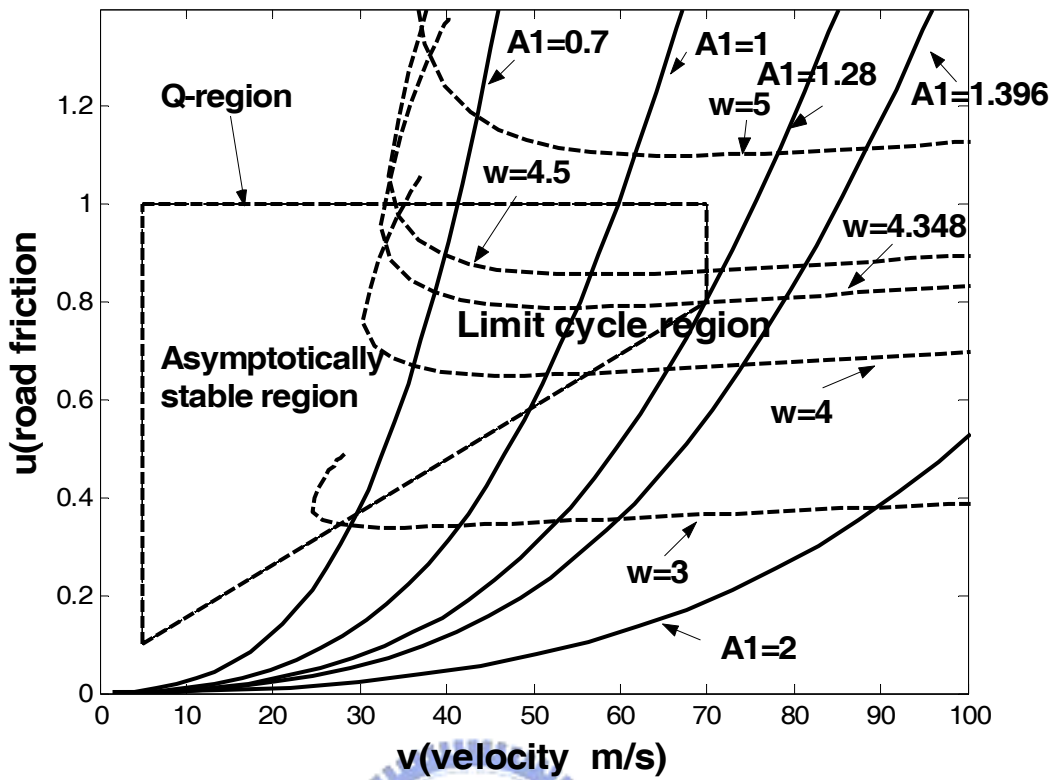
Fig. 4.3 The limit cycle loci in the parameter plane.
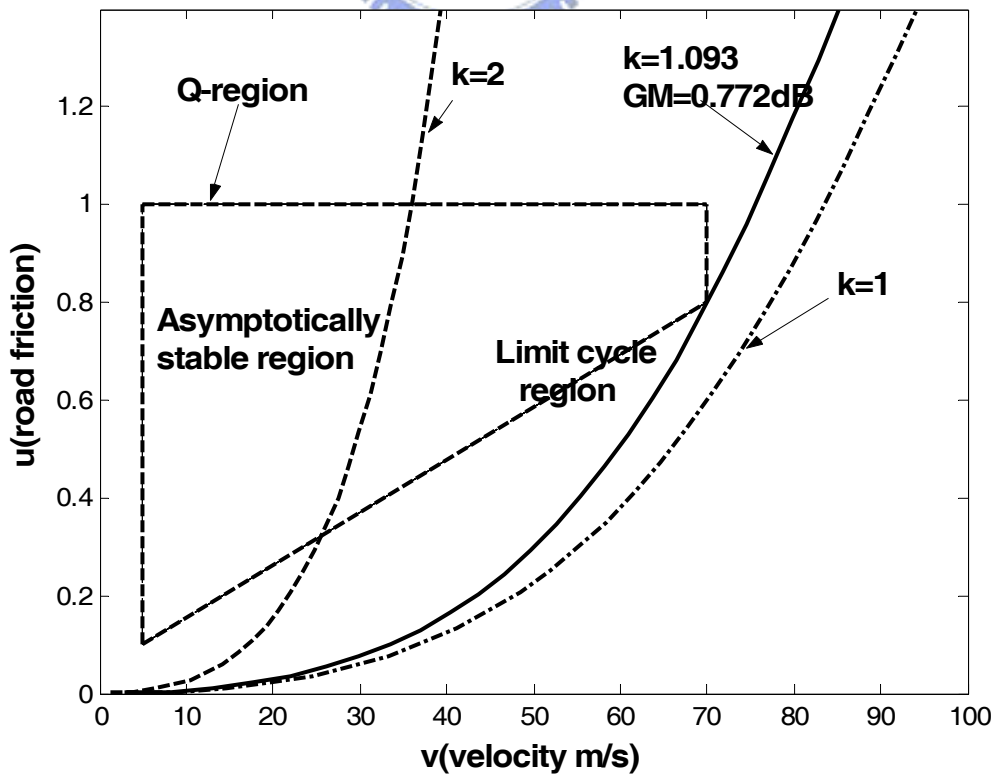
Fig. 4.4 Gain boundary curves with the vehicle weight 1830Kg (GM=0.772dB).
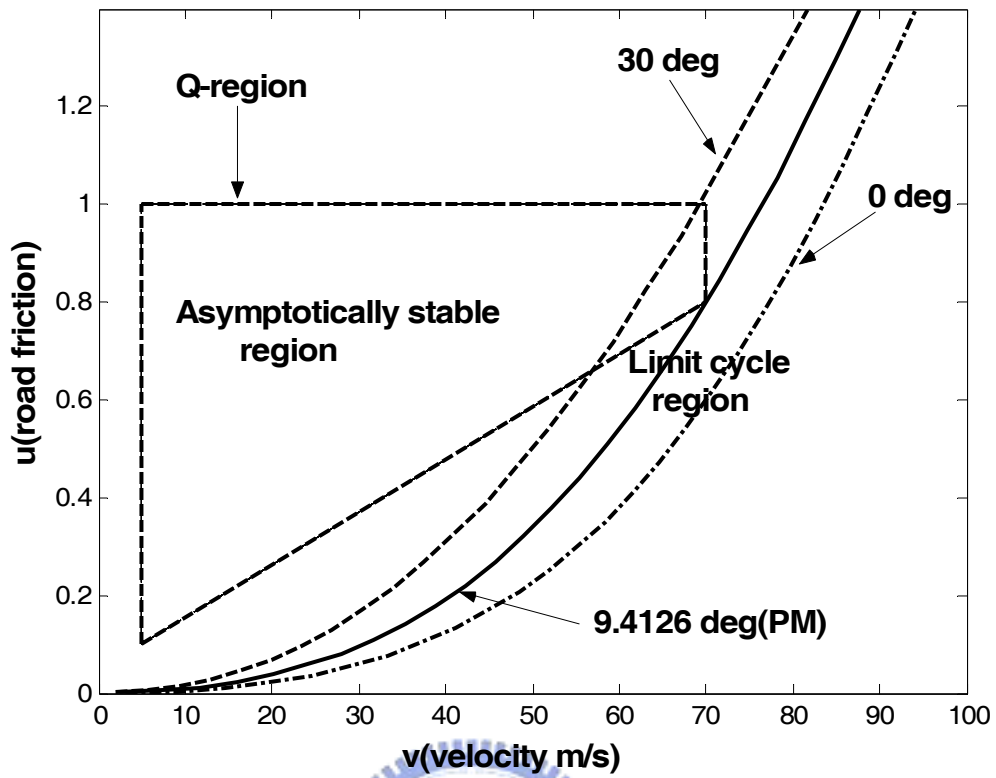
Fig. 4.5 Phase boundary curves with the vehicle weight 1830Kg (PM=9.4126 deg).
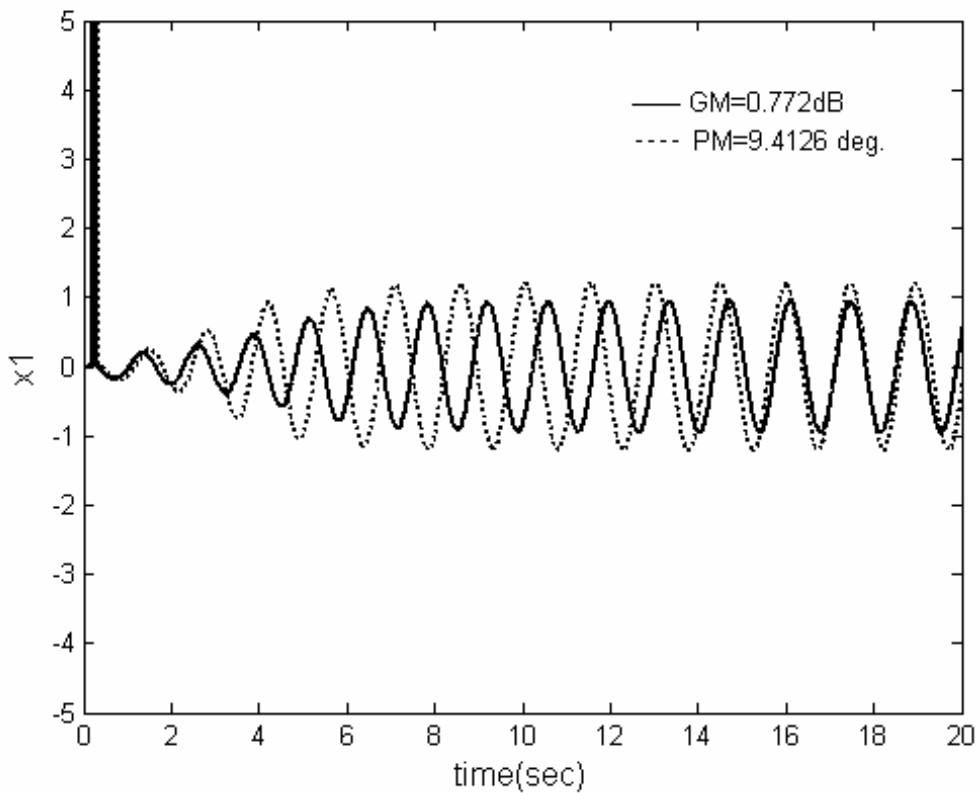
Fig. 4.6 Simulation results in time-domain with increased gain and phase.
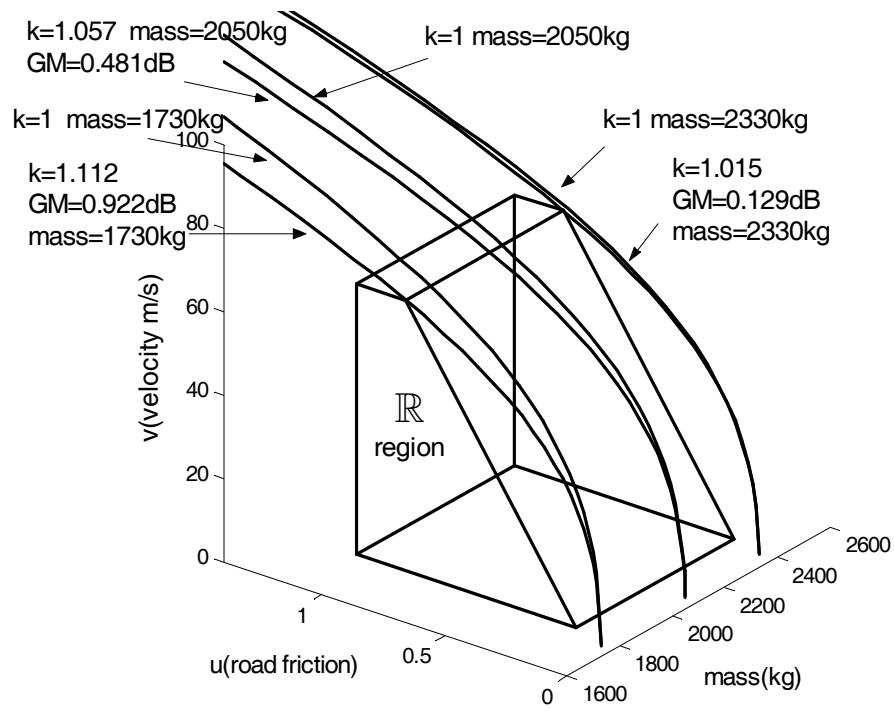
Fig. 4.7 Gain boundary curves in 3-dimension.
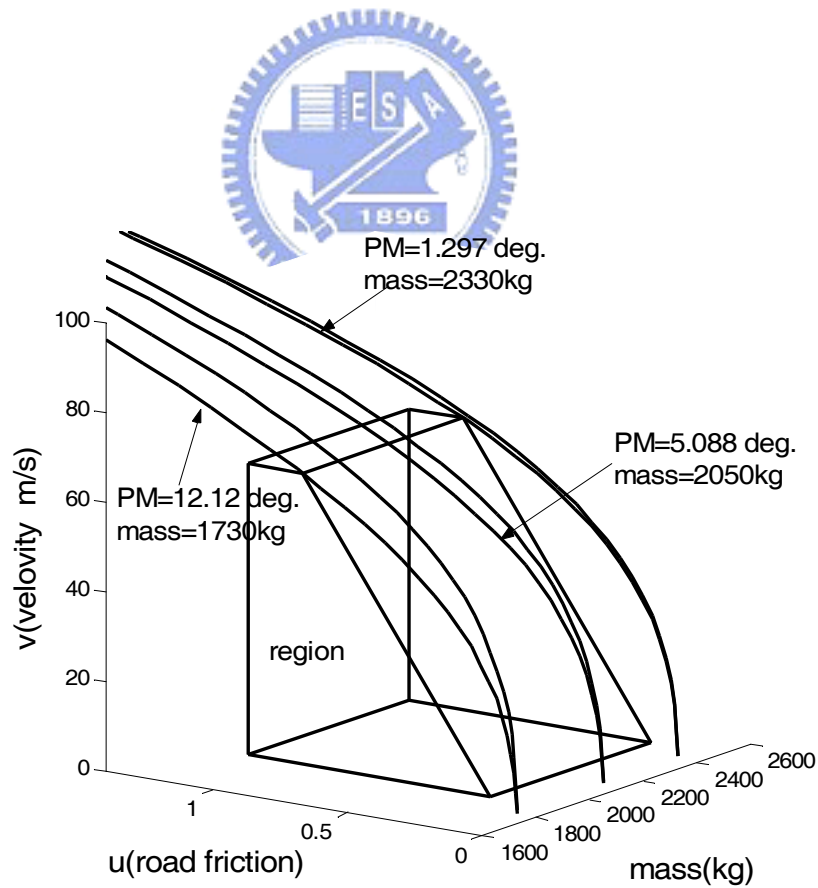
Fig. 4.8 Phase boundary curves in 3-dimension.

Chapter 5

Parameter Plane Analysis of Fuzzy Vehicle Steering Control Systems

5.1 Overview

The main purpose of this chapter is to analyze the robust stability for a fuzzy vehicle steering control system. In general, fuzzy control system is a nonlinear control system. Therefore, the fuzzy controller may be linearized by the use of describing function first. After then, parameter plane method is then applied to determine the conditions of robust stability when the system has perturbed or adjustable parameters. A systematic procedure is proposed to solve this problem. The effects of plant parameters and control factors are both considered here. Furthermore, the problem of relative stability by using a gain-phase margin tester is also addressed. The limit cycles provided by a static fuzzy controller can be easily suppressed if the control factors are chosen properly. Simulation results show the efficiency of our approach.

5.2 Vehicle Model

Fig. 5.1 shows the single track vehicle model and the related symbols are listed in Table 5.1. The equations of motion are [22]

$$\begin{bmatrix} mv(\dot{\beta}+r) \\ ml_fl_r\dot{r} \end{bmatrix} = \begin{bmatrix} F_f + F_r \\ F_fl_f - F_rl_r \end{bmatrix} \tag{5.1}$$

The tire force can be expressed as

$$F_f(\alpha_f) = \mu c_{f0}\alpha_f, \quad F_r(\alpha_r) = \mu c_{r0}\alpha_r \tag{5.2}$$

with the tire cornering stiffness c_{f0}, c_{r0}, the road adhesion factor μ and the tire side slip angles

$$\alpha_f = \delta_f - (\beta + \frac{l_f}{v}r), \alpha_r = -(\beta - \frac{l_r}{v}r) \tag{5.3}$$

The state equation of vehicle dynamics with β and r can be represented as

$$\begin{bmatrix} \dot{\beta} \\ \dot{r} \end{bmatrix} = \begin{bmatrix} -\dfrac{\mu(c_{f0}+c_{r0})}{mv} & -1+\dfrac{\mu(c_{r0}l_r-c_{f0}l_f)}{mv^2} \\ \dfrac{\mu(c_{r0}l_r-c_{f0}l_f)}{ml_fl_r} & -\mu\dfrac{(c_{f0}l_f^2+c_{r0}l_r^2)}{ml_fl_rv} \end{bmatrix}\begin{bmatrix} \beta \\ r \end{bmatrix} + \begin{bmatrix} \dfrac{\mu c_{f0}}{mv} \\ \dfrac{\mu c_{f0}}{ml_r} \end{bmatrix}\delta_f \tag{5.4}$$

Hence, the transfer function from δ_f to r is

$$G_{r/\delta_f} = \frac{c_{f0}ml_f\mu v^2 s + c_{f0}c_{r0}l\mu^2 v}{l_fl_rm^2v^2s^2 + l(c_{r0}l_r+c_{f0}l_f)m\mu vs + c_{f0}c_{r0}l^2\mu^2 + (c_{r0}l_r-c_{f0}l_f)m\mu v^2} \tag{5.5}$$

The numerical data are listed in Table 5.2. According to the above analysis of a single track vehicle model, the transfer function from the input of front deflection angle δ_f to the output of yaw rate r can be obtained as

$$G_{r/\delta_f}(s,\mu,v) = \frac{(1.382\times10^8\mu v^2 s + 1.415\times10^{10}\mu^2 v)}{6.675\times10^6 v^2 s^2 + 1.08\times10^9 \mu vs + (1.034\times10^8 \mu v^2 + 4\times10^{10}\mu^2)} \tag{5.6}$$

The operating range Q of the uncertain parameters μ and v is depicted in Fig. 5.2.

In addition, the steering actuator is modeled as

$$G_a(s) = \frac{\omega_a^2}{s^2 + \sqrt{2}\omega_a s + \omega_a^2} \tag{5.7}$$
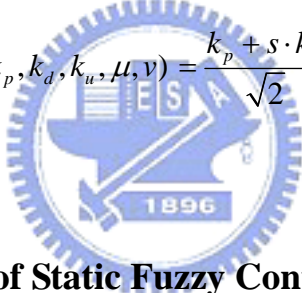
where $\omega_a = 4\pi$.

In our study, a fuzzy vehicle control system is presented in Fig. 5.3. The open loop transfer function $G_O(s)$ is defined as

$$G_O(s,\mu,v) = G_a(s)G_{r/\delta_f}(s,\mu,v) \tag{5.8}$$

The control factors k_p, k_d and k_u can be determined by the designer. By transferring Fig. 5.3 to Fig. 5.4, the overall open loop transfer function can be obtained as

$$G(s,k_p,k_d,k_u,\mu,v) = \frac{k_p + s \cdot k_d}{\sqrt{2}} \cdot \frac{k_u}{s} \cdot G_O(s,\mu,v) \tag{5.9}$$

5.3 Describing Function of Static Fuzzy Controller

The describing function N_1 of static fuzzy controller shown in Fig. 5.4 can be obtained, which depends only on the amplitude of A and is independent of the frequency of ω, and can be expressed as follows [32]:

$$
\begin{aligned}
N_1 &\underline{\underline{\Delta}} N_1(A) \\
&= \frac{4}{\pi A} \sum_{i=0}^{n} \{ \frac{\Delta u_i A}{2\Delta \Phi_i} ((\delta_{i+1} - \sin \delta_{i+1} \cos \delta_{i+1}) - (\delta_i - \sin \delta_i \cos \delta_i)) \\
&\quad + \frac{1}{\Delta \Phi_i} \cdot (\Phi_i u_{i+1} - \Phi_{i+1} u_i)(\cos \delta_{i+1} - \cos \delta_i) \},
\end{aligned} \tag{5.10}
$$

where n satisfies $\Phi_n \leq A < \Phi_{n+1}$, $n > 0$, and varies with A; new variables $\{\delta_i\}$ are defined to be the angles where the input sinusoidal signal $x = A \sin \delta$ intersects the centers

of fuzzy membership functions (Φ_i's) as follows:

$$\delta_0 = 0,$$

$$\delta_i = \sin^{-1}\left(\frac{\Phi_i}{A}\right), \ \left(i = 1, \cdots, n, \ 0 < \delta_i < \frac{\pi}{2}\right), \tag{5.11}$$

$$\delta_{n+1} = \frac{\pi}{2}.$$

The detail definitions of n and δ_i's are visualized in [32].

5.4 Stability Analysis of Fuzzy Vehicle Control Systems

If the gain-phase margin tester $Ke^{-j\theta}$ is added in the open loop of Fig. 5.4, the closed

loop transfer function is

$$\frac{Ke^{-j\theta}N_1G(s,k_p,k_d,k_u,\mu,v)}{1 + Ke^{-j\theta}N_1G(s,k_p,k_d,k_u,\mu,v)} = 0 \tag{5.12}$$

Case 1: *Perturbed Plant Parameters*

Arrange (5.12), the following characteristic equation is obtained.

$$f(s,k_p,k_d,k_u,\mu,v,K,\theta) = C_4\mu^2 + C_3v^2 + C_2\mu v + C_1\mu^2 v + C_0\mu v^2 = 0 \tag{5.13}$$

where

$$C_0 = 1.4621 \times 10^8 s(s^2 + 17.7688s + 157.9137)$$
$$+ 2.1818 \times 10^{10} Ke^{-j\theta}N_1k_u s(k_p + k_d s)$$
$$C_1 = 2.2345 \times 10^{12} Ke^{-j\theta}N_1k_u(k_p + k_d s)$$
$$C_2 = 1.5271 \times 10^9 s^2(s^2 + 17.7668s + 157.9137)$$
$$C_3 = 9.4384 \times 10^6 s^3(s^2 + 17.7668s + 157.9137)$$
$$C_4 = 5.656 \times 10^{10} s(s^2 + 17.7668s + 157.9137)$$

$$\tag{5.14}$$

Let $s = j\omega$, $K = 0\,\text{dB}$ and $\theta = 0°$. Equation (5.13) is divided into two stability equations with real part X_R and imaginary part X_I of characteristic equation, one has

$$f(j\omega, k_p, k_d, k_u, \mu, v) = X_R + jX_I = 0 \qquad (5.15)$$

where

$$
\begin{aligned}
X_R =\ & -1.0064 \times 10^{12}\,\omega^2\mu^2 + 1.6776 \times 10^{8}\,\omega^4 v^2 + (1.5179 \times 10^{9}\,\omega^4 \\
& -2.3999 \times 10^{11}\,\omega^2)\mu v + 2.2345 \times 10^{12}\, N_1 k_p k_u \mu^2 v - (2.5986 \\
& \times 10^{9}\,\omega^2 + 2.1818 \times 10^{10}\, N_1 k_d k_u \omega^2)\mu v^2, \\
X_I =\ & (8.9429 \times 10^{12}\,\omega - 5.656 \times 10^{10}\,\omega^3)\mu^2 + (9.4399 \times 10^{6}\,\omega^5 \\
& -1.4907 \times 10^{9}\,\omega^3)v^2 - 2.7008 \times 10^{10}\,\omega^3 \mu v + 2.2345 \\
& \times 10^{12}\, N_1 k_d k_u \omega\mu^2 v + (2.3091 \times 10^{10}\,\omega - 1.4621 \times 10^{8}\,\omega^3 + \\
& 2.1818 \times 10^{10}\, N_1 k_p k_u \omega)\mu v^2.
\end{aligned}
\qquad (5.16)
$$

In order to obtain the solution of μ and v, the following equation is solved

$$\begin{cases} X_R = 0 \\ X_I = 0 \end{cases}, \qquad (5.17)$$

when k_p, k_d, k_u, N_1 are fixed and ω is changed from 0 to ∞. As the amplitude A is also changed, the solutions of μ and v called limit cycle loci can be displayed in the parameter plane.

Case 2: Control Factors

After some simple manipulations, the characteristic equation of (5.12) can be obtained as

$$f(s, k_p, k_d, k_u, \mu, v, K, \theta) = U \cdot k_p + V \cdot k_d + W = 0 \qquad (5.18)$$

where

$$U = Ke^{-j\theta} N_1 k_u (2.1818 \times 10^{10}\,\mu v^2 s + 2.2345 \times 10^{12}\,\mu^2 v),$$

$$V = Ke^{-j\theta}N_1k_u s(2.1818\times10^{10}\,\mu v^2 s + 2.2345\times10^{12}\,\mu^2 v)$$
$$W = 1.414s(s^2 + 17.7688s + 157.9137)(6.675\times10^6 v^2 s^2 + 1.0746\times10^9\,\mu vs \quad (5.19)$$
$$+4.0045\times10^{10}\,\mu^2 + 1.034\times10^8\,\mu v^2)$$

Let $s = j\omega$, $K = 0\,\text{dB}$ and $\theta = 0^\circ$. Equation (5.18) is divided into two stability equations

with real part and imaginary part of characteristic equation

$$f(j\omega, k_p, k_d, k_u, \mu, v) = X_R + jX_I = 0, \tag{5.20}$$

where

$$X_R = U_1 \cdot k_p + V_1 \cdot k_d + W_1 = 0, \tag{5.21}$$

and

$$X_I = U_2 \cdot k_p + V_2 \cdot k_d + W_2 = 0. \tag{5.22}$$

Therefore, k_p and k_d are solved from (5.21) and (5.22) when μ, v, k_u, N_1 are fixed

and ω is changed from 0 to ∞, one has

$$k_p = \frac{V_1 \cdot W_2 - V_2 \cdot W_1}{U_1 \cdot V_2 - U_2 \cdot V_1}, \tag{5.23}$$

and

$$k_d = \frac{W_1 \cdot U_2 - W_2 \cdot U_1}{U_1 \cdot V_2 - U_2 \cdot V_1} \tag{5.24}$$

Case 3: Gain-phase Margin Analysis

The gain-phase margin tester can be expressed as

$$Ke^{-j\theta} = K\cos\theta - jK\sin\theta = K_R - jK_I \tag{5.25}$$

where

$$K_R = K\cos\theta, \tag{5.26}$$

56

and

$$K_I = K \sin \theta . \qquad (5.27)$$

It is noted that $K = \sqrt{K_R^2 + K_I^2}$ and $\theta = \tan^{-1}(\frac{K_I}{K_R})$.

Then, the characteristic equation can be written as

$$f(s, k_p, k_d, k_u, \mu, v, K_R, K_I) = U \cdot K_R + V \cdot K_I + W = 0 \qquad (5.28)$$

where

$$
\begin{aligned}
U &= N_1 k_u (2.1818 \times 10^{10} \mu v^2 s + 2.2345 \times 10^{12} \mu^2 v)(k_p + k_d s) \\
V &= (-j) N_1 k_u (2.1818 \times 10^{10} \mu v^2 s + 2.2345 \times 10^{12} \mu^2 v)(k_p + k_d s) \\
W &= 1.414 s(s^2 + 17.7688 s + 157.9137)(6.675 \times 10^6 v^2 s^2 \\
&\quad + 1.0746 \times 10^9 \mu v s + 4.0045 \times 10^{10} \mu^2 + 1.034 \times 10^8 \mu v^2)
\end{aligned}
\qquad (5.29)
$$

Let $s = j\omega$, (5.28) is divided into two stability equations with real part and imaginary part of

characteristic equation

$$f(j\omega, k_p, k_d, k_u, \mu, v, K_R, K_I) = X_R + jX_I = 0, \qquad (5.30)$$

where

$$X_R = U_1 \cdot K_R + V_1 \cdot K_I + W_1 = 0, \qquad (5.31)$$

and

$$X_I = U_2 \cdot K_R + V_2 \cdot K_I + W_2 = 0. \qquad (5.32)$$

Therefore, K_R and K_I are solved from (5.31) and (5.32) when k_p, k_d, μ, v, k_u, N_1

are fixed and ω is changed from 0 to ∞, one has

$$K_R = \frac{V_1 \cdot W_2 - V_2 \cdot W_1}{U_1 \cdot V_2 - U_2 \cdot V_1}, \qquad (5.33)$$

and

$$K_I = \frac{W_1 \cdot U_2 - W_2 \cdot U_1}{U_1 \cdot V_2 - U_2 \cdot V_1},$$ (5.34)

5.5 Simulation Results

In our work, five fuzzy rules and parameters are adopted and listed in Tables 5.3 and 5.4, respectively. Fig. 5.5 shows the premise triangle membership functions of fuzzy controller. The consequent parts are singletons. Fig. 5.6 shows the control surface of fuzzy controller.

If $k_p = 0.2$, $k_d = 0.3$ and $k_u = 0.2$ are selected first, (5.14) can be solved when A is fixed and ω is changed from 0 to ∞. Fig. 5.7 shows the stability boundary and some limit cycle loci in the μ-ν parameter plane. Two stability regions including asymptotically stable and limit cycle are divided. In order to verify the accuracy of Fig. 5.7, four operating points Q1-Q3 (limit cycle region) and Q4 (asymptotically stable region) are illustrated for testing. Fig. 5.8 shows the time responses of input signal $x(t)$. It is obvious that the results shown in Fig. 5.8 consist with the predicted results in Fig. 5.7. For examples, if Q1($\mu = 1$ and $\nu = 70$) is chosen, the limit cycle occurs and the amplitude is 0.0465. Besides, if Q4 ($\mu = 1$ and $\nu = 5$) is chosen, the system is stable and no limit cycle happens. On the other hand, if $k_p = 0.1$, $k_d = 0.27$ and $k_u = 0.1$ are selected, Fig. 5.9 shows the stability boundary. We can find that no limit cycle will occur in the overall operating region Q.

If $k_u = 0.2$, $\mu = 1$ and $\nu = 70$ are selected, (5.19) and (5.20) can be solved in the

k_p-k_d parameter plane when A is fixed and ω is changed from 0 to ∞. Fig. 5.10 shows the stability boundary and some limit cycle loci. Four testing points Q5-Q8 are illustrated.

If Q8 ($k_p = 0.1$, $k_d = 0.1$, $k_u = 0.2$, $\mu = 1$, $v = 70$) in Fig. 5.10 is selected, (5.23) and (5.24) can be solved in the K_R-K_I parameter plane when A is fixed and ω is changed from 0 to ∞. Because Q8 is in asymptotically stable region, the gain-phase margin tester can be viewed as a compensator to generate the limit cycle (from stable region to limit cycle region). For example, if $A = 0.05$ is expected, the related gain margin (Q9: GM $= 3.2$, $\theta = 0°$) and phase margin (Q10: PM $= 46.6°$, $K = 1$) to generate limit cycles can be easily obtained in Fig. 5.11. On the other hand, when the original system is in limit cycle region like Q5-Q7, the related gain margin and phase margin to suppress limit cycle could be also obtained in the parameter plane.

5.6 Concluding Remarks

Based on the parameter plane approach, the complete stability analysis of a fuzzy vehicle steering control system is proposed in this chapter. A systematic procedure is presented to deal with this problem. In addition, the effects of control factor and gain-phase margins are also considered. Simulation results show that more information can be obtained by this approach.
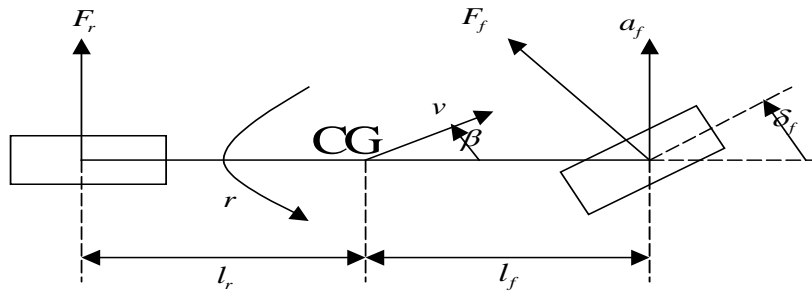
Fig. 5.1 Single track vehicle model.

Table 5.1 Vehicle system quantities

F_f, F_r	lateral wheel force at front and rear wheel
r	yaw rate
β	side slip angle at center of gravity (CG)
v	velocity
a_f	lateral acceleration
l_f, l_r	distance from front and rear axis to CG
$l = l_f + l_r$	wheelbase
δ_f	front wheel steering angle
m	mass

Table5.2Vehicle system parameters

c_{f0}	5000 N/rad
c_{ro}	100000 N/rad
m	1830Kg
l_f	1.51 m
l_r	1.32 m
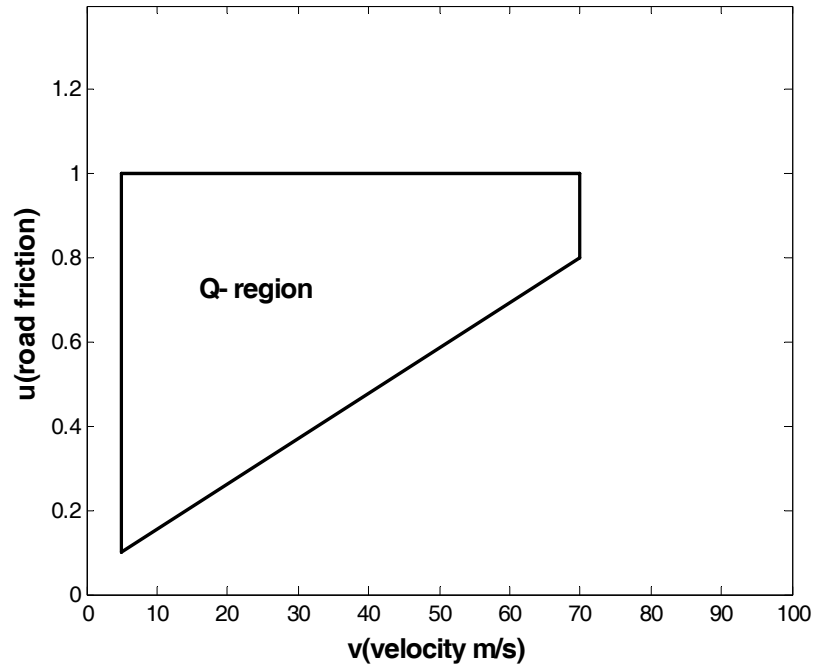
Fig. 5.2 Operating Range.
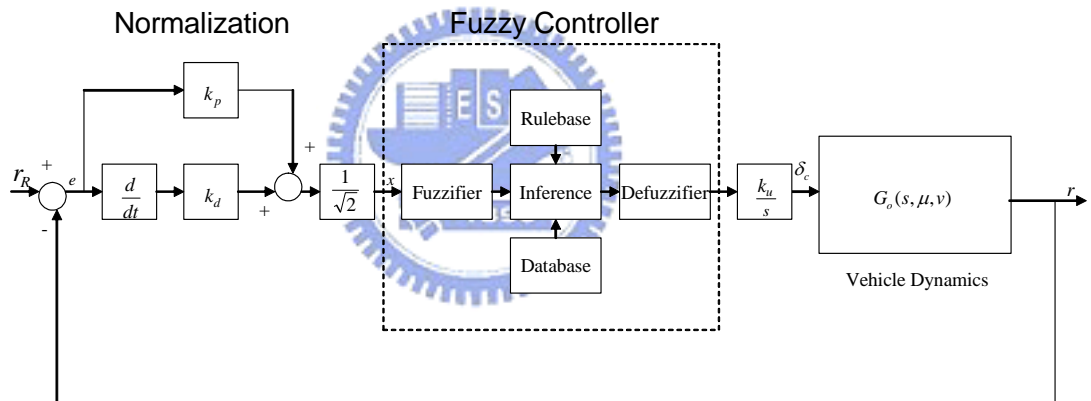
Fig. 5.3 Block diagram of a fuzzy vehicle control system.
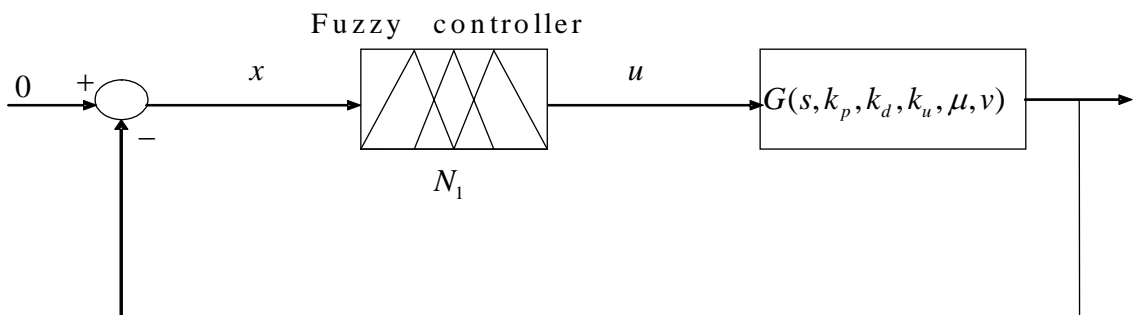
Fig. 5.4 Block diagram of a fuzzy vehicle control system.

Table 5.3 Rules of fuzzy controller

e	NBE	NSE	ZRE	PSE	PBE
u	NBU	NSU	ZRU	PSU	PBU

Table 5.4 Parameters of fuzzy controller

	nbe	nse	zre	pse	pbe
e	-1	-0.02	0	0.02	1
	nbu	nsu	zru	psu	pbu
u	-1	-0.7	0	0.7	1
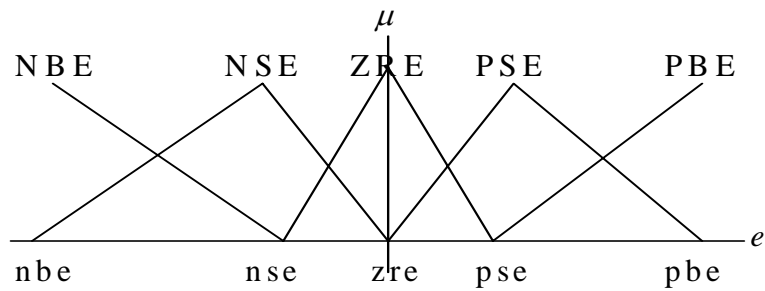
Fig. 5.5 Membership functions of fuzzy controller.
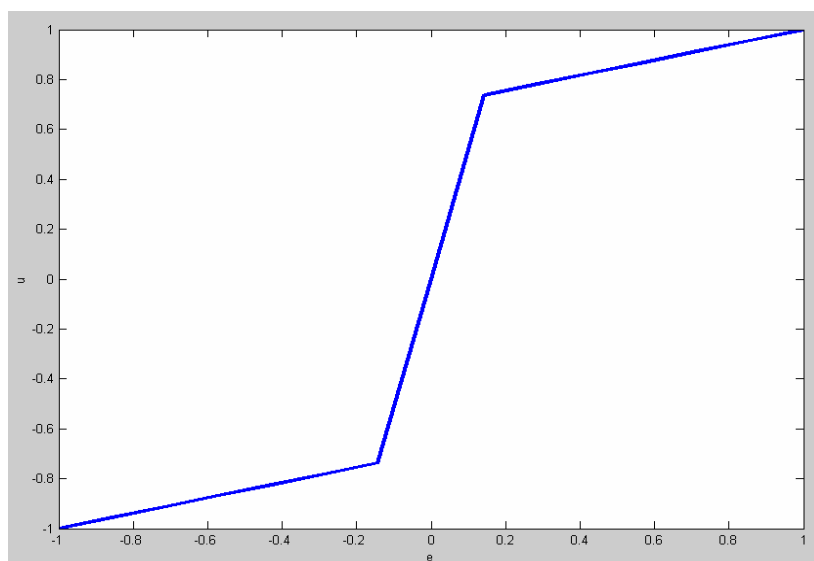
Fig. 5.6 Control surface.
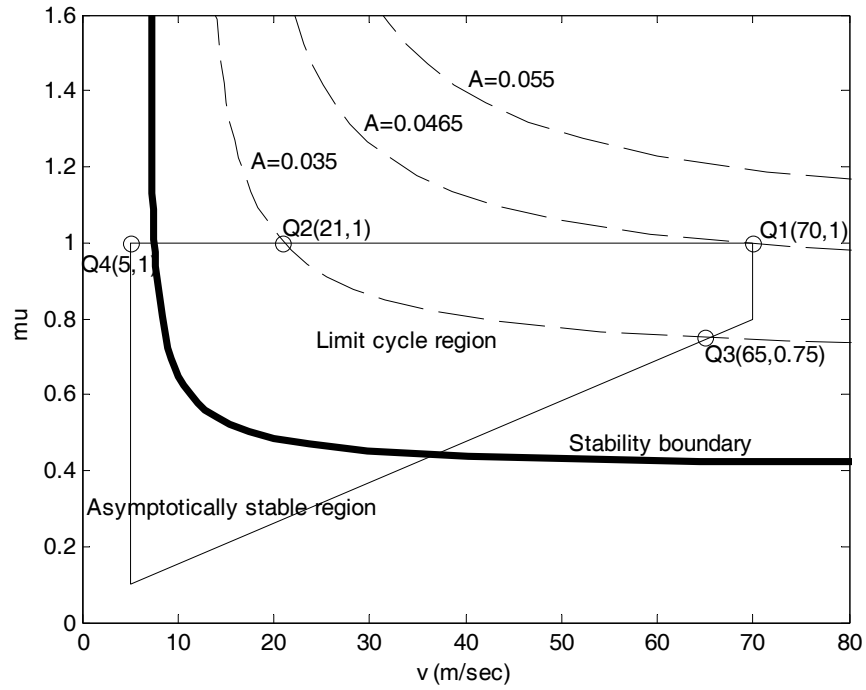
Fig. 5.7 Limit cycle loci.
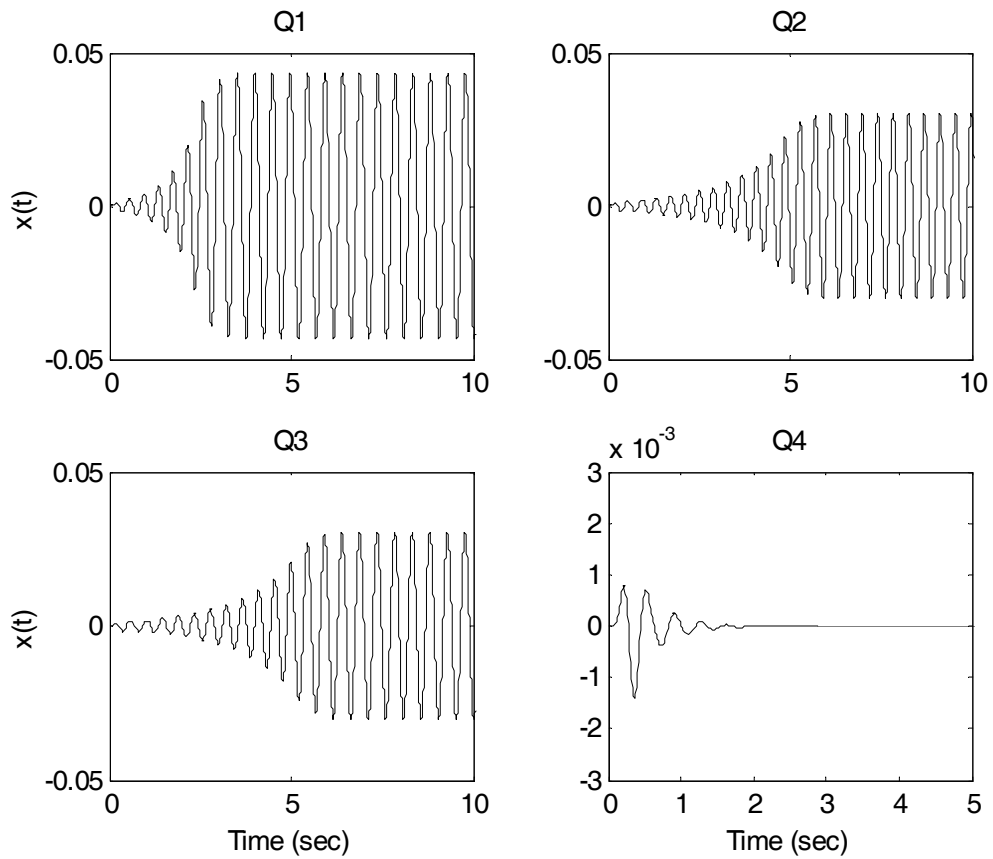
Fig. 5.8 Time responses of input signal.
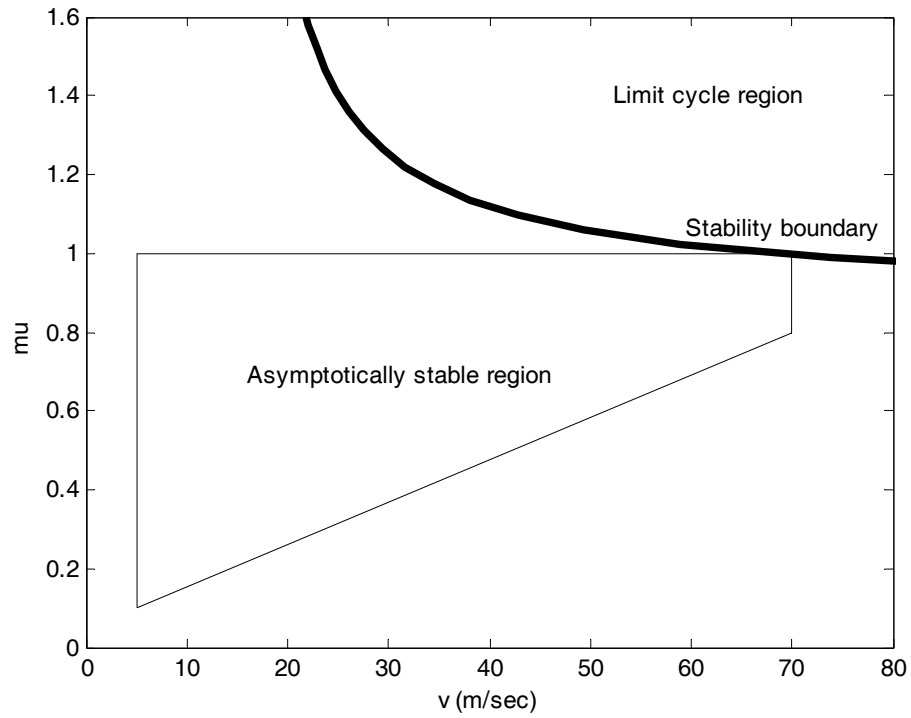
Fig. 5.9 Stability boundary.
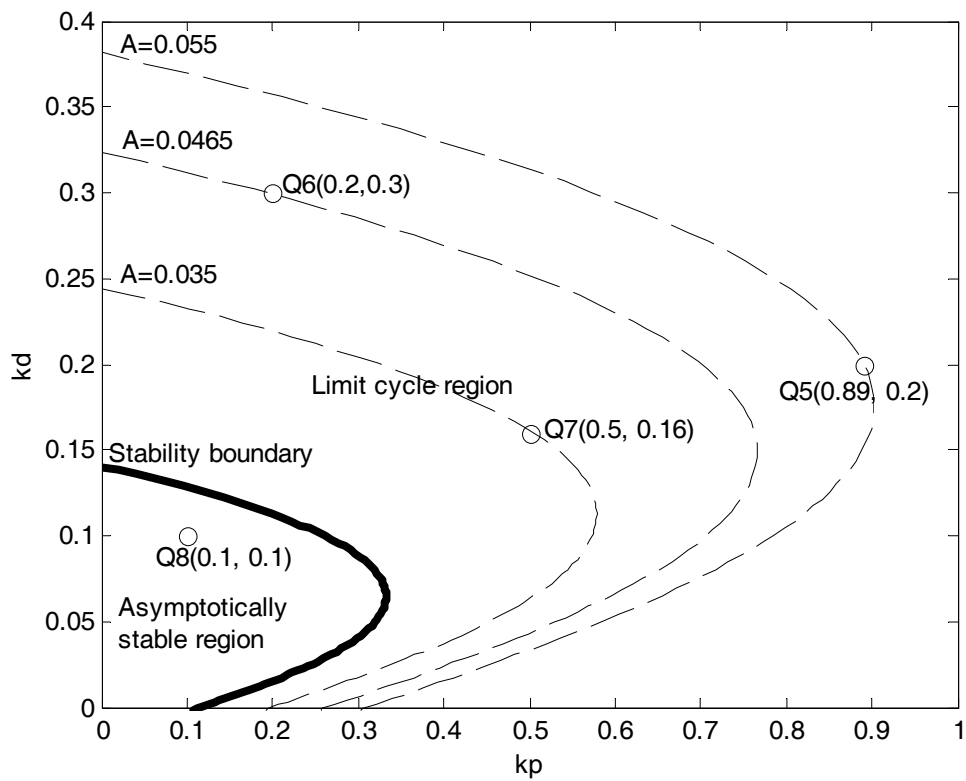
Fig. 5.10 Stability boundary.
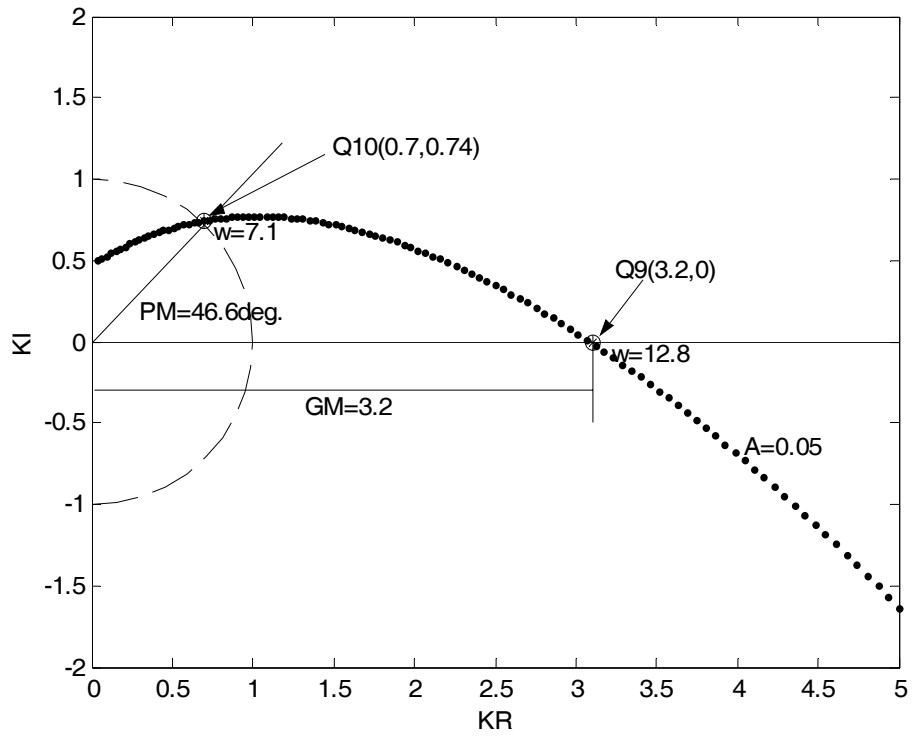
Fig. 5.11 GM and PM analysis.

Chapter 6

Robust Design for Perturbed Phase-Locked Loops

6.1 Overview

A control algorithm is presented in this chapter for phase-locked loop (PLL) design with perturbed parameters satisfying frequency-domain specifications. By the use of a gain-phase tester, the parameter plane method and robust stability criteria, the range of the designed parameters of PLL is determined based on specified constraints of gain and phase margins (GM and PM) on frequency domain with uncertain parameters perturbed in some intervals. The PLL model used in this design is assumed to be a linearized one if in the locked state. The proposed method is applied to a PLL model with first and second order low-pass filters as examples. With the help of stability boundary curves, the area in the selected designed parameters of the corresponding coordinate plane is found out such that the whole PLL system with the desired parameters in that area will meet given conditions. Simulation results are provided to illustrate the design technique based on GM and PM, and the resulted PLL is

to robustly meet the specified constraints as expected with uncertain parameters varying in intervals.

6.2 Basic Concept of PLL

PLL is an electronic circuit which causes a output signal to keep track of the input reference signal applied to it and the output signal keeps synchronization with the input one. Three basic functional blocks, a phase detector (PD), a loop filter (LF) and a voltage controlled oscillator (VCO), are contained in a PLL depicted in Fig. 6.1.

Assume the reference input $v_i(t) = A\sin(\omega_i t + \theta_i)$ and the VCO output $v_o(t) = B\sin(\omega_o t + \theta_o)$, where ω_i and ω_o are angular frequencies, θ_i and θ_o are phases, A and B are amplitudes of $v_i(t)$ and $v_o(t)$, respectively.

In a PLL, the function of the PD is to measure the phase difference between $v_i(t)$ and $v_0(t)$ and produces an output voltage $v_d(t)$ proportional to the phase error of $v_i(t)$ and $v_0(t)$. Assume the PD be a linear multiplier in linear PLL (LPLL) through this chapter.

The LF is a low-pass filter and is used to suppress noise and high-frequency signal components which are unwanted signals. The lower frequency and dc parts are passed through the LF and delivered to control the frequency of the VCO output.

The VCO is an oscillator which produces a periodic signal with the frequency that is

proportional to the dc voltage from the LF.

When the PLL is locked, the frequencies ω_i and ω_o are identical. The PD is linear and the LF output voltage is proportional to the phase error. The linearized mathematical model of the PLL is shown in Fig. 6.2 if the phase difference $\left|\theta_i - \theta_o\right|$ is very small. As seen in this figure, the PLL structure is in fact a feedback control mechanism. The phase transfer function $\Gamma(s)$ that relates the phase θ_i of the reference input to the phase θ_o of the VCO output is

$$\Gamma(s) = \frac{\Theta_0(s)}{\Theta_i(s)} = \frac{k_v k_d F(s)}{s + k_v k_d F(s)} , \qquad (6.1)$$

where $\Theta_i(s)$ and $\Theta_0(s)$ are the Laplace transforms of θ_i and θ_o, respectively. k_d is the PD gain in rad per volt and k_v is the VCO gain with the unit of rad s^{-1} volt^{-1}. $F(s)$ is the transfer function of the LF.

6.3 Stability Boundary Analysis

Consider a gain-phase tester $ke^{-j\theta}$ included in series with the original control system as in Fig. 6.3, and its transfer function is given by

$$H(s,q,m,k,\theta) = \frac{ke^{-j\theta}G(s,q,m)}{1 + ke^{-j\theta}G(s,q,m)} , \qquad (6.2)$$

where $G(s,q,m)$ is an open-loop system function and $G(s,q,m) = G_m(s,m)F(s,q)$. $F(s,q)$ is the transfer function of the LF with the perturbed parameter vector q.

$m = [m_1, m_2, ..., m_r]$ is a designed parameter vector of PLL in the $m_1 - m_2 - .... - m_r$ coordinate

space under user-defined specifications.

The closed-loop characteristic polynomial is $P(s, q, m, k, \theta)$ and

$$
\begin{aligned}
P(s, q, m, k, \theta) &= \text{the numerator of} \quad [1 + ke^{-j\theta} G(s, q, m)] \\
&= \sum_{i=0}^{n} d_i(q, m, k, \theta) s^i \\
&= d_0(q, m, k, \theta) + d_1(q, m, k, \theta)s + \cdots + d_n(q, m, k, \theta)s^n
\end{aligned} \qquad (6.3)
$$

$P(j\omega, q, m, k, \theta)$ is divided into the real part $U(\omega, q, m, k, \theta)$ and imaginary part.

$V(\omega, q, m, k, \theta)$. Assume $d_i(q, m, k, \theta)$ is a continuous function in q for $i = 1, 2, ..., n$.

The equation

$$
\begin{cases}
U(\omega, q, m, k, \theta) = 0 \\
V(\omega, q, m, k, \theta) = 0
\end{cases} \qquad (6.4)
$$

can be solved for m with specific ω, k, θ and q in PLL design. Gain and phase boundary

curves are developed in the $m - \text{space}$ according to different gain k and θ by varying ω,

respectively.

6.3.1 Gain Boundary Curves

Let $\theta = 0^O$ and q be a specific perturbed parameter. Equation (6.4) is rewritten into

the form

$$
\begin{cases}
U(\omega, m, k) = 0 \\
V(\omega, m, k) = 0
\end{cases} \qquad (6.5)
$$

A gain boundary curve is generated in $m - \text{space}$ from the solutions m of (6.5) by

varying ω for every k. Given a specific gain k, a gain boundary curve will be generated

and a region of the designed parameters in $m-$space is to be found out so that the whole

PLL system with the designed parameters chosen from the above determined region will

satisfy the GM condition. The GM of the control system at a point on one side of a specific

gain boundary curve is greater than that at a point on the boundary curve. But it is less at the

points on the other side.

6.3.2   Phase Boundary Curves

Given $k=1$ and a specific q, (6.4) is written into the form

$$\begin{cases} U(\omega,m,\theta) = 0 \\ V(\omega,m,\theta) = 0 \end{cases}.$$
(6.6)

Phase boundary curves are developed under the PM specification in a similar way. They

are generated in $m-$space from the solutions m of (6.6) by varying ω for every θ.

Given a specific θ, a phase boundary curve will be generated and a region of the designed

parameters in $m-$space is to be found out so that the whole PLL system with the designed

parameters chosen from the above determined region will satisfy the PM condition. The PM

of the control system at a point on one side of a specific phase boundary curve is greater than

that at a point on the boundary curve. But it is less at a point on the other side.

6.3.3   PLL Robust Design

In physical systems, uncertainties usually exist in system parameters. The LF is usually

connected to a PLL IC externally and implemented by the designer under the specified

constraints. The system parameters are separated into the designed parameters, which are the parameters of PD and VCO, and the perturbed parameters, which are the ones of the LF. The designed parameters are the parameters the range of which is to be determined so that the performance of the whole PLL system can meet the specified conditions under the perturbed parameters varying in a region as long as the designed parameters are within the determined range.

In this chapter, the LFs with different order are used as examples to demonstrate the proposed design method of PLL robust design. The robust design is based on gain and phase boundary curves with respect to k and θ of a gain-phase margin tester and they are drawn in $m-\text{space}$ from the locations of the roots of (6.5) and (6.6) with respect to different k and θ, respectively. The range of the designed parameters is going to be found out in $m-\text{space}$ under the constraints of specified GM and PM.
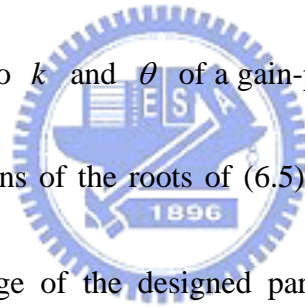
Based on the discussions mentioned above, the design algorithm is as the followings:

Step (1) Set up user-defined specifications on GM and PM.

Step (2) For every system parameter q at the vertices of the perturbed system parameter region in q-plane, draw the gain boundary curves corresponding to the specified GM in m-plane by solving (6.5).

Step (3) For every q at the vertices of the perturbed system parameter region in q-plane,

draw the phase boundary curves corresponding to the specified PM in m-plane by

solving (6.6).

Step (4) Determine a gain region in m-space with the help of the gain boundary curves as

in step (2)

so that the designed parameters with the coefficients in that region satisfy the

specified GM constraints.

Step (5) Determine a phase-region in m-space with the help of the phase boundary curves

as in step (3) so that the designed parameters with the coefficients in that region

satisfy the specified PM constraints.

Step (6) Find out the common region of the determined gain and phase ones as in steps (4)

and (5). The perturbed PLL system with the designed parameters in that region is the

desired one satisfying the specified GM and PM conditions.

6.4 Simulation Results of PLL Design for $\text{GM} \geq 3\text{dB}$ and $\text{PM} \geq 30^{\circ}$

6.4.1 The First Order LF

The transfer function $F_1(s)$ of the first order filter as in Fig. 6.4 is given by

$$F_1(s) = \frac{1 + s\tau_1}{1 + s\tau_2}, \tag{6.7}$$

where $\tau_1 = R_1 C_1$ and $\tau_2 = (R_1 + R_2) C_1$. R_1 and C_1 are perturbed parameters inside the

$\mathbb{S}$ region as in Fig. 6.6, where the $\mathbb{S}$ region is

$$R_1 \in [200 \text{Kohm}, 800 \text{Kohm}]$$
$$C_1 \in [5 \text{nf}, 15 \text{nf}]$$. \hfill (6.8)

R_2 and $k_d k_v$ are the selected designed parameters in this case and $m = [k_d k_v, R_2]$.

In (6.2),

$$G(s, q, m) = \frac{k_d k_v (1 + \tau_1 s)}{s(1 + \tau_2 s)}, \hfill (6.9)$$

and its closed-loop transfer function is

$$H_1(s, q, m, k, \theta) = \frac{ke^{-j\theta} k_d k_v (1 + \tau_1 s)}{\tau_2 s^2 + (1 + ke^{-j\theta} k_d k_v \tau_1) s + ke^{-j\theta} k_d k_v} \hfill (6.10)$$

In (6.4), the coefficients of the real part of the characteristic polynomial $U(\omega, q, m, k, \theta)$ are

$$r_0 = kk_d k_v \cos(\theta)$$
$$r_1 = kk_d k_v R_2 C_1 \sin(\theta) . \hfill (6.11)$$
$$r_2 = -(R_1 + R_2) C_1$$

The coefficients of the imaginary part of the polynomial $V(\omega, q, m, k, \theta)$ are

$$i_0 = -kk_d k_v \sin(\theta)$$
$$i_1 = 1 + kk_d k_v R_2 C_1 \cos(\theta), \hfill (6.12)$$
$$i_2 = 0$$

where $q = [q_1, q_2] = [R_1, C_1]$ is a specific point within $\mathbb{S}$.

By solving (6.5) and (6.6) for every specific k and θ, gain and phase boundary curves are

generated to determine the designed parameters m. The m-desired region is determined

solely by phase boundary curves because of the GM of the closed PLL system is infinity. Let

$\theta = 30^\circ$. The phase boundary curves corresponding to PM=30° are drawn with the perturbed

parameters at the vertices S1, S2, S3 and S4 of the region $\mathbb{S}$ in Fig. 6.6. The shaded area in

$k_d k_v$-R_2 plane, seen in Fig. 6.7, is the desired one so that the designed parameters R_2 and $k_d k_v$ in the determined area cause the PLL system to meet the phase requirement $PM \geq 30^\circ$.

Choose $k_v = 13000$ rad/(sec × volt) which signifies that the frequency created by the VCO changes about 20KHz if the input signal $v_f(t)$ of the VCO in Fig. 1 changes by 1 volt. The shaded area in k_d-R_2 plane in Fig. 6.8 is found. The point $Q_1 = (k_d, R_2) = (1.8, 14K$ ohm) is selected as an example point in this area and the PMs at the vertices and other points of S are listed in Table 6.1. The corresponding bode plots are also shown in Fig. 9. The simulation results are achieved as desired.

Choose designed parameters $m = [k_v, R_2]$ with $k_d = 0.6$. In a similar way, the desired parameters in the k_v-R_2 plane satisfying the condition $PM \geq 30^\circ$ are shown in Fig. 6.10. If the point $Q_2 = (k_v, R_2) = (3 \times 10^6, 5.1Kohm)$ is chosen, the bode plots and the PMs at the point $[R_1, C]$ inside S are depicted in Fig. 6.11 and Table 6.2, respectively.

6.4.2 The Second Order LF

The transfer function of the LF as in Fig. 6.5 is

$$F_2(s) = \frac{1 + s(\tau_3 + \tau_4)}{1 + s(\tau_3 + \tau_4 + \tau_5) + \tau_3 \tau_5 s^2}, \tag{6.13}$$

where $\tau_3 = R_1 C_1$, $\tau_4 = R_2 C_1$, and $\tau_5 = R_2 C_2$.

For the closed PLL system, the transfer function is given by

$$H_2(s,q,m,k,\theta) = \frac{ke^{-j\theta}k_dk_v + ke^{-j\theta}k_dk_v(\tau_4+\tau_5)s}{\tau_3\tau_5 s^3 + (\tau_3+\tau_4+\tau_5)s^2 + ke^{-j\theta}k_dk_v(\tau_4+\tau_5)s + ke^{-j\theta}k_dk_v} \quad (6.14)$$

The coefficients of the real part of the characteristic polynomial are

$$
\begin{aligned}
r_0 &= kk_dk_v\cos(\theta) \\
r_1 &= kk_dk_v(R_2C_1+R_2C_2)\sin(\theta) \\
r_2 &= -(R_1C_1+R_2C_1+R_2C_2) \\
r_3 &= 0
\end{aligned}
\quad (6.15)
$$

and the coefficients of the real part of the characteristic polynomial are

$$
\begin{aligned}
i_0 &= -kk_dk_v\sin(\theta) \\
i_1 &= 1 + kk_dk_v(R_2C_1+R_2C_2)\cos(\theta) \\
i_2 &= 0 \\
i_3 &= -R_1C_1R_2C_2
\end{aligned}
\quad (6.16)
$$

The perturbed parameters are chosen as $q=[q_1,q_2,q_3]=[R_1,C_1,C_2]$ and the perturbed space

$\mathbb{R}$ is depicted in 3D-coordinate in Fig. 6.12.

The 3D perturbed space $\mathbb{R}$ is defined by

$$
\begin{aligned}
R_1 &\in [200\text{Kohm}, 800\text{Kohm}] \\
C_1 &\in [5\text{nf}, 15\text{nf}] \\
C_2 &\in [1\text{nf}, 3\text{nf}]
\end{aligned}
\quad (6.17)
$$

and the locations of the vertices of $\mathbb{R}$ are listed in Table 6.3. Select R_2 and $k_d k_v$ as the

designed parameters. By the same way as above, solve (6.4) for R_2 and $k_d k_v$ and phase

boundary curves as in Fig. 6.13 with respect to $PM=30^\circ$ are created at the vertices of $\mathbb{R}$.

The desired R_2 and $k_d k_v$ in $k_d k_v$-R_2 plane are shown as in the shaded area of this plot.

Let $k_v = 13000$ rad/(sec×volt) and $m=(k_d, R_2)$ is the designed parameters. The

chart of phase boundary curves is developed in Figs. 6.14 and 6.15 in k_d-R_2 plane. Choose

an example point $Q_3(k_d=0.2, R_2=60\text{Kohm})$ in the shaded area in Fig. 6.15. The

corresponding bode plots and the PMs are shown and listed in Fig. 6.16 and Table 6.4.

Assume $m = [k_v, R_2]$ and $k_d = 0.8$. The phase boundary curves are shown in Fig. 6.17 and the desired shaded area are found in Fig. 6.18 in the k_v-R_2 plane. $Q_4(k_v = 50000, R_2 = 45\text{Kohm})$ is the selected point. The bode plots and the PMs at the vertices and other points in $\Re$ are depicted and listed in Fig. 6.19 and Table 6.5, respectively.

6.5 Concluding Remarks

This chapter introduces a new method on PLL design by frequency domain approach for a perturbed PLL control system. Based on parameter space method and robust stability criteria, the desired system parameters of PLLs in the selected coordinate plane are determined in graphical portrayals. With the help of gain and phase boundary curves resulting from the roots of characteristic polynomial equation in the closed PLL system, a methodology is proposed for portraying regions in a selected designed parameter plane so that the performance of the whole PLL system can meet the specified requirements on frequency-domain constraints. Simulation results have demonstrated the objectives have been achieved as desired.
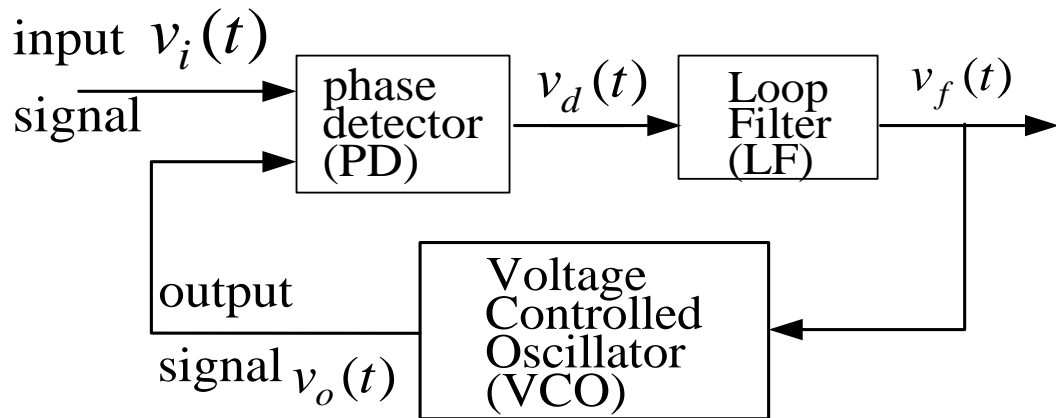
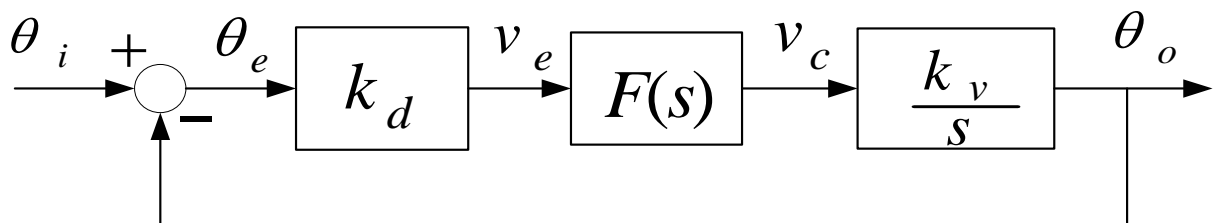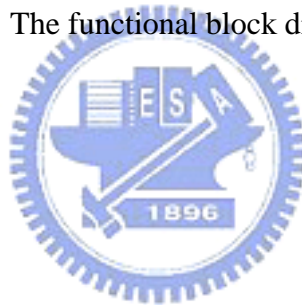Fig. 6.1 The functional block diagram of PLL.

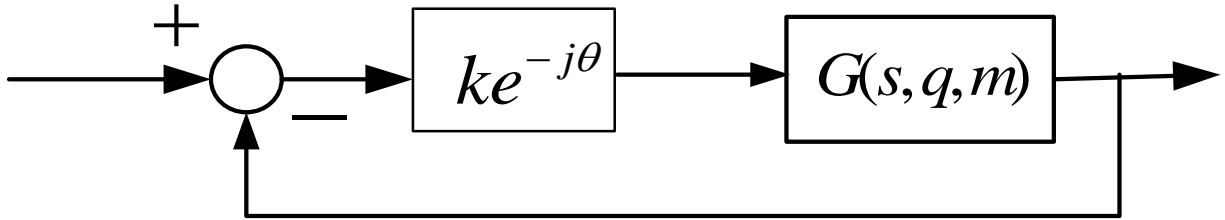Fig. 6.2 The linearized mathematical model of PLL.

Fig. 6.3 The closed feedback system with a gain-phase margin tester $ke^{-j\theta}$.
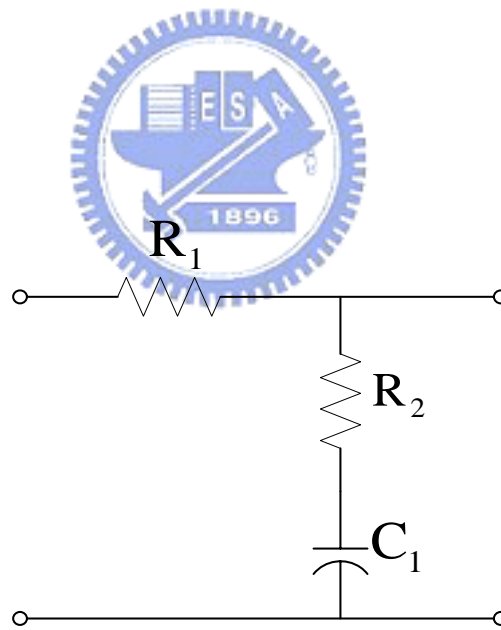
Fig. 6.4 The first order loop filter.

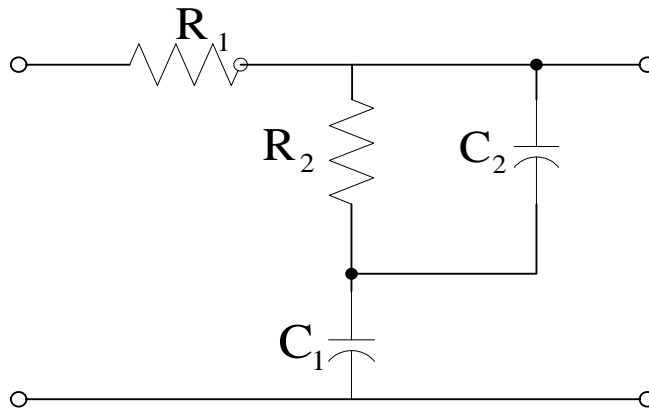Fig. 6.5 The second order filter.
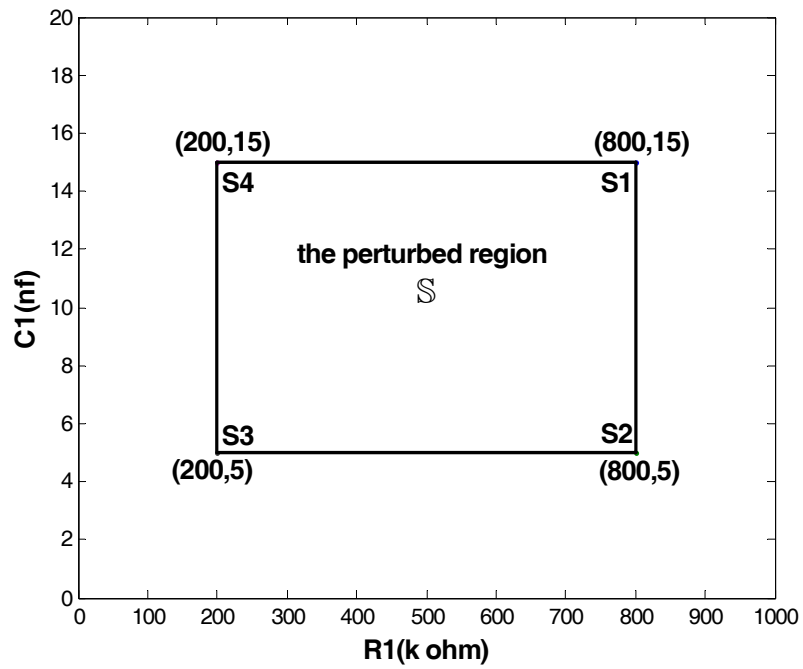
Fig. 6.6 The 2D perturbed plane $\mathbb{S}$ with the perturbed parameters R_1 and C_1.

Fig.6.7 The designed-parameter shaded area in $k_d k_v$-R_2 plane meeting

the phase specifications $PM \geq 30°$ with the first order LF.

Fig.6. 8 The designed-parameter shaded area in k_d-R_2 plane meeting

the phase specifications $PM \geq 30°$ with $k_v = 130000$.
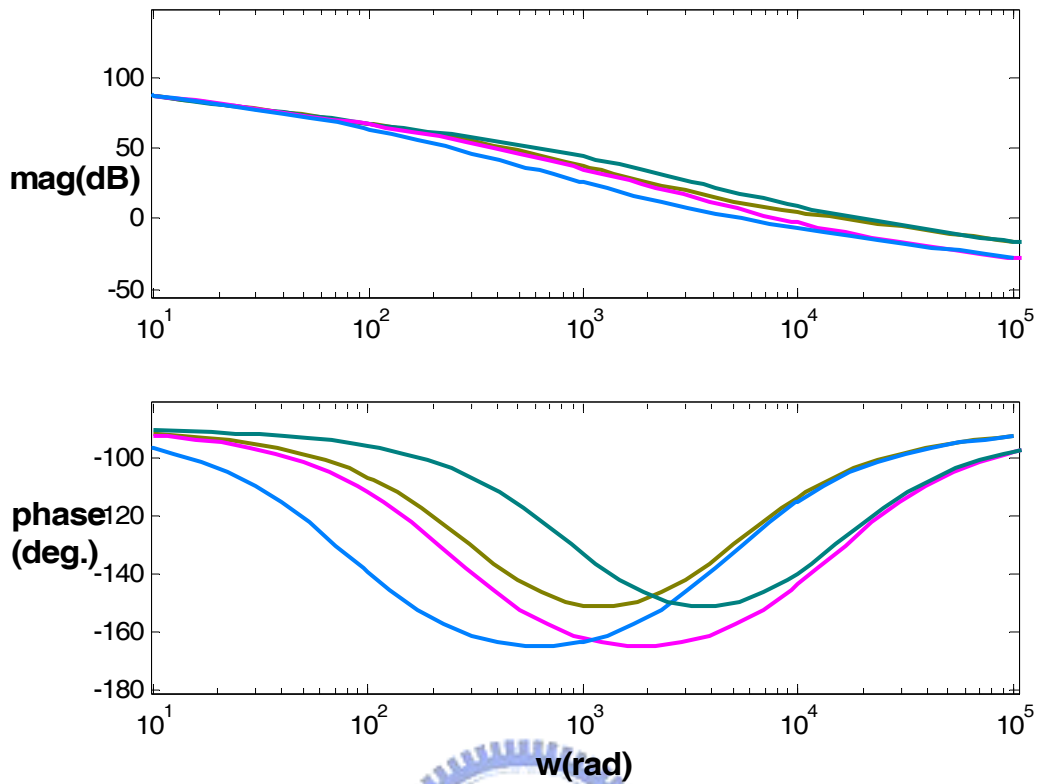
Fig. 6.9 The bode plots of the PLL system at the vertices of the region $\mathbb{S}$ with $Q_1 = (k_d, R_2) = (1.8, 14\text{Kohm})$ and $k_v = 130000$.
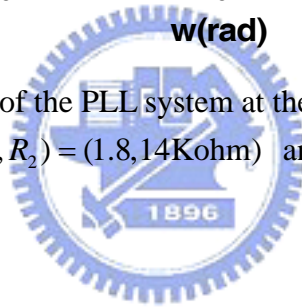
Table 6.1 The PMs of the PLL system with the first order LF at the points of $\mathbb{S}$ at $Q_1 = (k_d, R_2) = (1.8, 14\text{Kohm})$ and $k_v = 130000$..

the point (R_1, C_1)	PM	the point (R_1, C_1)	PM
S1	49.3°	S2	31.4°
S3	56°	S4	74.5°
(350,12)	70.3°	(650,8)	51.2°

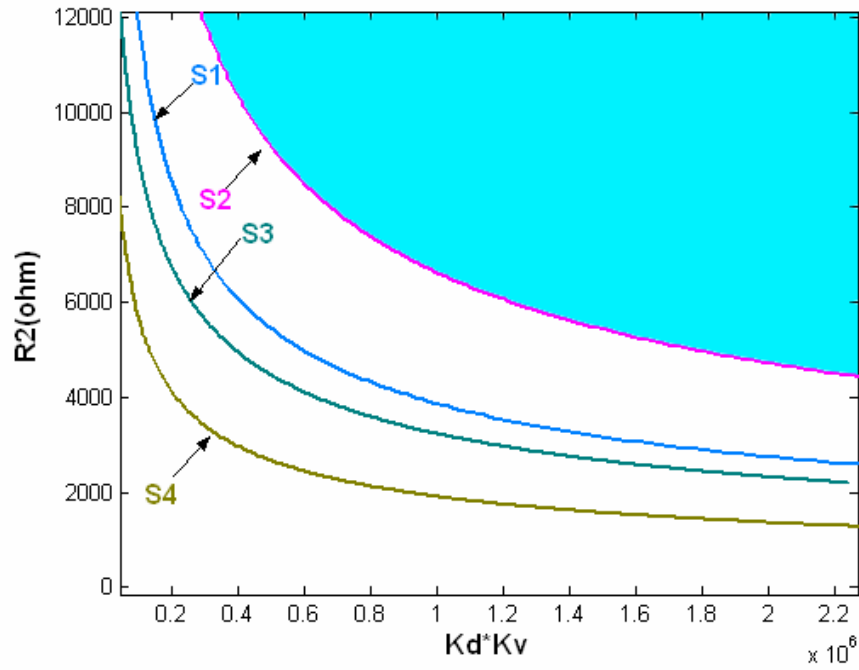Fig. 6.10 The designed-parameter shaded area in k_v-R_2 plane meeting the phase specifications $PM \geq 30^\circ$ with $k_d = 0.6$.

Fig 6.11 The bode plots of the PLL system at the vertices of the region $\mathbb{S}$ with $Q_2 = (k_v, R_2) = (3 \times 10^6, 5.1 \text{Kohm})$ and $k_d = 0.6$.

Table 6.2 The PMs of the PLL system with the first order LF at the points of $\mathbb{S}$ at $Q_2 = (k_v, R_2) = (3 \times 10^6, 5.1 \text{Kohm})$ and $k_d = 0.6$.

the point (R_1, C_1)	PM	the point (R_1, C_1)	PM
S1	49.4°	S2	30.7°
S3	55.5°	S4	74.7°
(350,12)	61.5°	(650,8)	41.6°
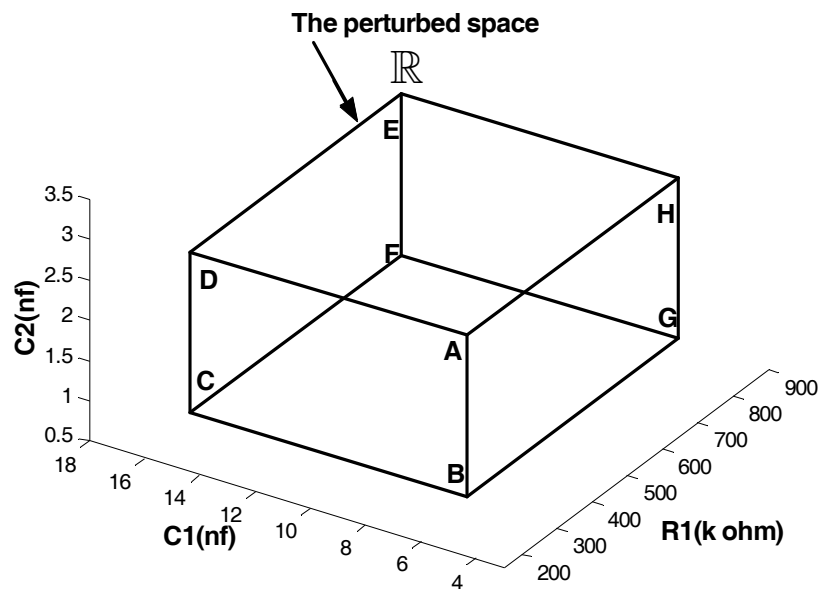
Fig. 6.12 The 3D perturbed plane $\mathbb{R}$ with the perturbed parameters R_1, C_1 and C_2.

Table 6.3 The Coordinates of the vertices of The 3D Perturbed Parameter Space $\mathbb{R}$

(R1, C1, C2)=(Kohm, nf, nf)	
A(800,15,1)	E(200,15,3)
B(800, 5,1)	F(200, 5,3)
C(200, 5,1)	G(800, 5,3)
D(200,15,1)	H(800,15,3)

Fig. 6.13 The designed-parameter shaded area in $k_d k_v$-R_2 plane meeting the phase specifications $PM \geq 30^\circ$ with the second order LF.
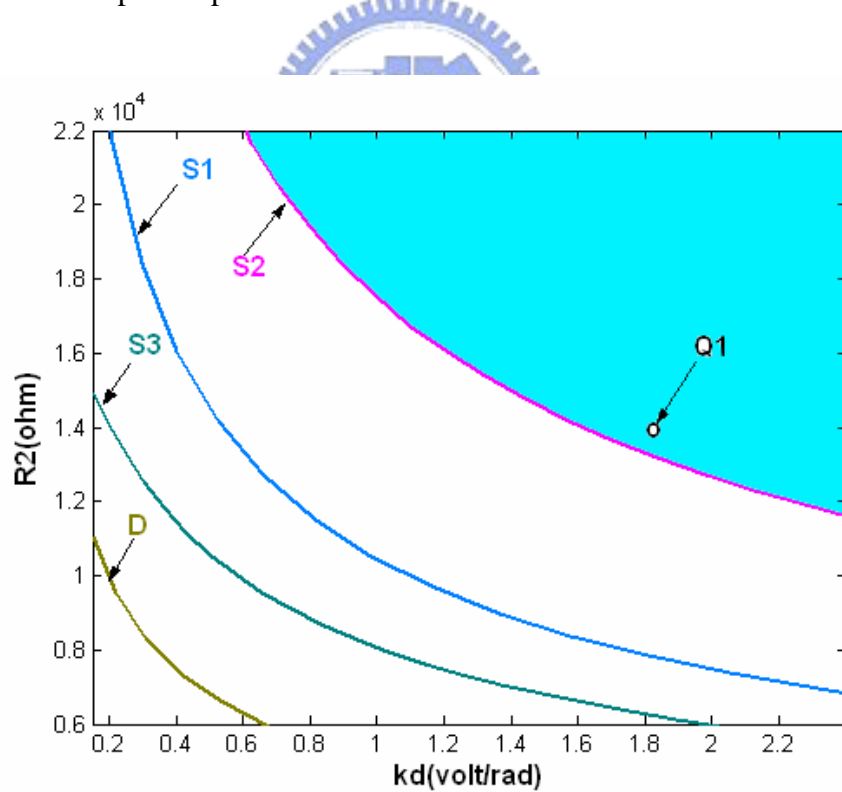
Fig. 6.14 The designed-parameter shaded area in k_d -R$_2$ plane meeting the phase specifications PM $\geq 30^\circ$ and $k_v = 130000$ with the second order LF.

Fig. 6.15 The enlarged designed-parameter shaded area in k_d -R$_2$ plane meeting the phase specifications PM $\geq 30^\circ$ and $k_v = 130000$ with the second order LF.
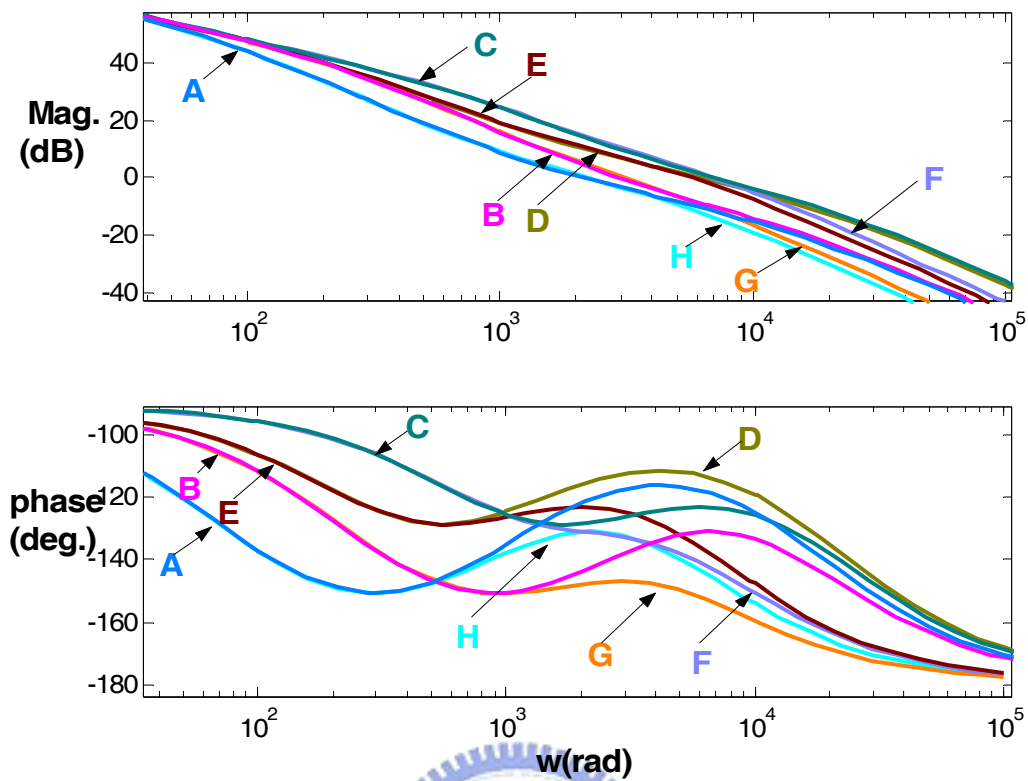
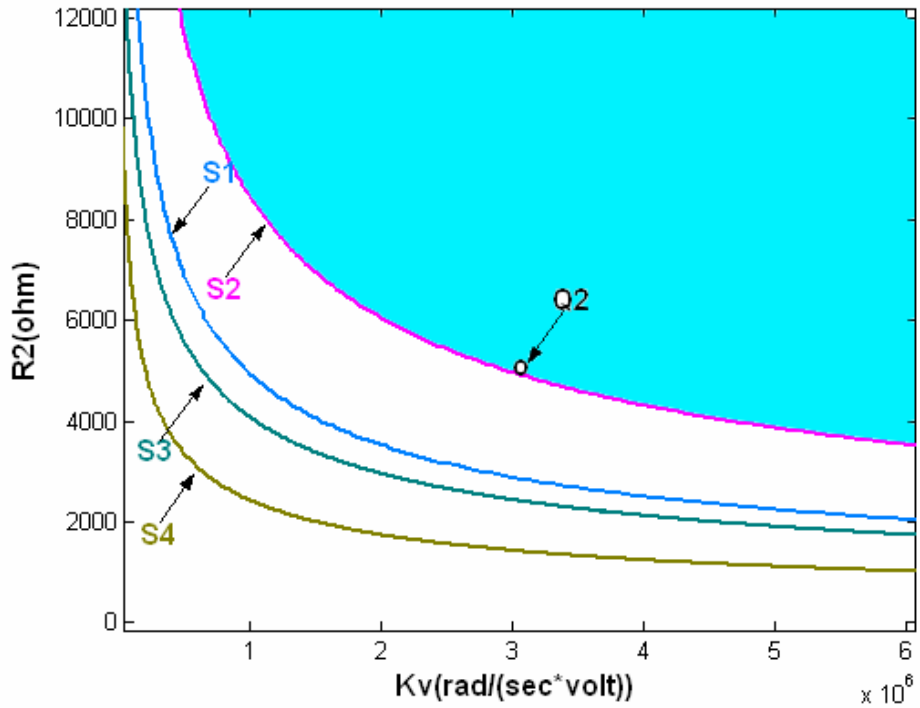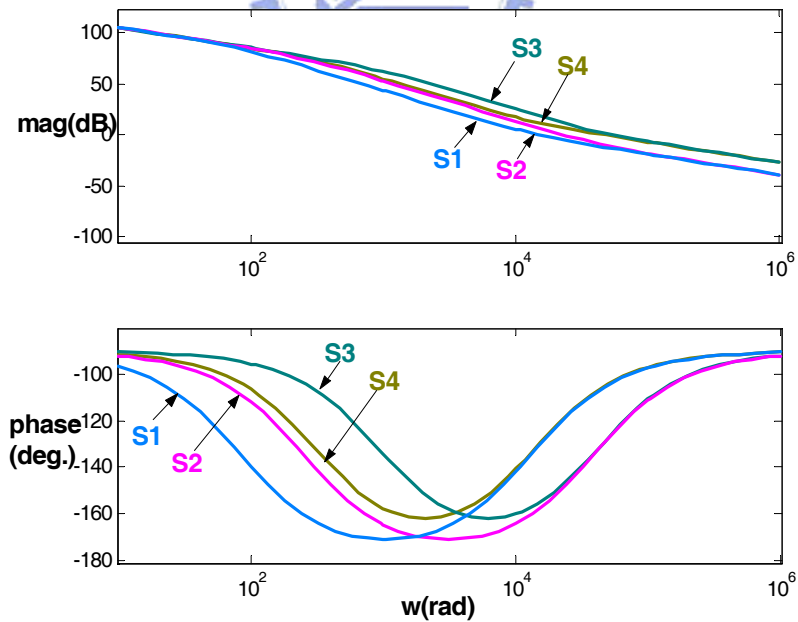Fig. 6.16 The bode plots of the PLL system at the vertices of the region $\mathbb{R}$ at $Q_3 = (k_d, R_2) = (0.2, 60\text{Kohm})$ and $k_v = 130000$ with the second order LF.

Table 6.4 The PMs of the PLL system with the second order LF at the points of $\mathbb{R}$ at $Q_3 = (k_d, R_2) = (0.2, 60\text{Kohm})$ and $k_v = 130000$.

The point (R_1, C_1, C_2)	PM	The point (R_1, C_1, C_2)	PM
A	59.3°	B	41.8°
C	56.7°	D	66.9°
E	45.4°	F	36.3°
G	33°	H	49°
(500,10,2)	50.8°	(650,7,1.6)	46.4°
(350,12,2.5)	49.3°	(700,9,2.2)	46.2°
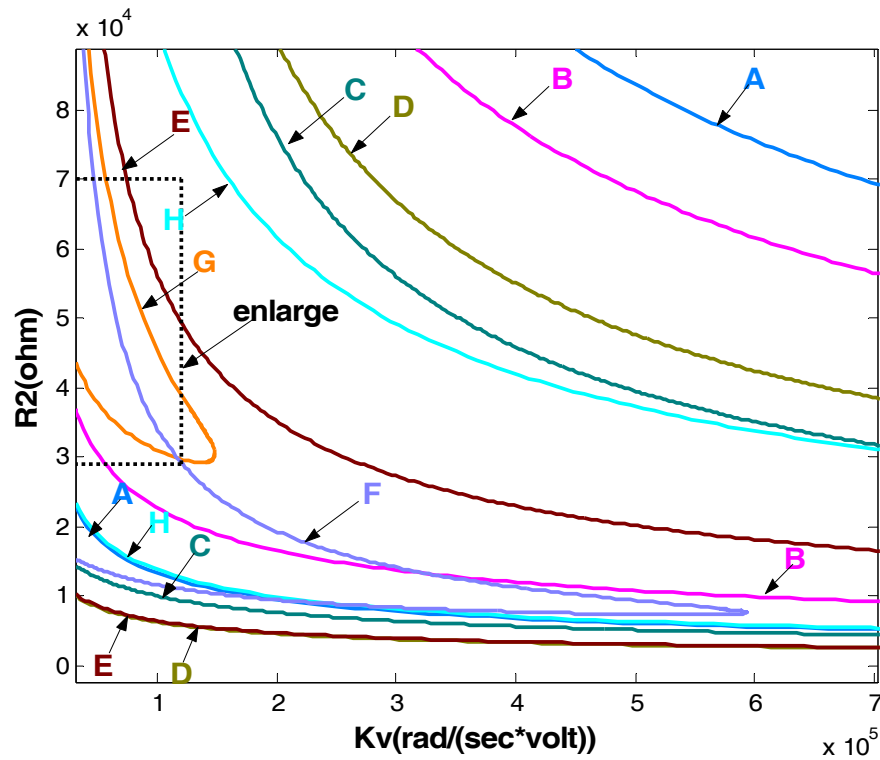
Fig. 6.17 The designed-parameter shaded area in k_v-R_2 plane meeting the phase specifications $PM \geq 30°$ and $k_d = 0.8$ with the second order LF.

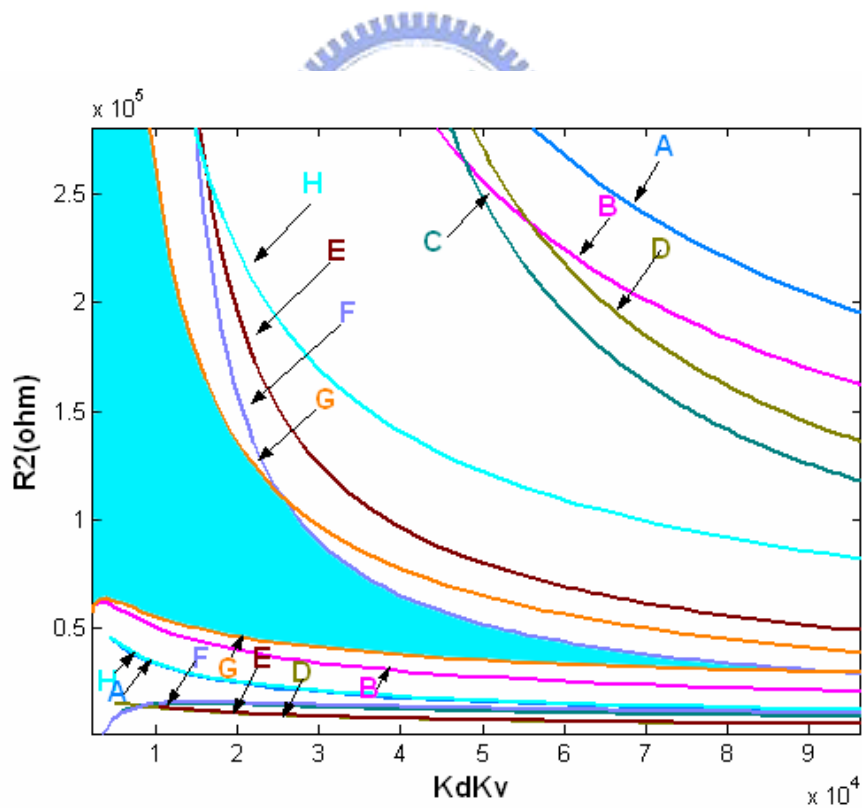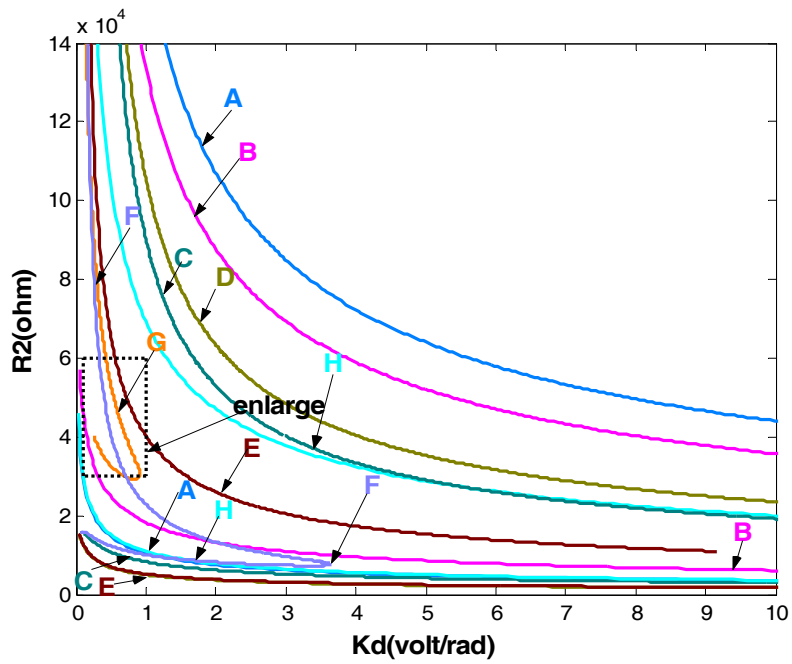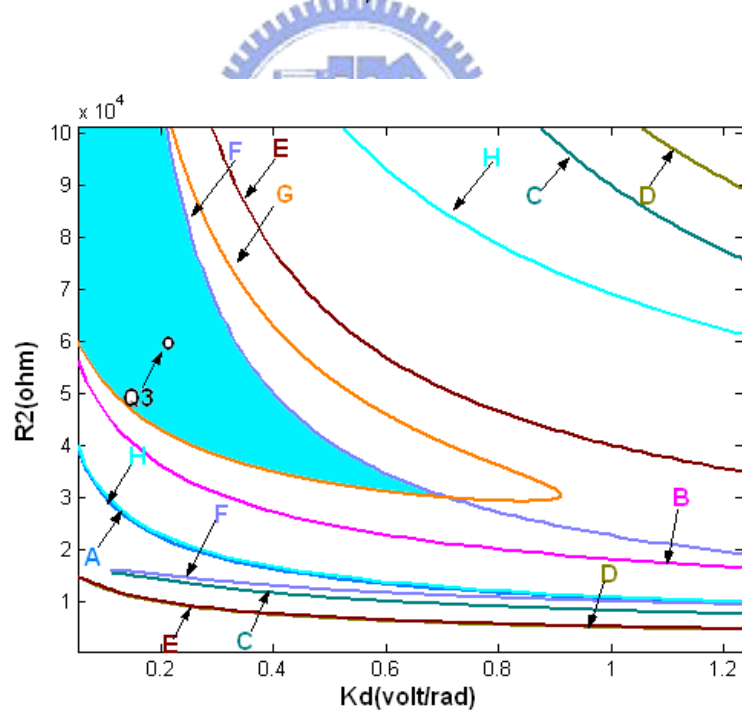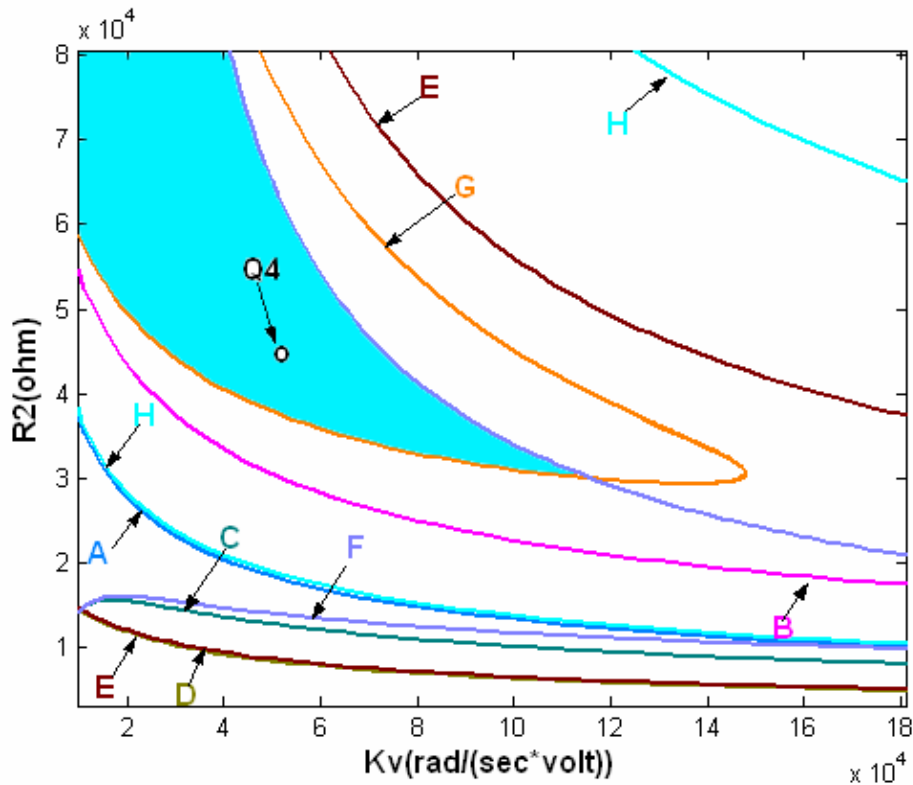Fig. 6.18 The enlarged designed-parameter shaded area in k_v-R_2 plane meeting the phase specifications $PM \geq 30°$ and $k_d = 0.8$ with the second order LF.
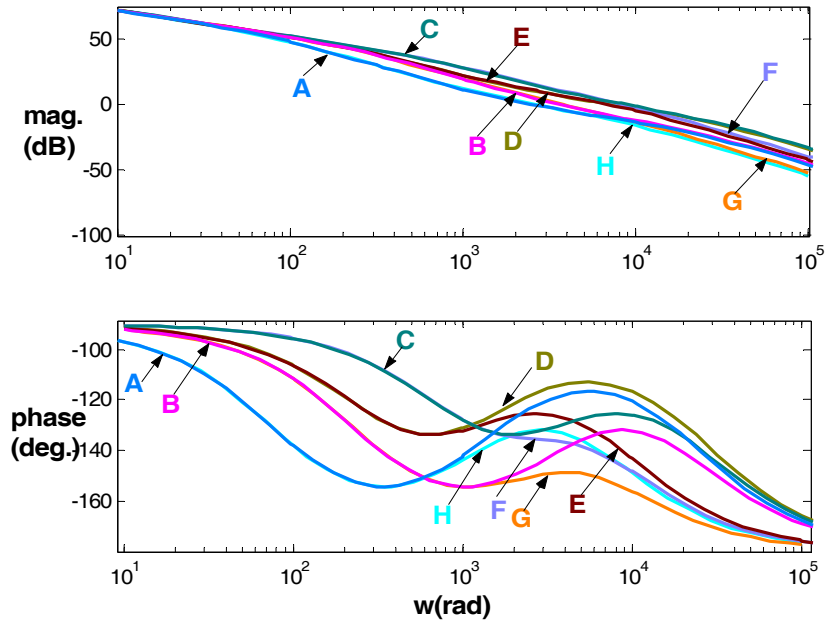
Fig. 6.19 The bode plots of the PLL system at the vertices of the region $\mathbb{R}$ at $Q_4 = (k_v, R_2) = (5 \times 10^4, 45\text{Kohm})$ and $k_d = 0.8$ with the second order LF.

Table 6.5 The PMs of the PLL system with the second order LF at the points of $\mathbb{R}$ at $Q_4 = (k_v, R_2) = (5 \times 10^4, 45\text{Kohm})$ and $k_d = 0.8$.

The point (R_1, C_1, C_2)	PM	The point (R_1, C_1, C_2)	PM
A	57.1°	B	39.3°
C	54.6°	D	66.1°
E	44.6°	F	34.3°
G	31.5°	H	48°
(500,10,2)	49.6°	(650,7,1.6)	44.4°
(350,12,2.5)	48.7°	(700,9,2.2)	44.6°

Chapter 7

Conclusions and Suggestions for Future Research

7.1 Conclusions

The main subject of this dissertation is to propose a systematic method based on parameter space method and robust stability criteria to predict the limit cycles occurred, analyze the system performances of gain margin and phase margins (GM and PM), and design a desired controller by adjusting the controller coefficients for perturbed control systems to meet specified conditions including GM, PM and sensitivity in frequency domain. Robust PLL design is also studied.

Based on parameter space method and robust stability criteria, the following objectives are achieved in this dissertation.

1. A systematic method is proposed to predict the limit cycles for perturbed control systems with nonlinearities.

2. Gain and phase margins are defined for system parameters perturbed in given intervals

and performance analysis on frequency domain is analyzed.

3. Robust stability is also analyzed for fuzzy dynamic control systems.

4. Controller design for perturbed control systems with uncertain parameters is solved in

    portraying way based on the proposed techniques.

5. The desired parameters of perturbed PLL systems are determined under specified

    constraints in frequency-domain.

7.2 Suggestions for Future Research

In this dissertation, some linear and nonlinear practical perturbed control systems have

been considered. However, the proposed approach may be further applied to other control

systems. The suggestions of future works planned to do are given as follows.

1. Nonlinear PLL systems.

2. Discrete time systems

3. Filter design systems

4. Power electronic systems

References

[1] C. H. Lee and C. C. Teng, "Tuning of PID Controllers for Stable and Unstable Process with Specifications on Gain and Phase Margins," *Int. Journal of Fuzzy Systems*, vol. 3, no. 1, pp. 346-355, March 2001.

[2] G. F. Franklin, J. D. Powell and A. E. Baeini, *Feedback Control of Dynamic Systems*, New York: Addison-Wesley, 1986.

[3] K. J. Astrom and T. Hagglund, "Automatic Tuning of Simple Regulators with Specifications on Phase and Amplitude Margins," *Automatica*, vol. 20, no. 5, pp. 645-651, 1984.

[4] M. Nagurka and O. Yaniv, "Robust PI Controller Design Satisfying Gain and Phase Margin Constraints," *in Prco. IEEE Conf. American Control*, vol. 5,pp. 3931-3936, Denver, Colorado, June 4, 2003.

[5] W. K. Ho, C. C. Hang and L. S. Cao, "Tuning of PID Controllers Based on Gain and Phase Margin Specifications," *Automatica,* vol. 31, no. 3, pp. 497-502, 1995.

[6] O. Yaniv and M. Nagurka, "Robust PI Controller Design Satisfying Sensitivity and Uncertainty Specifications," *IEEE Trans. Automatic Control*, vol. 48, no. 11, pp. 2069-2072, Nov. 2003.

[7] T. Chai and G. Zhang, "A New Self-tuning of PID Regulators Based On Phase and Amplitude Margin Specifications," *ACTA Automata Sinica*, vol. 23, no. 2, pp. 167-172, 1997.

[8] W. K. Ho, C. C. Hang and J. H. Zhou, "Self-tuning PID Control of a Plant with Underdamped Response with Specifications on Gain and Phase Margins," *IEEE Trans. Control Systems Technology*, vol. 5, no. 4, pp. 446-452, 1997.

[9] W. K. Ho and W. Xu, "PID Tuning for "Unstable Processes Based On Gain and Phase Margin Specifications," in *Proc. IEE Control Theory and Applications*, vol. 145, pp. 392-396, 1998

[10] G. L. Chao, J. W. Perng and K. W. Han, "Robust Stability Analysis of Time Delay Systems Using Parameter–plane and Parameter-space Method," *J. of Franklin Institute*, vol. 335B, no. 7, pp. 1294-1262, 1998.

[11] S. P. Bhattacharyya, H. Chapellat and L. H. Keel, *Robust Control (The Parametric Approach)*, Prentice-Hall, NJ, 1994.

[12] A. Cavallo, G. E. Maria, and L. Verde, "Robust Control Systems: A Parameter Space Design," *J. of Guidance, Control, and Dynamics*, vol. 15, no. 5, pp. 1207-1215, 1992.

[13] D. D. Siljak, "Parameter Space Methods for Robust Control Design: A Guide Tour," *IEEE Trans. Automatic Control*, vol. 34, no. 7, pp. 674-688, 1989.

[14] D. D. Siljak, "Analysis and Synthesis of Feedback Control Systems in the Parameter Plane," *IEEE Trans. Industry and Application*, vol. 83, pp. 466-473, 1964.

[15] J. Ackermann, "Parameter Space Design of Robust Control System," *IEEE Trans. Automatic Control*, vol. 25, no. 6, pp. 1058-1072, 1980.

[16] K. W. Han and G. J. Thaler, "Control System Analysis and Design Using a Parameter Space Method," *IEEE Trans. Automatic Control*, vol. 11, no. 3, pp. 560-563, 1966.

[17] R. A. Frazer and W. J. Duncan, "On the Criteria for the Stability of Small Motions," *in Proc. R. Soc*. A, 125, pp. 642-654, 1929.

[18] J. Ackermann, D. Kaesbauer and R. Muench,, "Robust Gamma-stability Analysis in a Plant Parameter Space," *Automatic Control*, vol. 27, no. 1, pp. 75-85, 1991.

[19] A. T. Shenton and Z. Shafiei, "Relative Stability for Control Systems with Adjustable Parameters," *J. of Guidance, Control, Dynamics*, vol. 17, no. 2, pp. 304-310, 1994.

[20] B. F. Wu, H. I Chin and J. W. Perng, "Gain-phase Margin Analysis of Perturbed Vehicle Control Systems," in *Proc. IEEE Conf Networking, Sensing & Control,* pp. 589-594, Taipei, Taiwan, 2004.

[21] C. H. Chang and K. W. Han, "Gain Margins and Phase Margins for Control Systems with Adjustable Parameters," *J. of Guidance, Control, and Dynamics*, vol. 13, no. 3, pp. 404-408, 1990.

[22] J. Ackermann and T. Bünte, "Actuator Rate Limits in Robust Car Steering Control," in *Proc. IEEE Conference on Decision & Control*, pp. 4726-4731, San Diego, U.S.A., 1997.

[23] J. Ackermann, "Robust Control Prevents Car Skidding," *IEEE Control Systems Magazine*, vol. 17, no. 3, pp. 23-31, June 1997.

[24] J. W. Smith and D. T. Berry, "Analysis of Longitudinal Pilot-Induced Oscillation Tendencies of the YF-12 Aircraft," *NASA TND-7900*, Feb.1975.

[25] R. Wang, Z. Jing, L. Chen, "Periodic Oscillators in Genetic Networks with Negative Feedback Loops," *WSEAS Int. Conf. Applied Mathematics(MATH 2004)*, Miami, Florida, April 21-23,2004.

[26] J. Ackermann and T. Bünte, "Robust Prevention of Limit Cycles for Robustly Decoupled Car Steering Dynamics," in *Proc. IEEE Mediterranean Conf. Control and Systems*, (Paphos, Cyprus), 1997.

[27] A. Gelb and W. E. Vander Velde, *Multiple input Describing Functions and Nonlinear System Design*, McGraw-Hill, New York, pp. 520-524, 1968.

[28] K. W. Han, *Nonlinear Control Systems: Some Practical Method*s, Academic Cultural Company, California, pp. 254-268, 1977.

[29] A. I. Mees and A. R. Bergen, "Describing Functions Revisited," *IEEE Trans. Automatic*

*Contro*l, vol. AC-2, pp. 473-478, Apr. 1975.

[30] Shlomo Engelberg, "Limitations of the Describing Function for Limit Cycle Prediction," *IEEE Trans. Automatic Contro*l, vol. 47, no. 11, pp. 1887-1890, Nov. 2002.

[31] F. Gordillo, J. Aracil and T. Alamo, "Determining Limit Cycles in Fuzzy Control Systems," in *Proc. IEEE Conf. Fuzzy Syst.*, vol. 1, pp. 193-198, 1997.

[32] E. Kim, H. Lee and M. Park, "Limit-Cycle Prediction of a Fuzzy Control System Based on Describing Function Method," *IEEE Trans. Fuzzy Syst.*, vol. 8, no. 1, pp. 11-21, 2000.

[33] S. Gomariz, F. Guinjoan, E. V. Idiarte, L. M. Salamero and A. Poveda, "On the Use of the Describing Function in Fuzzy Controllers Design for Switching DC-DC Regulators," *IEEE Int. Symp. Circuits Syst*., vol. 3, pp. 247-250, 2000.

[34] A. Delgado, "Stability Analysis of Neurocontrol Systems Using a Describing Function," in *Proc. Int. Join. Conf. Neural Network*, vol. 3, pp. 2126-2130, 1998.

[35] A. Blanchard, *Phase-Locked Loops: Application to Coherent Receiver Design*. New York: Wiley, 1976.

[36] F. M. Gardner, *Phaselock Techniques*, 2nd ed. New York: Wiley, 1979.

[37] W. C. Lindsey and C. M. Chie, "A Survey of Digital Phase-locked Loops," in *Proc. IEEE*, vol. 69, pp. 410-431, Apr. 1981.

[38] G. C. Hsieh and J. C. Hung, "Phase-locked Loop Techniques-a Survey," *IEEE Trans. Ind. Electron.*, vol. 43, no, 6, pp. 609-615, Dec. 1996.

[39] R. E. Best, *Phase-Locked Loops: Design, Simulation, and Application*, fifth ed. New York: McGraw-Hill, 2003.

[40] B. K. Bose and K. J. Jentzen, "Digital Speed Control of a DC Motor with PLL Regulation," *IEEE Ind. Electron.*, vol. IECI-27, pp. 10-13, Feb. 1978.

[41] P. Janiczek and S. Gilbert, *Global Positioning Systems Papers*, vol. 3, Washington, DC: The Institute of Navigation, 1986.

[42] V. Manassewitsch, *Frequency Synthesizers: Theory and Design*, 3rd edition. New York: Wiley, 1987.

VITA

博 士 候 選 人 學 經 歷 資 料

姓名：秦弘毅
性別：男
生日：民國 41 年 12 月 20 日
出生地：台灣省基隆市
論文題目：
    中文：參數空間法用於擾動控制系統之分析與設計
    英文：Analysis and Design of Perturbed Control Systems Based on
            Parameter Space Method
學歷：
1. 民國 65 年 6 月　　　國立交通大學控制工程系畢業
2. 民國 75 年 9 月　　　美國紐約州立大學 Buffalo 分校電機研究所畢業
3. 民國 85 年 9 月　　　國立交通大學電機與控制工程研究所博士班

經歷：
1. 民國 67 年 08 月~74 年 8 月　中山科學研究院研究助理

2. 民國 75 年 10 月~76 年 1 月　工業技術研究院副研究員

3. 民國 76 年 2 月～迄今　　　明新科技大學電子工程系專任講師

Publication List

博 士 候 選 人 著 作 目 錄

姓名：秦弘毅 (Hung-I Chin)

已被接受之期刊論文：

[1] Bing-Fei Wu, Jau-Woei Perng and Hung-I Chin, "Limit Cycle Analysis of Nonlinear Sampled-Data Systems by Gain-Phase Margin Approach," *Journal of the Franklin Institute*, Vol. 342, No. 7, pp. 175-192, 2005.

[2] Hung-I Chin, Jau-Woei Perng and Bing-Fei. Wu, "Parameter Plane Analysis of Fuzzy Vehicle Steering Control Systems," *WSEAS Trans. on Circuits and Systems*. Vol. 4, No. 2, pp. 59-65, 2005.

[3] Jau-Woei Perng, Bing-Fei Wu, Hung-I Chin and Tsu-Tian Lee, "Gain-Phase Margin Analysis of Dynamic Fuzzy Control Systems," *IEEE Trans. on Systems, Man and Cybernetics Part B*, Vol. 34, No. 5, pp.2133-2139, 2004.

[4] Bing-Fei Wu, Hung-I Chin and Jau-Woei Perng, "Gain-Phase Margin Analysis of Nonlinear Perturbed Vehicle Control Systems for Limit Cycle Prediction," *WSEAS Trans. on Systems*, Vol. 3, No. 5, pp. 1881-1886, 2004.

待審之期刊論文：

[1] Bing-Fei Wu, Hung-I Chin, Jau-Woei Perng and Tsu-Tian Lee, "Robust Control Design for Perturbed Systems by Frequency Domain Approach," submitted to *ASME Journal of Dynamic Systems, Measurement and Control*, 2005. (DS-05-1112)

[2] Bing-Fei Wu, Hung-I Chin, Li-Shan Ma and Jau-Woei Perng, "Robust Design for Perturbed Phase-Locked Loops," submitted to *IEEE Trans. on Circuits and Systems I*, 2005. (control number:1958)

研討會之期刊論文：

[1] Jau-Woei Perng, Bing-Fei Wu, Hung-I Chin and Tsu-Tian Lee, "Stability Analysis of a Robust Fuzzy Vehicle Steering Control System," accepted for publication in *IEEE Intelligent Vehicles Symposium*, Las Vegas, Nevada, USA, June 6-8, 2005.

[2] Jau-Woei Perng, Bing-Fei Wu, Hung-I Chin and Tsu-Tian Lee, "Limit Cycle Analysis of Uncertain Fuzzy Vehicle Control Systems," *IEEE International Conference on Network,*

Sensing & Control, Tucson, Arizona, USA, pp. 626-631, March 19-22, 2005.

[3] Jau-Woei Perng, Bing-Fei Wu, Hung-I Chin, Tsu-Tian Lee and Kuang-Wei Han, "Robust Analysis of Fuzzy Vehicle Control System by Parameter Space Approach," *The Twelfth National Conference on Fuzzy Theory and Its Applications*, July, 2004, I-Lan, Taiwan.

[4] Jau-Woei Perng, Hung-I Chin, Bing-Fei Wu and Tsu-Tian Lee, "Analysis of Pilot-Induced Oscillations from Parameter Plane Approach," *Proceedings of the IASTED Conference on Circuits, Signals and Systems,* Clearwater Beach, FL, USA, pp. 344-349, Nov. 28- Dec. 1, 2004.

[5] Bing-Fei Wu, Hung-I Chin and Jau-Woei Perng, "Gain-Phase Margin Analysis of Perturbed Vehicle Control Systems," *IEEE International Conference on Network, Sensing & Control*, Taipei, Taiwan, pp. 589-594, March 21-23, 2004.

[6] Hung-I Chin, Chih-Hsu Yen, and Bing-Fei Wu, "An observer-based secure system with chaotic signals," *Proceedings of 1998 Conference on Industrial Automatic Control & Power* Applications, Kaohsiung, pp. A2-28-A2-32, 1998.